Electrospinning of Thermo-and *pH*-Sensitive Polymers as Potential Drug Delivery Systems

by

Marwa STA

MANUSCRIPT-BASED THESIS PRESENTED TO ÉCOLE DE TECHNOLOGIE SUPÉRIEURE IN PARTIAL FULFILLMENT FOR THE DEGREE OF DOCTOR OF PHILOSOPHY
Ph. D.

MONTRÉAL, NOVEMBER 15, 2021

ÉCOLE DE TECHNOLOGIE SUPÉRIEURE
UNIVERSITÉ DU QUÉBEC

BOARD OF EXAMINERS

THIS REPORT HAS BEEN EVALUATED

BY THE FOLLOWING BOARD OF EXAMINERS

Mrs. Nicole R. Demarquette, Thesis Supervisor
Department of Mechanical Engineering, École de technologie supérieure

Mr. Amilton M. Dos Santos, Thesis Co-Supervisor
Department of Chemical Engineering, University of São Paulo

Mr. Simon Joncas, President of Board of Examiners
Department of Systems Engineering, École de technologie supérieure

Mr. Ricardo J. Zednik, internal Member of Board of Examiners
Department of Mechanical Engineering, École de technologie supérieure

Mr. Milan Maric, external Member of Board of Examiners
Department of Chemical Engineering, McGill University

THIS THESIS WAS PRESENTED AND DEFENDED

IN THE PRESENCE OF A BOARD OF EXAMINERS AND THE PUBLIC

ON, NOVEMBER 9, 2021

AT ÉCOLE DE TECHNOLOGIE SUPÉRIEURE

ACKNOWLEDGMENTS

I would particularly like to thank my research directors, Nicole Demarquette and Amilton Santos, who supervised me throughout this project, for their availability and patience regarding the technical and personal difficulties associated with this PhD. Their scientific support and sound advice helped to fuel the reflection in this project and improve its rigor and precision. I thank them for their support and encouragement in the pursuit of this thesis and for giving me the opportunity to work on this project in their labs.

I also thank the members of the jury Simon Joncas, Ricardo J. Zednik, and, Milan Maric for agreeing to evaluate my thesis, as well as for their advice and constructive criticism.

Thank you to the researchers, research staff and technician from the École de technologie supérieure for their collaborations on the various aspects of the project and their expertise.

A big thank you to all the members of Laboratoire d'ingénierie des polymères et composites (LIPEC) that I have integrated into the École de technologie supérieure.

I would like to address a special thank you to Simone F. Medeiros Sampaio, Dayane Batista Tada and Mazen Samara for their availability and for their contribution in the articles.

I would like also to thank the University Mission of Tunisia in Montreal for their availability and supervision.

I would like to express my gratitude to my family, who have always supported and accompanied me, whatever my dreams and ambitions.

Electrofilage de polymères thermo-sensibles et *pH*-sensible en tant que système d'administration de médicaments potentiel

Marwa Sta

RÉSUMÉ

Ce projet vise l'obtention d'une membrane électrofilée de PNVCL poly(N-Vinylcaprolactam), polymère thermosensible, comme système de délivrance de médicament. L'intérêt de l'utilisation de ce polymère et de la méthode de fabrication utilisée, pour cette application, résident en caractère thermosensible du polymère, qui pourrait permettre une libération de médicament contrôlée, et la surface spécifique élevée des membranes. Plusieurs routes ont été testées pour obtenir ces membranes.

Au cours d'une première étape, des membranes de PNVCL et de ses mélanges avec du poly(ε-caprolactone) (PCL) furent obtenues. Ces dernières furent testées quant à la capacité de délivrer de manière contrôlée du kétoprofène, un médicament hydrophobe. Même si des membranes furent obtenues, celles-ci ne présentaient pas la stabilité de morphologie nécessaire à leur utilisation. En effet, lors d'un contact avec l'eau elles se dissolvaient ce qui résultait en une libération de médicament trop rapide.

Afin de résoudre ces deux problèmes, le PNVCL fut modifié pour obtenir un copolymère à la fois thermo-et *pH*-sensible poly(N-vinylcaprolactam-*co*-acrylic acid) (Poly(NVCL-*co*-AA)). Deux compositions nominales de ce copolymère furent étudiées, un copolymère contenant 20 et un autre 30 % en moles d'AA. Les membranes obtenues furent testées quant à leur capacité d'encapsuler et de libérer une substance hydrophobe, le kétoprofène, et une substance hydrophile, la caféine. Des fibres régulières, dont le diamètre augmentait lors de l'incorporation de substance active, furent obtenues. Les résultats ont aussi montré qu'alors que le kétoprofène perdait sa forme cristalline lorsqu'incorporé dans les fibres, il n'en était pas de même pour la caféine. La cytotoxicité des différentes membranes obtenues a été évaluée par des tests de viabilité cellulaire utilisant des lignées cellulaires de MTT et de fibroblastes embryonnaires de souris (cellules MEF). La libération de kétoprofène et de caféine fut étudiée à des températures de 25 et 42°C et à un pH de 1,2 et 7,4. Pour le kétoprofène et la caféine, le profil de libération a montré un taux de libération plus élevé pour une température inférieure à LCST (température de solution critique inférieure : température à laquelle les polymères subissent des transitions de phase distincte solubles dans l'eau/non soluble dans l'eau) (25ºC) indiquant une libération basée sur le phénomène de diffusion. Il fut montré que le pH affectait aussi la cinétique de libération. Les résultats ont aussi montré que le copolymère contenant 20 % en mole d'AA était moins cytotoxique pour les cellules par rapport aux copolymères à 30 % molaire d'AA.

Les travaux menés ont permis de développer un nouveau système de délivrance de médicament électrofilé capable de contrôler la libération des modèles hydrophile et hydrophobe de médicaments. Ce système présente ainsi diffèrent profils de libération en fonction du modèle utilisé et des conditions fixées (température/pH). Le potentiel de la technique d'électrofilage ainsi que les copolymères thermo-et *pH*-sensible mis en valeur dans ce projet a indiqué que les poly(NVCL-*co*-AA) thermo-et *pH*-sensible sont des candidats prometteurs pour contrôler la libération de de médicament.

Mots-clés : thermosensible, *pH*-sensible, électrofilage, libération contrôlée, délivrance de médicament

Electrospinning of thermo-and *pH*-sensitive polymers as Potential Drug Delivery System

Marwa Sta

ABSTRACT

This project aims to obtain an electrospun membrane of poly(N-vinylcaprolactam) (PNVCL), a thermosensitive polymer, as a drug delivery system. The advantage of the use of this polymer and of the manufacturing method adopted for this application lies in the thermosensitive nature of the polymer, which could allow controlled drug release, and the high specific surface area of the membranes. Several routes have been tested to obtain these membranes.

During a first step, membranes of PNVCL and its mixtures with poly(ε-caprolactone) (PCL) were obtained. These were tested for the ability to deliver ketoprofen, a hydrophobic drug, in a controlled manner. Even if membranes were obtained, they did not exhibit the stability of morphology necessary for their use. Indeed, upon contact with water they dissolved which resulted in too rapid drug release.

In order to solve these two problems, the PNVCL was modified to obtain both thermo-and *pH*-sensitive copolymer poly(N-Vinylcaprolactam-*co*-acrylic acid) (Poly (NVCL-*co*-AA)). Two nominal compositions of this copolymer were studied, a copolymer containing 20 and another 30mol% AA. The membranes obtained were tested for their ability to encapsulate and release a hydrophobic substance, ketoprofen, and a hydrophilic substance, caffeine. Regular fibers, the diameter of which increased when the active substance was incorporated, were obtained. The results also showed that while ketoprofen lost its crystalline form when incorporated into fiber, the same was not true for caffeine. The cytotoxicity of the various membranes obtained was evaluated by cell viability tests using cell lines of MTT and mouse embryonic fibroblasts (MEF cells). The release of ketoprofen and caffeine was studied at temperatures of 25 and 42°C and at pH of 1.2 and 7.4. For ketoprofen and caffeine, the release profile showed a higher release rate for a temperature below LCST (lower critical solution temperature: temperature at which polymers undergo distinct water-soluble/non-soluble in water phase transitions) (25ºC) indicating a release based on the phenomenon of diffusion. pH has also been shown to affect the release kinetics. The results also showed that the copolymer containing 20 mol% AA was less cytotoxic to cells compared to the 30 mol% AA copolymers.

The work carried out led to the development of a novel electrospun drug delivery system able to control the release of the hydrophilic and hydrophobic models of drugs. This system thus presents different release profiles depending on the model used and the conditions set (temperature/pH). The potential of the electrospinning technique as well as the thermo-and *pH*-sensitive copolymers highlighted in this project have indicated that thermo-and *pH*-sensitive poly(NVCL-*co*-AA) are promising candidates for controlling drug release.

Keywords: thermo-sensitive, *pH*-sensitive, electrospinning, controlled release, drug delivery

TABLE OF CONTENTS

Page

LIST OF TABLES

Page

LIST OF FIGURES

Page

LIST OF ABBREVIATIONS, ABBREVIATIONS AND ACRONYMS

AA	Acrylic acid
AIBN	Azobisisobutyronitrile
AIC	Akaike Information Criterion
Caf	Caffeine
CF	Chloroforme
DE	Dissolution Efficiency
DMEM	Dulbecco's Modified Eagle Medium
DMF	Dimethylformamide
DMSO	Dimethyl sulfoxide
DSC	Differential Scanning Calorimetry
EE	Entrapment Efficiency
FTIR	Fourier Transform InfraRed
Ket	Ketoprofen
LCST	Lower critical solution temperature
MEF	Mouse Embryonic Fibroblasts
MTT	3-(4,5-dimethylthiazol-2-yl)-2,5-diphenyltetrazolium bromide
NMR	Nuclear magnetic resonance
NVCL	N-vinylcaprolactame
PAA	Poly(acrylic acid)
PBS	Phosphate buffer saline
PCL	Poly(ε-caprolactone)

PCL-*b*-PNVCL	poly(ε-caprolactone)-*b*-Poly(N-vinylcaprolactame)
PGS	Poly(glycerol sebacate) (PGS)
PNIPAm	Poly(N-isopropylacrylamide)
PNVCL	Poly(N-vinylcaprolactame)
Poly(NVCL-*co*-AA)	Poly(N-vinylcaprolactame-*co*-Acrylic Acid)
Poly(NVCL-*co*-MAA)	Poly(N-vinylcaprolactam-*co*-methacrylic acid)
PTFE	Polytetrafluoroethylene
PVA	Poly(vinyl alcohol)
PVP	Polyvinylpyrrolidone
RMSE	Root-Mean-Squared Error
SEM	Scanning Electron Microscopy
THF	Tetrahydrofuran
TFE	2,2,2-Trifluoroethanol
UCST	Upper critical solution temperature
XRD	X-ray diffraction

LIST OF SYMBOLS AND UNITS OF MEASUREMENT

SYMBOLES	
C	Concentration
ε	Conductivity
η	Kinematic viscosity
Đ	Dispersity
n	Release exponent
M_n	Number-Average Molar Mass
M_w	Weight-Average Molar Mass
K	kinetic constant
R^2	Coefficient of determination

UNITS OF MEASUREMENT	
cm	centimeter
cpm	counts per minute
cSt	centistokes
°C	Degree Celsius
g/mol kV	gramme par mole kilovolt
g	gramme
h	hour
nm	nanometer
mm	millimeter
MHz	megahertz
µL/h	microliter per hour
µm	micrometer
mL/h	milliliter per hour
mN/m	milli Newton per meter
mL	milliliter
min	minutes
ppm	parts per million
wt%	mass percentage

INTRODUCTION

The way a drug is delivered from pharmaceutical devices significantly affects its effectiveness and toxicity (Bhagwat & Vaidhya, 2013)(J. H. Lee & Yeo, 2015), for this reason, controlling the drug release at a controlled rate over a desired period is today one of the first challenges of the pharmaceutical industries (Bonnemain & Puisieux, 2005). The control of the drug release is possible using system called Drug Delivery System (DDS). These systems are based on interdisciplinary approaches that combine polymer science, pharmacies and polymer shaping (Bhagwat & Vaidhya, 2013)(Goh et al., 2013).

Polymers are widely used in drug delivery systems due to their beneficial properties and easy formation into different drug delivery devices (Srivastava et al., 2016). Current drug delivery systems, most often made from nontoxic, biodegradable, and biocompatible polymers, have limited effectiveness. Thus, stimuli-sensitive polymers, which have drawn particular attention to drug delivery systems over the past decade, would overcome the limitation of conventional polymers and therefore better control of drug release. These polymers and more precisely, the thermosensitive and pH sensitive polymers, can exhibit a changing affinity as a function of the temperature or of the *pH*. Thermosensitive polymers undergo distinct hydrophilic (water-soluble, swelling state)/hydrophobic (non-water soluble, collapsing state) phase transitions at a specific temperature: lower critical solution temperature (LCST), and upper critical solution temperature (UCST) (Chakraborty et al., 2018). Poly(N-vinylcaprolactam) (PNVCL) is one of the most popular temperature-sensitive polymers. Due to its LCST around 32ºC and its non-toxicity, PNVCL is widely used in biomedical applications include drug delivery system(Cortez-Lemus & Licea-Claverie, 2016). Depending on their chemical structure (basic or acid group) and at the suitable pH solution, the *pH*-sensitive polymers will swell or collapse (Kocak et al., 2017). Many *pH*-sensitive polymers can be designed using various electrolyte groups. The most common are weak poly-acids such as poly(acrylic acid) (PAA) collapse at low pH and swell at pH above its

pKa (Kocak et al., 2017). Furthermore, having polymers sensitive to both temperature and pH is even more advantageous.

Although, this is the goal of much research and despite the many technological advances in recent decades, drug delivery systems based on thermosensitive and pH-sensitive polymers have shown limitations. The two major limitations of these polymers are the high drug release especially at the temperature and *pH* at which the polymers swell and the loss of morphologies on contact with water due to its solubility in water. Furthermore, improving the efficiency of these systems also depends on the morphology of the structures adopted and therefore remains at the heart of the concerns for producing systems with flexible morphology and close to human body tissue.

Among the manufacturing methods commonly used to manufacture drug delivery systems, electrospinning is used for its ability to produce nano-to micro-sized fibrous structures with high specific surface area to volume and mechanical and morphological properties mimicking those of the extracellular matrix of human tissues (Persano et al., 2013). In order to overcome the problems observed with drug delivery systems, this technique could be employed for its ability to adjust the morphology of the fibers, control the thickness of the membrane and facilitate the encapsulation of the targeted drugs.

The general objective of this thesis is then to develop a new fibrous Drug Delivery System using the electrospinning process and based on the thermo-and *pH*-sensitive polymer, in order to have a better control of drug release under the effect of temperature and *pH*. To achieve this objective, three steps are put in place.

The first step consists in optimizing the electrospinning of the PNVCL and of the PNVCL blended with a hydrophobic polymer by controlling the solution and the process parameters. The idea is to obtain the fiber morphology most suitable for drug release and to assess its effect on the release of ketoprofen, a hydrophobic drug.

The second step consists in optimizing the electrospinning of a thermo-and *pH*-sensitive copolymer based on PNVCL in order to improve the stability of the morphology of the fibers in water. Two molar mass fractions of the copolymer will be studied in mixture with different concentrations of ketoprofen, a hydrophobic drug. The idea is to study the interaction between the copolymer and the drug and to assess its effect as well as the effect of temperature and pH on the release of ketoprofen.

The third and the last step consists in optimizing the electrospinning of the same two fractions of molar mass of the thermo-and *pH*-sensitive copolymer based on PNVCL in mixture with two concentrations of caffeine, a hydrophilic drug model. The idea is to study the interaction between the copolymer and the hydrophilic model and to evaluate its effect on the morphologies of the fibers and on the release of caffeine.

This thesis is divided in 5 chapters. After this introduction, chapter 1 brings an overview on drug delivery systems, thermo-and *pH*-sensitive polymers, and electrospinning process. The state of the art on electrospun membranes made from thermosensitive and *pH*-sensitive polymers for drug delivery systems is also reviewed in this first part. Following this first chapter, chapter 2 develops the objectives explored in this project. The following three chapters are copies of the papers originated from this PhD. While the first paper, chapter 3, deals with the first step of this thesis; Optimization of the electrospinning of PNVCL in blend with a hydrophobic polymer as a potential drug delivery system. The second paper (chapter 4) deals with the second step; Electrospinning of Thermo-and *pH*-Sensitive PNVCL based copolymers and evaluate it effect in the release of ketoprofen as potential drug delivery systems. Finally, the third (chapter 5) deals with the last step of the thesis; Electrospinning of Thermo-and *pH*-Sensitive PNVCL based copolymers and evaluate it effect in the release of caffeine, hydrophilic model, as a potential drug delivery system. We end up this thesis brings out the main conclusions as well as a summary of the contributions of this work and suggestions for future work.

In the annex a summary of experiments that have been performed with another system Pullulan are reported.

CHAPTER 1

LITERATURE REVIEW

1.1 Chapter outline

This literature review consists of four parts. In a first part, drug delivery systems and their importance in the drug's effectiveness are presented, then, the properties and the use of thermosensitive and *pH*-sensitive polymers in biomedical and drug release control applications are exposed. The third part describes the electrospinning technique that is the main processing technique used in this work. In particular, the impact of processing parameters on the morphology nanofibers produced using that processing method is discussed. The last part presents a state of the art on the use of electrospun membranes based on thermo-and *pH*-sensitive as drug delivery systems.

1.2 Drug Delivery System

The effectiveness of a drug is directly affected by the way it is delivered to the human body and for the last few decades lots of effort have been spent to develop a variety of Drug Delivery System (DDS) made out of different material to improve and optimize the performance of specific drugs (Lansdowne 2020; Bhagwat and Vaidhya 2013). Below, after introducing the principle of DDS, the various mathematical models which can be used to describe the kinetics of drug release are described.

1.2.1 Definition of Drug Delivery System

A Drug Delivery System (DDS) can be defined as a system composed by drugs and drug carriers designed to enable a drug release at a controlled rate over a desired period (Goh et al., 2013). This system is designed to maintain a sufficient amount of a therapeutic agent in

the body for an adequate period of time by controlling the drug release rate, in order to avoid side effects associated with unwanted fluctuations of the drug concentration in the body. As a result, this system improves the efficacy and the safety of the medicine (Zamani et al., 2013).

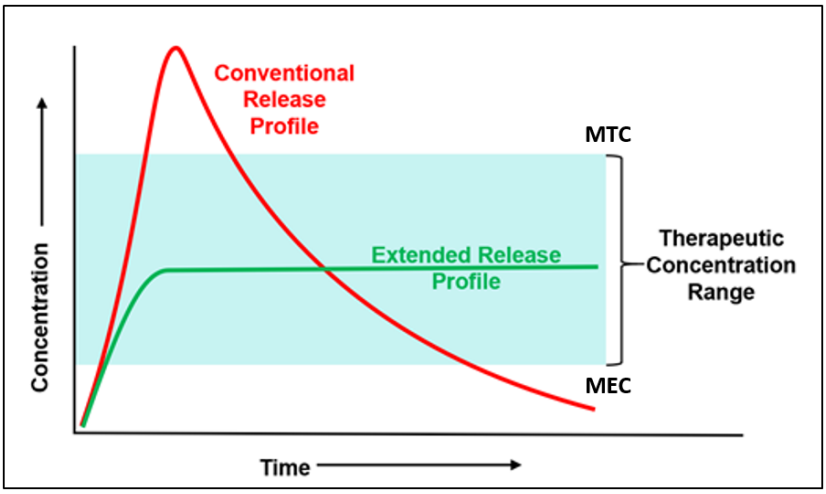

Figure 1.1 Example of drug concentration versus time for conventional and controlled release drug delivery systems

Maintaining the drug level within the therapeutic window between the minimum effective concentration (MEC) and the minimum toxic concentration (MTC), as shown in Figure 1.1, is the main objective of controlling the drug release kinetics. In particular, drug delivery systems avoid the administration of a single large dose of medication which would lead to drug level above MTC, causing toxic side effects, followed by a rapid drop below the MEC (J. H. Lee & Yeo, 2015).

Drug delivery system present several therapeutic benefits when compared to conventional or customary drug delivery systems including (Bhagwat & Vaidhya, 2013):

- Increased efficacy of the drug;
- Site-specific delivery;
- Decreased toxicity/side effects;
- Increased convenience;

- Viable treatments for previously incurable diseases;
- Potential for prophylactic applications;
- Better patient compliance.

A Drug delivery system can be described by three elements: drug routes, drug carriers and drug release mechanism. Those three elements are briefly described below.

1.2.2 Drug routes

The drug route defines the route by which drugs can be introduced into the body. Different routes can be considered and are generally classified according to their "starting point" where the drug is delivered as seen in Figure 1.2. For example, the drug can be administrated through the eyes, nose, orally or through the skin among other routes. The membranes produced in this work are intended to be used as transdermal Drug Delivery System. Transdermal drug delivery is a method of systemic drug delivery by applying a formulation (gel / cream) to the skin or applying a drug-encapsulating scaffold (dressing / patch) and which is the case of this work.

Figure 1.2 Different routes of drug delivery systems
Taken from Lansdowne (2020)

1.2.3 Drug carrier

Drug delivery systems have been used for the treatment of various diseases such as cancer therapy, transdermal systems and dressings. Depending on the disease targeted and the nature of the drug, carriers are formed and modified in various ways to achieve better control over the kinetics of drug release. As an example, for promoting wound healing and skin regeneration, many drug carrier can be adopted including liposomes, polymeric nanoparticles, inorganic nanoparticles, lipid nanoparticles, nanofibrous structures and nanohydrogels (Figure 1.3) (W. Wang et al., 2019).

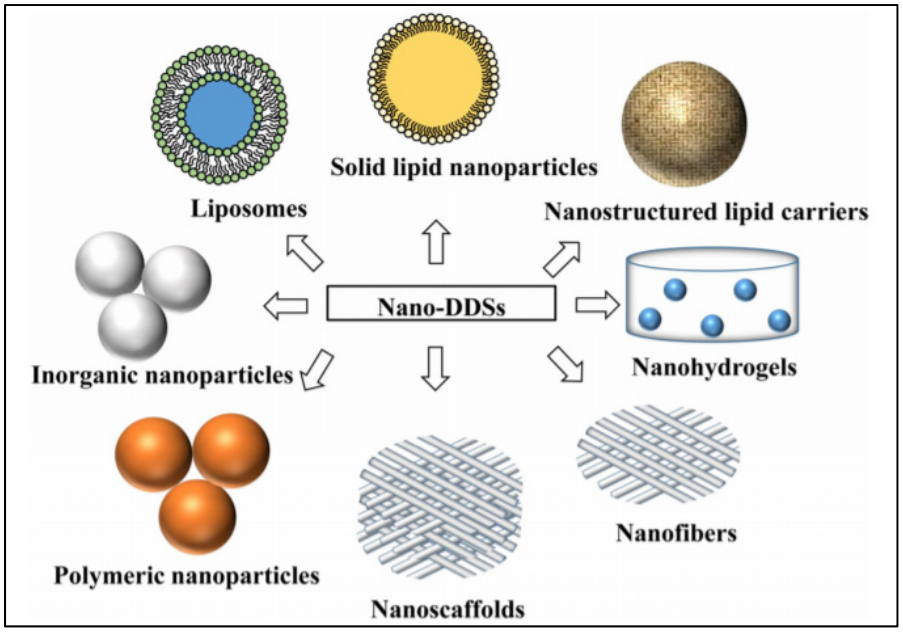

Figure 1.3 drug delivery systems in skin regeneration and wound treatment
Taken from Wang et al. (2019, p. 5)

In the case of the present work, particular attention was paid to carrier having a fibrous structure for many reasons, in particular the high surface/volume ratio, the flexibility, and the morphology very close to the morphology of the human body tissues.

1.2.4 Drug release mechanism

Several factors can influence the mechanism of drug release by the carriers and maybe the physical and/or chemical interactions between the components are the most important one. The drug release mechanism can be classified into four categories (J. H. Lee & Yeo, 2015):

- Diffusion-controlled release: the drug is first dissolved in the carrier and then diffuses through it.
- Solvent-controlled release solvent: the drug release is influenced by the solvent transport into the carrier.
- Degradation-controlled release drug: the drug release is determined by the degradation rate of the carrier.
- Stimuli-controlled release: the drug release is controlled by internal or external stimuli such as temperature and pH.

These different mechanisms will control the type of mathematical model that can be used to represent the data as shown below.

1.2.5 Mathematical models of Drug Delivery System

To study the release kinetics of a drug from a controlled release formulation, the methods can be classified into two major categories so called model-dependent and model-independent as explained below:

1.2.5.1 Model dependent methods

The model dependent methods describe the dissolution profile based on different mathematical functions which are fitted to experimental data obtained from in vitro drug

release as a function of time. The fitting parameters then provide an estimate of the effectiveness of drug delivery (Cohen, 2008)(Singhvi & Mahaveer, 2011). Some of the most commonly used are exposed in the table 1.1 below. The equations of each model present the cumulative amount of drug released versus time.

Table 1.1 The most commonly used model dependent methods to describe the dissolution profile
Taken from Singhvi & Mahaveer (2011)

Model	Equation	Systems/Remarks
Zero Order Model	$M = k.t + M_0$	Transdermal systems, Matrix tablets with low soluble drugs in coated forms
First Order Model	$M = M_0 e^{k.t}$	Water-soluble drugs in porous matrices, It is difficult to conceptualize this mechanism in a theoretical basis
Higuchi Model	$M = k.\sqrt{t}$	Insoluble matrix, Based on Fickian diffusion
Korsmeyer-Peppas Model	$M = k.t^n$	Cylindrical shaped matrices such the case of fibers
Weibull Model	$m = 1 - \exp\left[\frac{-(t)^b}{a}\right]$	This model is more useful for comparing the matrix type release profiles
Hixson-Crowell Model	$M^{\frac{1}{3}} = k.t + M_0^{\frac{1}{3}}$	Systems having a change in surface area and diameter of particles or tablets, The dissolution occurs in planes parallel to the surface of the drug and the tablet dimensions decrease proportionally
Baker-Lonsdale Model	$\frac{3}{2} \times \left[1 - (1 - M)^{\frac{2}{3}}\right] - M = k \times t$	Used to linearize of the release data from several microcapsules and microspheres formulations

M is the amount (%) of drug substance released at the time t
M_0 is the start value of M
t is the time
k is the release rate constant
n is the release exponent
m is the amount of drug released; M = 100% × m
a and b parameters describe the time dependence and the shape of the dissolution curve progression respectively

1.2.5.2 Model-independent methods

A model-independent method uses a difference factor and a similarity factor to compare dissolution profiles and calculate the dissolution efficiency (DE) represented by the equation (1.1) below:

$$DE = \left(\frac{\int_0^t M\,dt}{M_{max} \times t}\right) \times 100 \quad (1.1)$$

Where M_{max} is the maximum amount of drug released (=100%).
The difference factor calculates the percent of difference between two curves at each time point and the similarity factor is a measurement of the similarity in the percent of dissolution between two curves (Dash et al., 2010).

In general, in order to study the release model, the curve fitting of drug release data tested in vitro is used. The fitting process of the model parameters requires software such as KinetDS projects (Mendyk et al., 2012). KinetDS is curve-fitting software that describes the cumulative dissolution curve by a set of equations. The equations used are chosen from the mechanistic and empirical models (presented above) most applied to describe the drug dissolution curve (Mendyk et al., 2012). Several measure of fit accuracy are implemented to ensure the best model choice, which is based on the performance of the model on available data (Mendyk et al., 2012):

- R^2, coefficient of determination.
- AIC, Akaike Information Criterion;
- RMSE, root-mean-squared error.

The dissolution efficiency (DE) which represents the independent descriptions of the dissolution model is also automatically calculated for each available dataset (Mendyk et al., 2012). All those measures of fit accuracy are defined in the table 1.2.

Table 1.2 Independent and Dependent Kinetic Model Applied to Analyze the Drug Release Data

Approach	Method	Equation
Model-dependent	Empirical R^2	$R^2_{emp}= 1- \frac{\sum_{i=1}^{n}(yi_{obs}-yi_{pred})^2}{\sum_{i=1}^{n}(yi_{obs}-y_{AV})^2}$
	Akaike information criterion	$AIC= (2\times K) + n \times \left[\ln\left(\sum_{i=1}^{n}\left(yi_{obs} - yi_{pred}\right)^2\right)\right]$
	Root-mean-squared error	$RMSE= \sqrt{\frac{\sum_{i=1}^{n}(yi_{obs}-yi_{pred})^2}{n}}$
Model-independent	Dissolution Efficiency	$DE= \left(\frac{\int_0^t Mtdt}{Mt_{max}\times t}\right) \times 100$

yi_{obs}: observed value
yi_{pred}: model-predicted value
y_{AV}: average output value
Mt: amount of drug released at the time t
Mt_{max}: maximum amount of drug released
n: number of timepoints

In the case of matrix-type devices (fibers membrane), drug release is more likely to fit the Korsmeyer-Peppas model. The Korsmeyer-Peppas model is a Fickian diffusion driven, associating the concentration gradient to the diffusion distance. It is represented by the Equation 1.2 (Singhvi & Mahaveer, 2011)(Salome A et al., 2013).

$$\frac{M_t}{M_\infty} = kt^n \qquad (1.2)$$

Where M_t and M_∞ are the amount of drug released at an elapsed time (t) and at saturation, respectively, n is an exponent characterizing the diffusional mechanism and k is the release kinetic constant.

The n value is used to characterize different release mechanisms. For cylindrical shaped matrices such the case of fibers, an n value of 0.5 or less corresponds to a Fickian diffusion mechanism, which mean diffusion-controlled transport. For n values greater than 0.5 and less than 0.89 ($0.5 < n < 0.89$), anomalous transport (non-Fickian diffusion mechanism) is

obtained. Furthermore, in the case of n value of 0.89 and greater than 0.89 corresponds to a case-II transport mechanism super-case-II transport mechanism respectively. A case-II anomalous diffusion process is associated with controlled swelling (Singhvi and Mahaveer 2011; Dash et al. 2010; Salome A et al., 2013).

Korsmeyer-Peppas model was widely adapted and used in various drug release studies (Table 1.3).

Table 1.3 Examples of Modelling on Drug Release

Drug Carrier	Polymer	Drug model	Release model	Reference
Uniaxial fibers	Poly(NVCL-*co*-MAA)	Ketoprofen Captopril	$\frac{M_t}{M_\infty} = kt^n$	(L. Liu et al., 2016)
Hydrogel/micelle	Chitosan PVA	Aspirin Doxorubicin	$\frac{M_t}{M_\infty} = kt^n$	(Wei et al., 2009)
Microparticle	Poly(NVCL-*co*-AA)	Ketoprofen	$Mt = K_{KP}t^n$	(Medeiros et al., 2017)
Uniaxial fibers	PVA	Caffeine Riboflavin	$\frac{M_t}{M_\infty} = kt^n$	(Xiaoqiang Li et al., 2013)
Nanoferrosponges	Gelatin EDC (Carbodiimide Hydrochloride)	vitamin B12	$\frac{M_t}{M_\infty} = kt^n$	(Hu et al., 2007)
Uniaxial fibers	PDLLA	Chlortetracycline, tetracycline	$\frac{M_t}{M_\infty} = 1 - \left(1 - \frac{k_0}{C_{0L}}t\right)^N$	(Natu et al., 2010)
Coaxial fibers	PVP, HPMCAS	Paracetamol	$\frac{M_t}{M_\infty} = \left[e^{-tk_a} - e^{-tk_b}\right]$	(Tipduangta et al., 2016)
Uniaxial fibers	PLLA	Caffeine	$\frac{M_t}{M_\infty} = kt^n$	(Immich et al., 2017)

Diffusion occurs within the bulk polymer or through layers as in multilayered fibers. Several factors could affect the drug release rate:

- Polymer properties such as hydrophilicity, hydrophobicity, and biodegradability,
- Currier morphologies such as thickness and porosity,
- Drug loading locations,

- Drug solubility and stability,
- Drug-polymer compatibility and polymer-solvent-drug interactions.

In particular, drug solubility and stability are affected by the released environment condition such as temperature and *pH*. The drug release kinetics is also affected by the released environment condition and by the nature of the interaction between the polymer and the drug. For the last years, functional polymers, which change behavior according to the temperature and pH, have been developed and present interesting characteristics for drug delivery systems. In this work, special attention has been paid to thermo-and *pH*-sensitive polymers. The characteristics of those polymers and their application on drug delivery systems are presented below.

1.3 Thermo and *pH*-sensitive polymers

Stimuli-sensitive polymers are known as 'smart polymers' that may change property and dimension responding to specific stimulus (Temperature, *pH*, Electric field …) resulting from small changes in the environment (Aguilar et al., 2007).

The importance of the study of stimuli-sensitive polymers is due to the fact that their properties (water solubility, volume changes, conductivity, etc.) can be controlled by structure modification and chains organization (S.F. Medeiros et al., 2011)(A. Kumar et al., 2007)(Galaev & Mattiasson, 2008).

This work focuses on the temperature and *pH*-sensitive polymers and their most recent and relevant applications in the biomedical field in relation with drug delivery and tissue engineering. These polymers have advantages for this type of biomedical applications since they can interact directly with the temperature and *pH* changes of the body in particular in the case of tumors. Those two types of polymers are briefly described below.

1.3.1 Thermo-Sensitive Polymers

Thermo-sensitive polymers present a critical temperature at which the polymer passes from an hydrophilic polymer state to a hydrophobic polymer state (Ward & Georgiou, 2011). A small temperature change around this critical temperature causes chain extension to respond to the new adjustments of the hydrophobic and hydrophilic interactions between the polymers chains and aqueous media (Chakraborty et al., 2018).

Table 1.4 shows various thermosensitive polymers and their corresponding transition temperature.

Table 1.4 Transition temperature of thermo-sensitive polymers
Taken from Pasparakis and Tsitsilianis (2020) and Liu et al (2009)

Polymers	**Transition Temperature (°C)**
poly ((2- dimethylamino)ethyl methacrylate)	32-53
Poly(N-cyclopropymethacrylamide)	59
Poly(N-methyl-N-ethylacrylamide)	56
Poly(N-acryloylpyrrolidine)	56
Poly(N-ethylmethacrylamide)	50
Poly(N-cyclopropylacrylamide)	45.5
Poly(N-isopropylmethacrylamide)	44
Poly(N,N-diethylacrylamide)	32
Poly(N-isopropylacrylamide)	30.9
Poly(N-vinylcaprolactam)	31-34
Poly(N-n-propylmethacrylamide)	28
Poly(N-methyl-N-isopropylacrylamide) Poly(N-n-propylacrylamide)	22.3 21.5
Poly(N-methyl-N-n-propylacrylamide) Poly(N-acryloylpiperidine)	19.8 5.5

There are two types of thermosensitive polymers, the first type undergoes a reversible and rapid phase transition from a soluble configuration to an insoluble configuration in aqueous solutions at the lower critical solution temperature LCST, these types dissolve in cold water, but precipitate when the temperature of the solution exceeds the LCST. The second type

undergoes a reversible and rapid phase transition from an insoluble configuration to a soluble configuration in aqueous solutions at the upper critical solution temperature UCST. In contrast to the polymers having LCST temperature, the polymers having UCST temperature dissolve in hot water but precipitate when the temperature of the solution is lower than the UCST temperature.

LCST thermo-sensitive polymers are water-soluble polymers by making hydrogen bonds with the water molecules (Pasparakis & Tsitsilianis, 2020). The increase in temperature causes vibration of the water molecules; the displacement of the water molecules weakens the hydrogen bonds and increases the interactions between the macromolecules hydrophobic segments. Thus, the phase separation of the polymer takes place when the hydrogen bond with the water molecules becomes insufficient for the macromolecule solubility (Dimitrov et al., 2007)(S.F. Medeiros et al., 2011).

The LCST thermodynamics can be explained by the Gibbs free energy equation $\Delta G = \Delta H - T\Delta S$. For temperatures below the LCST, the formation of hydrogen bonds between the polymer chains and water molecules results in a negative enthalpy. Furthermore, the formation of hydrogen bonds between polymer and water molecules results in a negative entropy and therefore negative energy of mixing leading to dissolution. In contrast, at temperatures above the LCST, the entropy of the water in the system increases due to less ordered arrangement of water molecules (water–water associations) and predominates the enthalpy of mixture since the enthalpy is less negative due to the energy consuming to destroy the water hydrogen bonds. Therefore entropy of the system governs the LCST leading to de-mixing and phase separation (hydrophobic effect) (Q. Zhang et al., 2017)(Pasparakis & Tsitsilianis, 2020).

Figure 1.4 shows the effect of temperature on the phase transition of a thermosensitive polymer chain and on the hydrogen bonds between the polymer macromolecules and the water molecules.

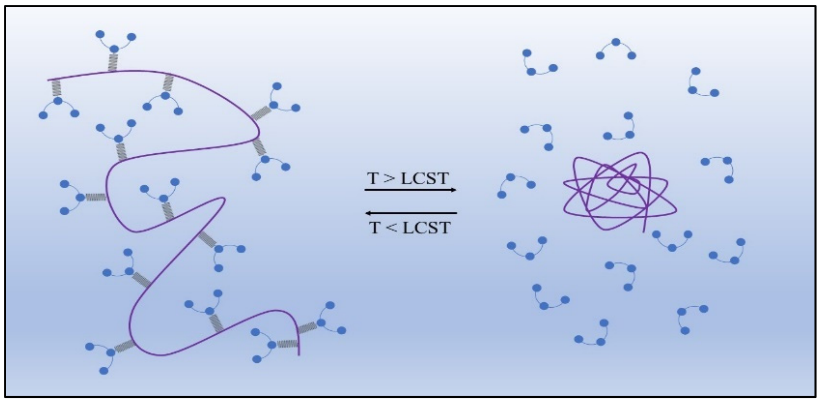

Figure 1.4 The effect of temperature on the phase transition of a thermosensitive polymer chain

This figure 1.4 shows that at temperatures below LCST, the hydrophilic part of the polymer provides hydrogen bonds with the water molecules, while increasing temperature above LCST causes weakness and breaking of hydrogen bonds and increase the interactions between the hydrophobic segments of macromolecules by forming hydrogen bonds with themselves (predomination of the hydrophobic interactions).

Some thermosensitive polymers have a critical temperature close to the physiological value such as Poly(N-isopropylacrylamide) PNIPAM (32-34ºC) (S.F. Medeiros et al., 2011) (Schmaljohann, 2006) and Poly(N-vinylcaprolactam) PNVCL (31-38 ºC) (S.F. Medeiros et al., 2011)(Cortez-Lemus & Licea-Claverie, 2016)(J. Liu et al., 2014), these polymers are the most attractive and used for biomedical applications and specially drug delivery systems. Although there are studies that have shown cytotoxicity of PNIPAM compared to the other thermosensitive polymers such as PNVCL (Vihola et al. 2008).

Poly (N-vinylcaprolactam) PNVCL has attracted more and more attention for various biomedical and biological applications. PNVCL can be used in a variety of materials such as micelles, nanogels, microgels and block copolymers, and for numerous applications such as cellular immobilization, tissue engineering, drug delivery for cancer therapy and separation

of proteins (J. Liu et al., 2014)(Zavgorodnya et al., 2017)(Cortez-Lemus & Licea-Claverie, 2016).

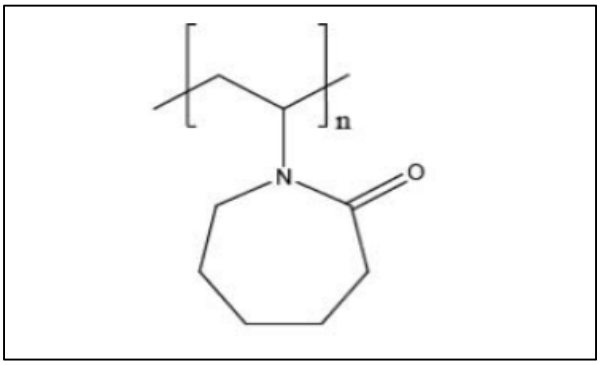

Figure 1.5 Chemical structure of PNVCL
Taken from Cortez-Lemus
and Licea-Claverie (2016)

The synthesis of PNVCL is carried out by polymerization of N-vinylcaprolactam (NVCL), which is a monomer of amphiphilic character which possesses a hydrophilic carbonyl group and a hydrophobic vinyl (lactam) group (J. Liu et al., 2014)(S.F. Medeiros et al., 2011).
Due to the direct connection of the amide group in the lactam ring to the carbon-backbone chain, in the case of PNVCL hydrolysis, a polymeric carboxylic acid builds up and small toxic amide compounds will not form and which is not the case for PNIPAM (Kozanoğlu et al., 2011)(Cortez-Lemus & Licea-Claverie, 2016). This makes PNVCL a biocompatible polymer compared to other thermosensitive polymers.

In addition to temperature sensitivity, *pH*-sensitivity can also be an interesting stimulus to control drug release of drug delivery system. The characteristics of this type of stimulus sensitive polymer will be detailed in this section.

1.3.2 *pH*-sensitive polymers

pH-sensitive polymers is another type of stimuli-sensitive polymers. Once in solution, their properties will change if the *pH* of the solution is changed (Kocak et al., 2017)(Dai et al., 2008). Due to their chemical structure, *pH*-sensitive polymers can be ionized by accepting or donating protons in response to the *pH* variation of the solutions. Having weak acid and base groups like carboxylic acids, phosphoric acid and amines, *pH*-sensitive polymers exhibit a change in the ionization state upon variation of the *pH*. This ionization can result in different structural and property changes such as surface activity, solubility, and a change in the ionization state.

There are two kinds of *pH*-sensitive polymers, *pH*-sensitive polymers which have basic monomers (having a basic groups such as -NH_2…) behave as cationic and swell under acidic conditions and polymers which have acidic monomers (having an acidic group such as –COOH,-SO_3H, etc…) behave as anionic polymer and swell at neutral and high *pH.* (Shaikh et al., 2010)(Kocak et al., 2017).

Being a polybasic or polyacid, these polyelectrolytes will accept and release protons according to the *pH* of the surrounding environment (Figure 1.6). Depending on their chemical structure (basic or acid group) and at the suitable *pH* solution, the polymer ionizes and expands because of the electrostatic repulsion generated by the polymer backbone charges. Because of the electrostatic repulsions of the generated charge along the polymer chain, the system increases its hydrodynamic volume and this could be explained by the imbalance of the ions concentration. (Kumar Thakur & Kumar Thakur, 2015).

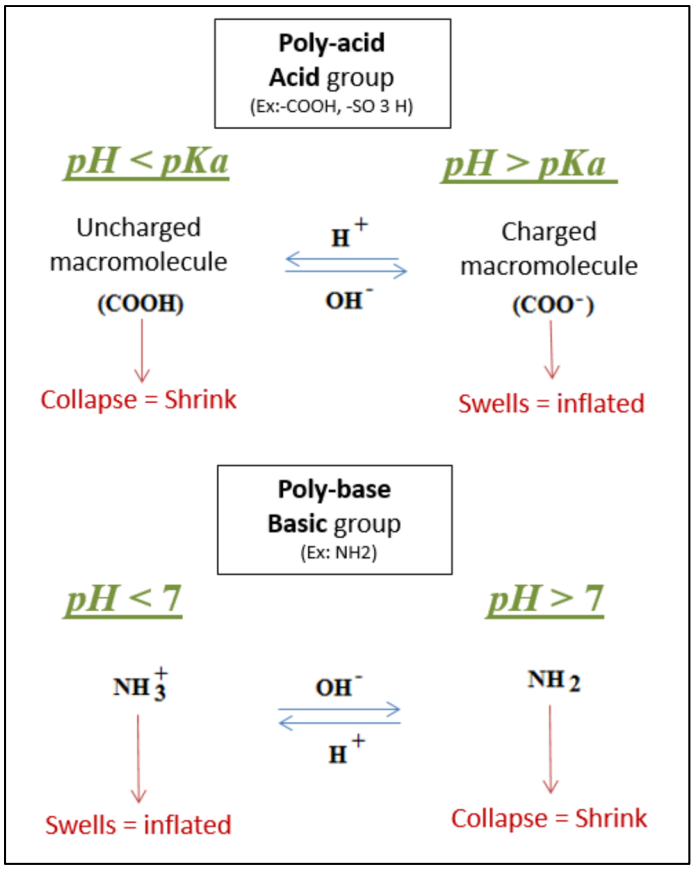

Figure 1.6 The Effect of pH on the *pH*-Sensitive poly-acid and poly-base

The classical *pH*-sensitive polymers used in biomedical application are poly(acrylic acid) (PAA), poly(methacrylic acid) (MAA) and poly(ethylacrylic acid) (PEAA) (Figure 1.7). These polymers lose acidic protons at *pH* values above their *pKa* (the hydrogen ion concentration (pH) at which 50% of the material is ionized), forming anionic polyelectrolytes and accept protons at *pH* values under *pKa*, resulting in an uncharged macromolecule (Figure 1.6)(Kocak et al., 2017).

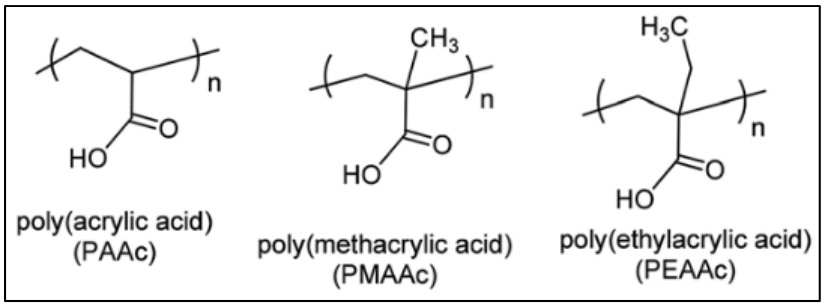

Figure 1.7 Chemical structures of *pH*-responsive poly(carboxylic acid) polymers
Taken from Kocak et al. (2017, p. 147)

Table 1.5 shows the different *pH*-sensitive polymers, their group and their abbreviation:

Table 1.5 *pH*-sensitive polymers, their group and their abbreviation
Adapted from Kocak et al. (2017, pp. 147-148)

Polymer groups	**Polymers**	**Abbreviation**
Carboxylic acid	Poly(acrylic acid) Poly(methacrylic acid) Poly(ethylacrylic acid) Poly(propylacrylic acid) Poly(4-vinylbenzoic acid) Poly(itaconic acid)	PAA PMAAc PEAAc PPAAc PVBA PIA
Phosphoric acid	Poly(ethylene glycol acrylate phosphate) Poly(vinylphosphonic acid) Poly(ethylene glycol methacrylate phosphate) Poly(4-vinyl-benzyl phosphoric acid)	PEGAP PVPA PEGMP PVBPA
Sulfuric acid	Poly(vinylsulfonic acid) Poly(4-styrenesulfonic acid) Poly(2-acrylamido-2-methylpropane sulfuric acid) Poly(3-sulfopropyl methacrylate potassium salt)	PVSA PSSA PAMPS PKSPMA
Aminoacid	Poly(aspartic acid) Poly(L-glutamic acid) Poly(histidine)	PASA PLGA PHIS
Boronic acid	Poly(vinylphenyl boric acid) Poly(3-acrylamidophenyl boronic acid)	PVPBA PAAPBA
Tertiary amine	Poly[(2-dimethylamino)ethylmethacrylate)] Poly[(2-diethylamino)ethylmethacrylate)] Poly[(2-dipropylamino)ethylmethacrylate)]	PDMAEMA PDEAEMA PDPAEMA

1.3.3 Combination of Thermo and *pH*-Sensitive Polymers

Multi-sensitive polymers are becoming more and more popular due to their various applications (Chakraborty et al., 2018). Sensitive polymers can have responses to a number of stimuli, such as *pH*, temperature, light, biomaterials, electrical field, and magnetic field. These polymers are normally the result of copolymerization of polymer segment that respond to different stimuli (Kocak et al., 2017).

In particular, polymers sensitive to both temperature and *pH* have received a lot of attention for biomedical applications and especially as Drug Delivery Systems because they can enable a more controlled drug release. By a simple combination of hydrophobic and ionizable functional groups, it is possible to obtain polymeric structures sensitive to both temperature and *pH*.

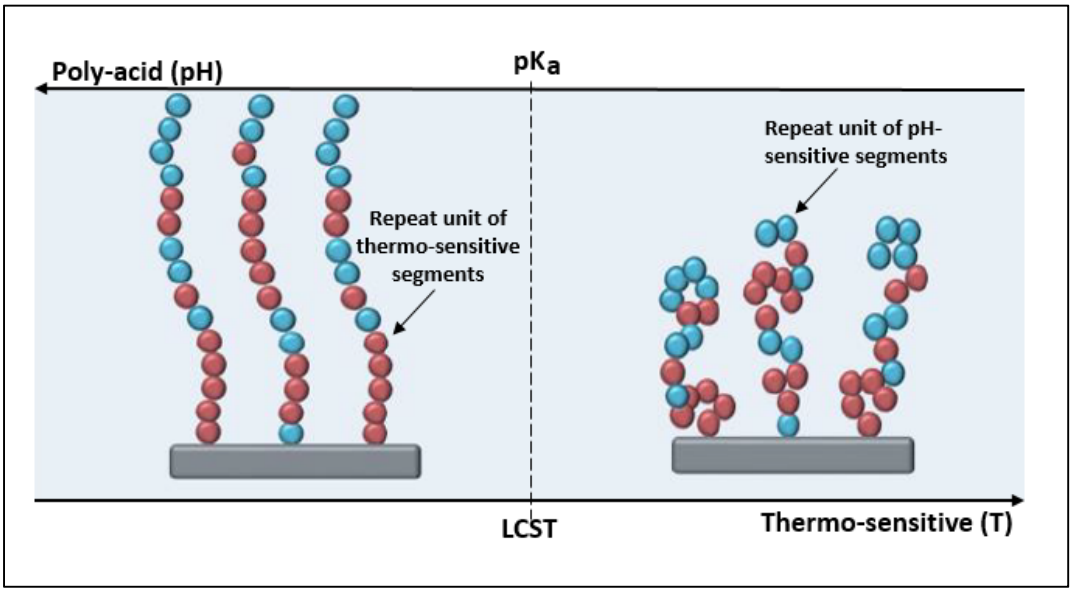

Figure 1.8 Schematic illustration of the thermo-sensitive behavior (below and above the LCST and *pH*-sensitive behavior (below and above the pKa) of thermo-and *pH*-sensitive copolymer

Figure 1.8 illustrates the behavior of a copolymer synthesized from monomers of thermosensitive polymer and monomers of poly-acid polymer to both temperature and *pH*.

Below the LCST and above the pK_a, the two temperatures and *pH*-sensitive segments are hydrophilic and swelling in the solution. Above this temperature and below the pK_a, copolymer chains become hydrophobic and collapse. Two other different situations can also appear presenting a partial collapse of the copolymer according to the temperature and *pH* of the medium Figure 1.9.

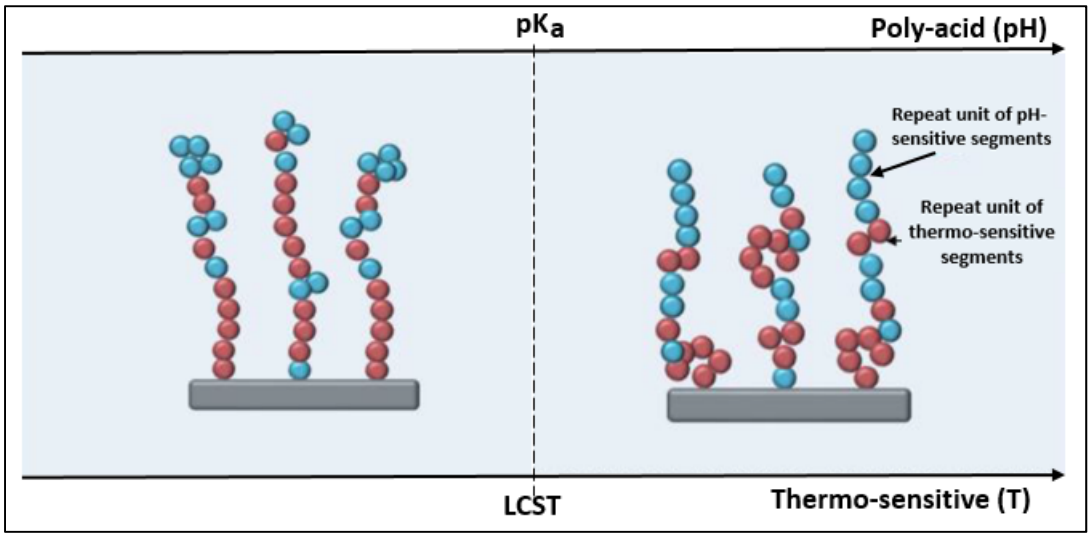

Figure 1.9 Schematic illustration of the thermo-sensitive behavior (below and above the LCST and *pH*-sensitive behavior (below and above the pKa) of thermo-and *pH*-sensitive copolymer

As we can see in the Figure 1.9, below the LCST and at acidic *pH*, the temperatures sensitive segments are hydrophilic and swelling in the solution and the *pH*-sensitive segments are collapsing. Moreover, the opposite happened at temperature above the LCST and at *pH* above the *pKa*. Some of these dual-sensitive polymers and their applications are given in Table 1.6.

Table 1.6 Thermo and *pH*-sensitive polymer system and their application

Polymers/Copolymers	System	Applications	References
Poly(N-vinylcaprolactam) (PNVCL) poly(N-vinylcaprolactam-*co*-acrylic acid) (poly(NVCL-*co*-AA))	Microparticles	Drug Delivery Systems	(Medeiros et al., 2017)
Chitosan chloride (HTCC) Glycerophosphate (GP)	Hydrogel system	Doxorubicin hydrochloride (DX) carrier	(Bin Wang et al., 2014)
Poly(N-Isoproylacrylamide) (PNIPAM) Polythylenimine (PEI)	Core-shell microgels	Drug Delivery	(Leung et al., 2005)
Poly(N-vinylimidazole-*co*-N-(1-hydroxy-3-methylbutan-2-yl)isobutyramide) P(VI-*co*-IMMA)	Copolymers	Organo-catalysts	(Bin Wang et al., 2014)
Poly(N-vinylcaprolactam) (PNVCL) Eudragit	Multicomponent membrane	Drug Delivery system	(H. Li, Liu, Williams, Wu, Wu, & Wang, 2018)
Polyethylene glycol (PEG) 4,4-Diphenylmethane diisocya-nate (MDI) Dimethylolpropionic acid (DMPA) PEG-i-MDI-DMPA	Polyurethane containing carboxyl groups	Triple-shape memory effec	(Song et al., 2016)
Carboxymethyl chitin (CMCH)	Injectable hydrogels	Drug delivery and tissue engineering	(H. Liu et al., 2016)
Cellulose nanofibrils (CNFs)	Hydrogel with biomass nanoparticles	reinforced hydrogel	(Lu et al., 2019)
N-dimethylacrylamide and N-isopropylamide N-acryl-N'-(quinolin-8-yl)thiourea (AQT) Poly(NIPAAm-*co*-DMAm-*co*-AQT)	Fluorescent polymer sensor	Selective detector of metal cations in aqueous solutions	(Y. Liu et al., 2008)

In order to lead to better drugs release control, the choice of material is a critical parameter for the drug delivery system. Further, the strategy used to incorporate the drug within the polymer is also of importance. In particular, it is important to control the localization and dispersion of the drug within the drug carriers.

In the present work, drug delivery systems were obtained in the form of flexible electrospun membranes having high surface area to volume ratio. Below the principles of electrospinning, process used to manufacture fibers, and the different techniques that can be used to incorporate drugs in electrospun fibers are presented.

1.4 Electrospinning

1.4.1 Principle of the technique

Electrospinning is a processing technique that can be used to obtain non-woven fabrics presenting many advantages for biomedical applications like artificial tissues and drug delivery systems (Kitsara et al., 2017)(Haider et al., 2015)(Haider et al., 2015). Based on electrostatic force this technique can enable the production of a membrane of fibers of various sizes, orientations, and morphologies to control the drug release through this membrane.

Typical electrospinning set-up consists of (Figure 1.10):

- A emitter, most commonly syringe, connected to a metal needle containing a polymer solution or a molten polymer;
- A pump for applying a defined flow rate to the molten polymer or solution;
- A high-voltage generator;
- A collector connected to the ground.

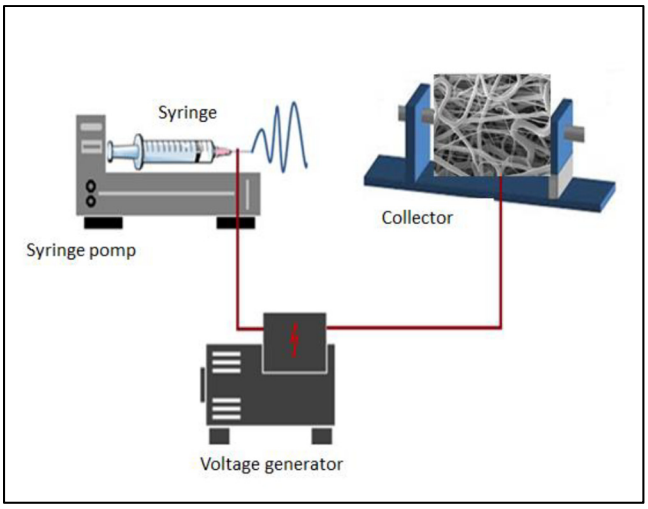

Figure 1.10 Electrospinning set up
Taken from Sta (2016, p. 5)

During electrospinning, the application of an electric field between the needle tip and the collector, using the high-voltage generator, causes the induction of charges in the polymer and results in repulsive interactions in the solution. This electrostatic force is then opposed to the surface tension of the solution (B.-S. Lee et al., 2014). When the electric force or charge repulsion overcomes the surface tension of the solution, a cone such as the one shown Figure 1.11, known as Taylor's cone, forms and a jet is then projected in the direction of the collector. During the flight of this jet, the solvent of the solution evaporates and the fibers are deposited on the surface of the collector(Haider et al., 2015)(Cheng et al., 2017)(Sarabi-Mianeji et al., 2015).

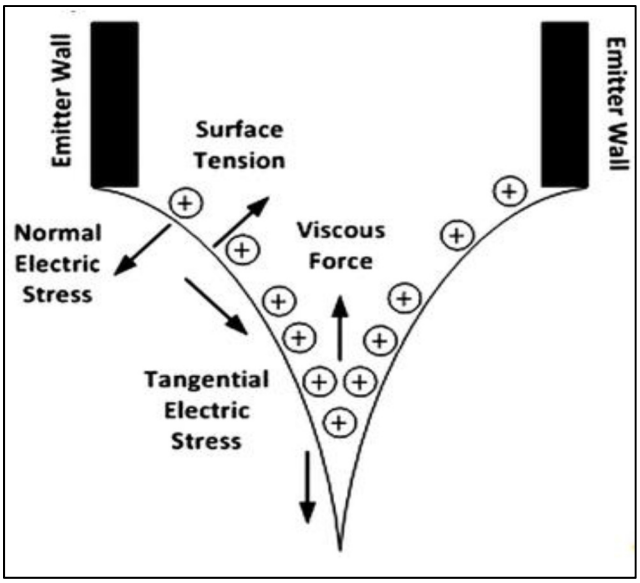

Figure 1.11 Force distribution on the liquid cone–jet based on the leaky dielectric model
Taken from Wu et al. (2012, p.4151)

1.4.2 Electrospinning Parameters

In general, all soluble polymers can be electrospun by controlling the physico-chemical parameters of the polymer solution (viscosity, surface tension, electrical properties), process parameters (electric field, needle/collector distance, flow rate, etc.) and environmental parameters (temperature, humidity) (Haider et al., 2015). All of these parameters affect directly the morphologies and the diameters of the fibers (Zamani et al., 2013).

In the following parts, a detailed presentation of the solution and process parameters of the electrospinning process and their effect in the fiber morphology will be presented.

1.4.2.1 Solution parameters

1.4.2.1.1 Viscosity

The viscosity of the polymer solution plays an important role in the electrospinning process. It is the critical key to have or not a fiber and to control the diameter and the morphology of fibers. The viscosity should be high enough to avoid breaking the polymer fibers into fragments before reaching the collector under the application of the electric field and overcome the surface tension of the solution to avoid creating pearls (Haider et al., 2015).
Generally, the viscosity of the solution can be controlled directly by adjusting the molecular weight and/or the solution concentration. Equation 1.3 shows the relationship between viscosity, concentration and molar mass of a polymer (Gupta et al., 2005).

$$C^* \sim \frac{1}{[\eta]} = \frac{1}{K M^a} \tag{1.3}$$

Where C* is the critical concentration of the solution (concentration for which the solution is electrospinnable), [ŋ] is the intrinsic viscosity, m is the average viscosimetric molar mass and a and K are constants that depend on the polymer, solvent and Temperature (taken from (Gupta et al., 2005))

1.4.2.1.2 Surface Tension

Surface tension is an important factor influencing the morphology of electrospun products. Indeed, the balance between viscosity and surface tension controls whether fibers or beads are obtained. Hence, an increase of surface tension increases the probability of obtaining beads. During the electrospinning process and with the application of the electric charges, the polymeric solution will charge, and the reciprocal repulsion of charges will produce a force that opposes the surface tension. This causes the formation of the Taylor cone, and ultimately

the resulting jet flows in the direction of the electric field to the collector (Haider et al., 2015).

1.4.2.1.3 Solvent properties

Two properties of the solvent are paramount to electrospinning: the electrical properties and the vapor pressure. The solution conductivity is mainly determined by the solvent. When choosing the solvent(s) to dissolve the polymer, it is essential that this solvent present a certain degree of conductivity. High conductivity solutions have a high surface charge density and are therefore more easily electrospun. In fact, with a highly conductive solution, the application of the electric field increases the elongation force on the jet which is caused by the self-repulsion of the excess charges on the surface (Khoo & Koh, 2016).

In general, high conductivity solution increases the charge of the droplet to form Taylor cone and yield smaller fibers diameters (Haider et al., 2015). When conductivity is not high enough, some researchers have shown that doping the solution with organic salt generates the total reduction or elimination of pearls (Teo, 2012).

The volatile nature of the solvent makes it possible to control the formation of pores on the surface of the fibers during the electrospinning process (Khoo & Koh, 2016).

1.4.2.2 Process parameters

1.4.2.2.1 Electric field

The electric force is the main factor in the electrospinning process because it affects the amount of charge applied to the solution. Apply a high electric field to the polymer solution (melt polymer) deforms the polymeric droplet into a conical shape (Taylor cone) from which nanofibers will emerge to the collector (Haider et al., 2015). For a given needle/collector distance the increase of the applied voltage, which means increase of the electric field, during

the electrospinning produces ultrafine fibers due to the increased traction intensity on the solution jet (Teo, 2012)(D. Li & Xia, 2004). However, some studies have shown that increasing the electric field could lead to an increase in the diameter of the fibers or the formation of multiple fibers of smaller diameter (Figure 1.12) (C. Zhang et al., 2005)(Teo, 2012).

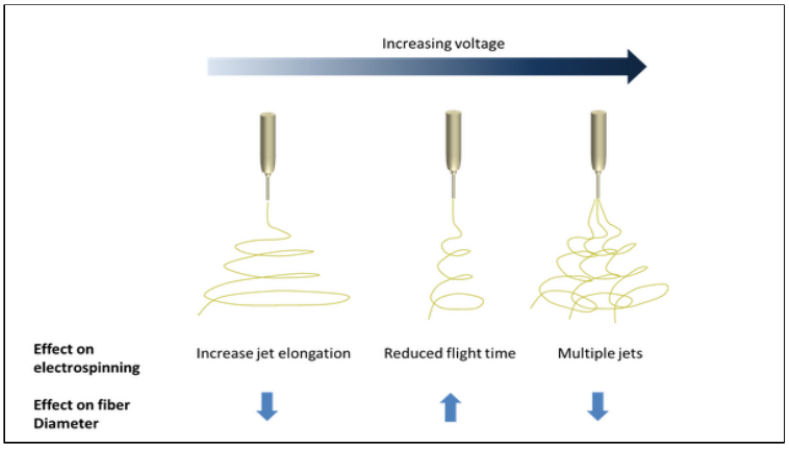

Figure 1.12 Effects of voltage increase on the diameter of electrospun fibers
Taken from Teo (2012, p.2)

1.4.2.2.2 Flow rate

The flow rate of the polymer solution inside the syringe is another important parameter of the electrospinning process. Generally, a low flow rate is most recommended to have enough time for polarization of the polymeric solution(C. Zhang et al., 2005). However, a balance must be kept between the rate of flow of the solution in the syringe and the rate of dispensing or ejection of the jet through the tip of the needle during electrospinning (Teo, 2012).

1.4.2.3 Environmental parameters

Electrospinning environment parameters such as humidity and temperature can also affect the fibers diameters and morphology. Low humidity can completely dry some type of solvent and increase the rate of its evaporation. On the contrary, high humidity will lead to the formation of thick fibers having fairly large diameters (Bhardwaj & Kundu, 2010). Furthermore, the environmental humidity can act as nonsolvent for system, which leads to the formation of surface porosity (Figure 1.13) (Rezabeigi et al. 2017).

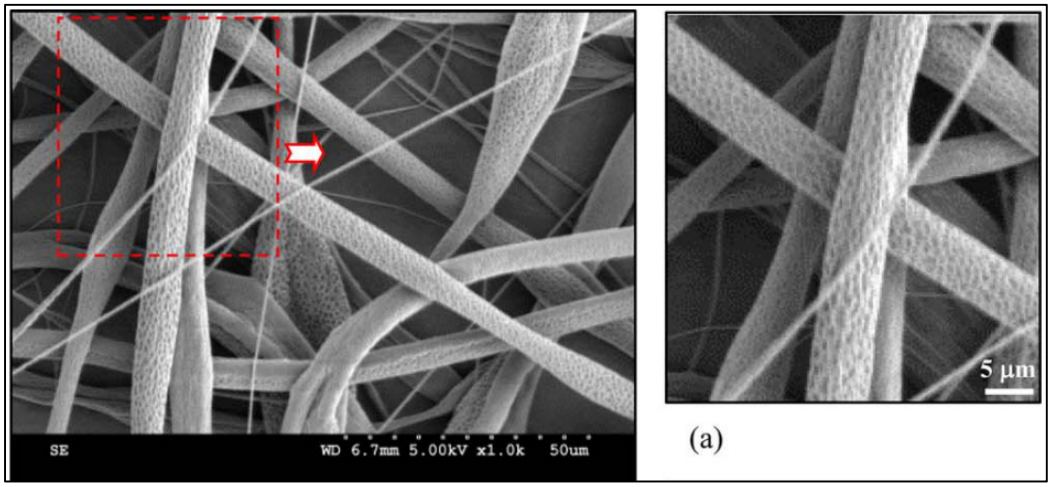

Figure 1.13 SEM images of the fibers in the early stages of electrospinability
Taken from Rezabeigi et al (2017, p. 44862)

A summary on the effect of certain parameters on the diameters and morphologies of the fibers are referenced in Table 1.7 below.

Table 1.7 Effect of the electrospinning parameters on the diameter and morphology of the fibers

Parameters		**Effect on the fibers diameter and morphology**
Solution	Viscosity	Increase fibers diameters Increase the uniformity of the fibers Too Low : no fibers/ beaded fibers Too High: no fibers/rubber like fibers
	Surface tension	Too high: beaded fibers
	Electrical conductivity/ solvent volatility	Decrease fibers diameters Low volatility: humid fibers High volatility: porous fibers
Process	Electric field	Increase/Decreases fibers diameters
	Flow rate	Increases fibers diameters Too Low: discontinuous fibers Too high: beaded fibers
	Collector-needle distance	Decreases fibers diameter Too low/high: beaded fibers/ no fibers
	Needle diameter	Increase fibers diameter
	Collector form	Fiber orientation (aligned fibers)
Environmental condition	Humidity	Porous fibers
	Temperature	Decreases fibers diameters

Other variants of the classic electrospinning technique exist, such as coaxial electrospinning, co-electrospinning, melt electrospinning and emulsion electrospinning.

In our project, we are particularly interested in the electrospinning process. This method of manufacturing nonwoven matrices has several advantages for biomedical applications, including ours. In the following part, the application of this process on a drug delivery system will be discussing.

1.5 Electrospinning for Drug Delivery System

Electrospinning process is extensively used in controlled drug release, due the ease of a process operation, the cost-effectiveness, the high fibers surface to volume ratio, the membrane flexibility and the high encapsulation efficiency of the obtained fiber (L. Liu et al., 2016)(Zamani et al., 2013). Different drugs can be incorporated into electrospun fibers: antimicrobial, anticancer drug and bioactive molecules such as protein using different

incorporation methods (Zamani et al., 2013)(Bochu Wang et al., 2010)(Yu et al., 2015)(H. Li, Liu, Williams, Wu, Wu, Wang, et al., 2018).

Various methods can be adopted for incorporating the desired therapeutic agents into electrospun fibers considering the specific requirements of the diseases and the wide variety of characteristics of the drug, such as stability and solubility. The most popular drug incorporation techniques will be discussed here.

1.5.1 Solution blending

Blending the therapeutic agent with the electrospun polymer solutions is perhaps the simplest, most popular, and predominant method of incorporating drugs into electrospun fibers. This method consists of dissolving or dispersing the drug into the polymer solution to obtain an encapsulated drug by a single-phase electrospinning process. However to achieve the desired results, certain requirements must be taken into consideration such as (Zamani et al., 2013):

1.5.1.1 Drug localization and distribution into electrospun fibers

Drug localization into the fiber highly affects the drug release from the fiber. Having drugs located in the surface of the fiber results to high drug release rate especially in the case of fast-dissolving model such as caffeine. Contrariwise, good distribution of the drug inside the fibers leads to stable a sustained drug release rate, since the drug molecule must travel through the thickness of the fiber to diffuse through it.

1.5.1.2 Fiber morphology

The fiber morphology affects the drug release rate as well as the drug localization and distribution. First, the diameter of the fibers reflects the distance that the drug molecules must travel to reach the delivery medium. Second, having non-homogeneous fiber diameters results in unstable drug release. Finally, the presence of pearls can also affect the distribution and localization of the drug and, consequently, the rate of drug release.

1.5.1.3 Polymer physicochemical properties

Regardless of the carriers and the morphology of the carriers, each drug has its own physicochemical properties which can define its degree and method of diffusion and its interaction with the carriers.

1.5.1.4 Drug Crystallinity

In general, amorphous substances dissolve more easily in an aqueous medium; however, prolonged dissolution of the amorphous drug can be expected because the amorphous drug will be well dispersed in the fibrous matrices.

1.5.1.5 Polymers-Drug interaction

The polymer-drug interaction is quite possibly the interaction that most affects the drug release rate. Because this interaction effects directly and indirectly all the property discussed previously. Good polymer-drug interaction can be reflected in better distribution of the drug inside fibers in the amorphous state and in the formation of fibers with homogeneous morphology.

1.5.1.6 Drug hydrophobic-hydrophilic properties

Being a hydrophobic or hydrophilic drug will certainly affect the rate of drug release. Generally, for the same release medium and the same carrier properties, a high release rate is always expected from a hydrophilic drug.

1.5.2 Surface modification

The second most used method for functionalizing fibers with therapeutic agents is the surface modification of the electrospun fibers. This technique involves binding or conjugating the surface of the fibers by therapeutic agents or biomolecules in a way that the release of the therapeutic agents would be attenuated. However, this technique is recommended when a slow and sustained release is required such as genes or growth factors because the chemical immobilization of the target molecules on the surface generates an attenuated release (Sun et al., 2013) (Zamani et al., 2013)(J. Jiang et al., 2014).

1.5.3 Coaxial electrospinning process

Coaxial electrospinning is a modified version of the electrospinning technique, allowing the production of fibers with core-shell fiber morphology. With the coaxial electrospinning, two solutions are used and electrospun simultaneously through co-concentric design needles (one needle inside the other) and the shear stress generated by the shell solution in the core cause the formation of core-shell fibers (B.-S. Lee et al., 2014).

Using this modified electrospinning process in biomedical applications presents many advantages. Through this technique, the polymer used for the shell could contribute to the sustained release of the therapeutic agent and play an essential role in protecting the agent and the cells located in the core of the fiber from direct exposure to the biological environment (Figure 1.14) (Perez & Kim, 2015).

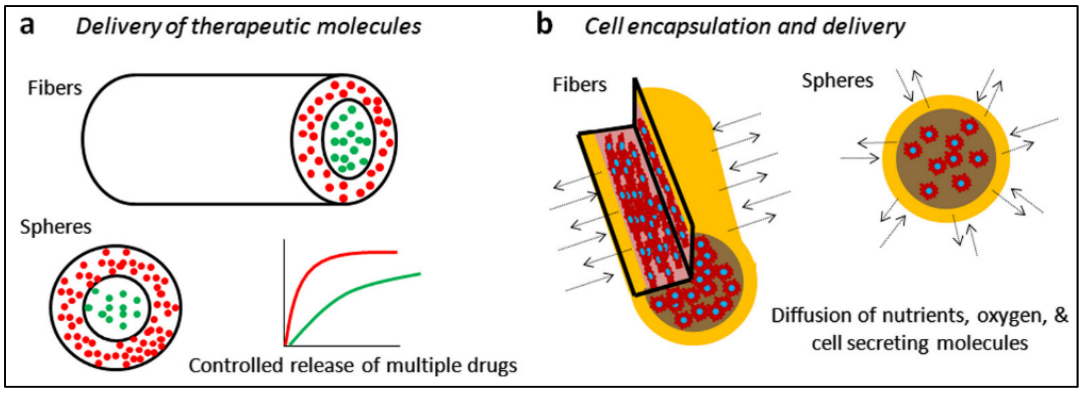

Figure 1.14 (a) Illustration of the general features of core-shell designs that are useful for the delivery of therapeutic molecules and (b) for the cell encapsulated tissue engineering
Taken from Perez and Kim (2015, p. 3)

Numerous articles have used the electrospinning technique as a manufacturing process for drug delivery systems. Research on the 'Web of science' shows that since 2000 over 1000 articles have been written on the subject. Below two examples of the most relevant paper of electrospun drug delivery system of each drug incorporation techniques (Table 1.8) (Goh et al., 2013).

Table 1.8 Examples of the application of electrospinning process in drug delivery systems and its drug incorporation method

Papers	**Polymers**	**Additives**	**Drug incorporation method**	**References**
Preservation of FGF-2 bioactivity using heparin-based nanoparticles, and their delivery from electrospun chitosan fibers	Chitosan	Heparin-Polyelectrolyte complex nanoparticles (PCNs) Fibroblast growth factor (FGF-2)	Surface modification	(Zomer Volpato et al., 2012)

Papers	Polymers	Additives	Drug incorporation method	References
MMPs-responsive release of DNA from electrospun nanofibrous matrix for local gene therapy: In vitro and in vivo evaluation	Polycaprolactone(PCL) - Polyethylene glycol(PEG) block copolymers	Deoxyribonucleic acid (DNA)	Surface modification	(Kim & Yoo, 2010)
Chitosan–bacterial nanocellulose nanofibrous structures for potential wound dressing applications	Chitosan Poly(ethylene oxide) (PEO)	Bacterial nanocellulose (BNC)	Coaxial electrospinning	(Ardila Nelson; Arkoun ,Mounia; Heuzey,Marie-Claude; Ajji,Abdellah; Panchal,Chandra J., 2016)
Fabrication of chitosan-polycaprolactone composite nanofibrousscaffold for simultaneous delivery of ferulic acid and resveratrol	Chitosan Polycaprolactone (PCL)	Resveratrol ferulic acid	Coaxial electrospinning	(Poornima & Korrapati, 2017)
Fast dissolving paracetamol/caffeine nanofibers prepared by electrospinning	Polyvinylpyrrolidone (PVP)	Paracetamol caffeine	Solution blending	(Illangakoon et al., 2014)
Electrospun polyvinyl-alcohol nanofibers as oral fast-dissolving delivery system of caffeine and riboflavin	Polyvinyl alcohol (PVA)	Caffeine riboflavin	Solution blending	(Xiaoqiang Li et al., 2013)

1.6 Application of thermo-and *pH*-sensitive polymer membrane on Drug Delivery System

In view of the interesting properties of thermo-and *pH*-sensitive polymers and the electrospinning process for biomedical applications and especially drug delivery system, several studies of drug delivery system and tissue engineering have been carried out.

On the 'Web of science' there are around 50 articles reported on this topic. The following table shows some examples of the most relevant applications of these polymers and copolymers membranes in drug delivery systems and tissue engineering.

Table 1.9 Examples of the application of Thermo and *pH*-sensitive polymer fibers membranes in drug delivery systems and tissue engineering

Papers	**Polymers/ Additive**	**Processing methods**	**Purpose**	**Referen-ces**
Dual temperature and *pH* responsive nanofiber formulations prepared by Electrospinning	Ethyl cellulose (EC) PNVCL Eudragit KET : ketoprofen (drug)	Blend electrospin-ning	Demonstrates that multicomponent membrane composed by fibers of (PNVCL/EC/KET) blend and fibers of (Eudragit/ KET) blend comprises effective and biocompatible materials for targeted drug delivery	(H. Li, Liu, Williams, Wu, Wu, Wang, et al., 2018)
Bioactive thermoresponsive polyblend nanofiber formulations for wound healing	PNIPAM Gati (antibacterial drug) EA : egg albumen	Blend electrospin-ning	Electrospinning of thermosentive polymer membrane for drug delivery and wound healing applications	(Pawar et al., 2015)
Tunable Thermo-Responsive Poly(Nvinylcaprolact am) Cellulose Nanofibers: Synthesis, Characterization, and Fabrication	PNVCL Carboxylic acids Cellulose acetate (CA)	Blend electrospin-ning	Electrospinning of PNVCL, PNVCL-COOH (synthesis polymer) and PNVCL/CA (blend) nanofibers membranes have potential applications in developing affinity membranes.	(Webster et al., 2013)
Controlled release from thermo-sensitive P(NVCL-*co*-MAA) electrospun nanofibers: The effects of hydrophilicity/hydro phobicity of a drug	Poly(N-vinylcaprolactam-*co*-methacrylic acid) captopril (hydrophilic drug) ketoprofen (hydrophobic drug)	Electrospin -ning process	Controlled release of hydrophobic/hydro phillic drug from thermo-sensitive P(NVCL-*co*-MAA) electrospun nanofibers	(L. Liu et al., 2016)

Papers	Polymers/ Additive	Processing methods	Purpose	Referen-ces
Thermo-sensitive drug controlled release PLA core/ PNIPAM shell fibers fabricated using a combination of electrospinning and UV photo-polymerization	PLA (dichloromethane) PNIPAM (cross-linked with MBA in deionized water) Combretastatin A4 (CA4)	Electrospin ning of PLA and followed by PNIPAM the UV photo-polymerizat ion of NIPAM	drug loaded core–shell fibers membrane to control drug release	(H. Zhang et al., 2015)
Fabrication of PVCL-co-PMMA nano fibers with tunable volume phase transition temperatures and maintainable shape for anti-cancer drugs release	Poly(NVCL-*co*-MMA) (MBA cross linker and varied amounts of MMA) PNVCL (free radical polymerization) Erlotinib (anti-cancer drugs)	Electrospin ning technique	Thermo-responsive nano fibers for drug delivery applications that could maintain shapes after heating–cooling cycles	(Yu et al., 2015)
Preparation of a thermo- and *pH*-sensitive nanofibrous scaffold with embedded chitosan-based nanoparticles and its evaluation as a drug carrier	poly(NIPAAm-*co*-N-methylolacrylamide) (PNN) Chitosan Doxycycline hyclate (drug)	Electrospin ning technique	Controlled release of hydrophilic drug from thermo-and pH sensitive nanofibrous	(C. H. Huang et al., 2014)
Poly(N-isopropylacrylamide) /polyurethane core–shell nanofibres by coaxial electrospinning for drugs controlled release	Poly(N-isopropylacrylamide) polyurethane nifedipine (drug)	Coaxial electrospin ning technique	core–shell fibers membrane to control drug release	(Lin et al., 2016)

After an extensive review of the literature, the two major limitations or problem of thermosensitive polymers problem were identified.

- The high drug release especially at temperature below the LCST. (Yu et al., 2015) (Cortez-Lemus & Licea-Claverie, 2016) (Medeiros et al., 2017).

- The stability of the fiber morphology in contact with water after the electrospun of thermosensitive polymers (Yu et al., 2015)(C. H. Huang et al., 2014).

Reducing the drug release at temperature below the LCST can be possible using thermo-and *pH*-sensitive copolymer such as poly(NVCL-*co*-AA) or a thermo-and *pH*-sensitive polymers blend such as PNVCL/Eudragit (Simone F. Medeiros et al., 2017) (Li, Liu, Williams, Wu, Wu, Wang, et al., 2018).

In their study, Medeiros et al. showed that higher release rates of ketoprofen were obtained from PNVCL microparticles when compared to poly(NVCL-*co*-AA) copolymer microparticles for temperatures below the LCST (25ºC) (Simone F. Medeiros et al., 2017). Figure 1.15 illustrates the results obtained by Medeiros et al. It can be seen that the incorporation of acrylic acid within the molecule (red and green curve) result in a decrease of drug release most likely due to the interaction of the drug, in this case ketoprofen, with the acrylic acid.

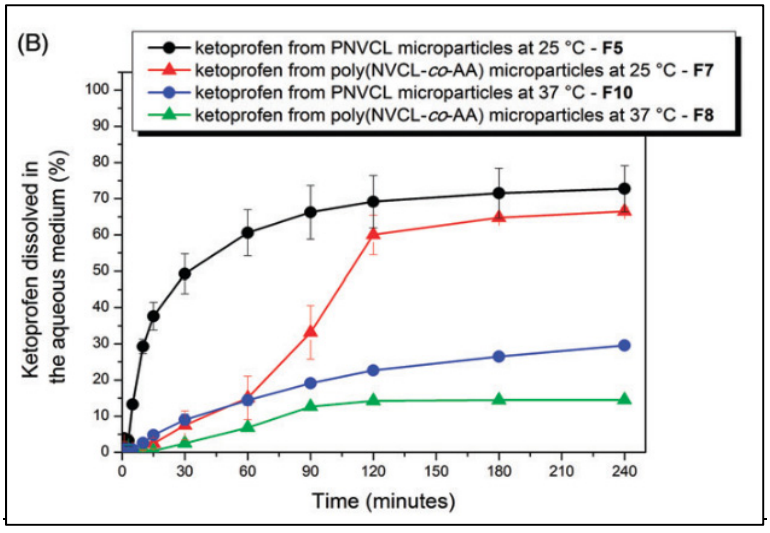

Figure 1.15 In vitro release of ketoprofen from PNVCL and poly(NVCL-*co*-AA) microparticles (pH 7.4)
Taken from Medeiros et al. (2017, p. 23)

In another study, Li et al. simultaneously electrospun two polymers; a thermo-sensitive polymer (PNVCL) with a *pH*-sensitive polymer (Eudragit) to formulate a hybrid mats (H. Li, Liu, Williams, Wu, Wu, Wang, et al., 2018). Encapsulating ketoprofen in the two electrospun solutions and evaluating its release shows a decrease of the ketoprofen release by changing the *pH* of the releasing media for temperature below the LCST (25ºC) (Figure 1.16)(H. Li, Liu, Williams, Wu, Wu, Wang, et al., 2018). It can be seen that, a greater extent of release was observed at pH 7.4 than at 4.5, and at temperature below the LCST (25°C) than at temperature above the LCST (37 °C) (H. Li, Liu, Williams, Wu, Wu, Wang, et al., 2018).

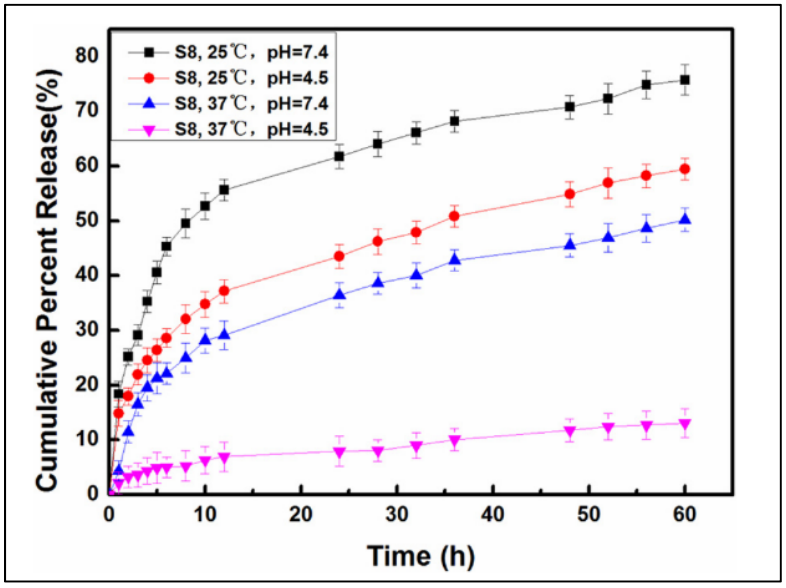

Figure 1.16 In vitro KET release profiles from the hybrid electrospun fiber mats of Eudragit/Ket blend and PNVCL/EC/Ket blend (S8)
Taken from Li et al. (2018, p. 147)

In other research, Lin et al. were able to control the release of hydrophilic drug (captopril) in blend with PNVCL base copolymer Poly(N-vinylcaprolactam-*co*-meth acrylic acid) (Poly(NVCL-*co*-MAA)). The electrospinning solutions were prepared by adding Poly(NVCL-*co*-MAA) with different molecular weights to a mixture of methanol and dimethylacetamide (DMAC) at a ratio of 85:15 (v:v). The captopril powder was added into

the Poly(NVCL-*co*-MAA) solution under continuous stirring to give a final drug concentration of 20 mg/ml. The same thing was also done using hydrophobic drug (ketoprofen) in order to compare its release. The release test of these drugs at 20ºC (temperature below LCST) and 40ºC (temperature above LCST) demonstrated that drug release was faster at temperatures below and above the LCST with hydrophilic drugs (Figure 1.17 b and d). These could be explained by the hydrophobic interaction that prevents the drug dissolution and the hydrophilic interaction facilitates the drug dissolution (L. Liu et al., 2016).

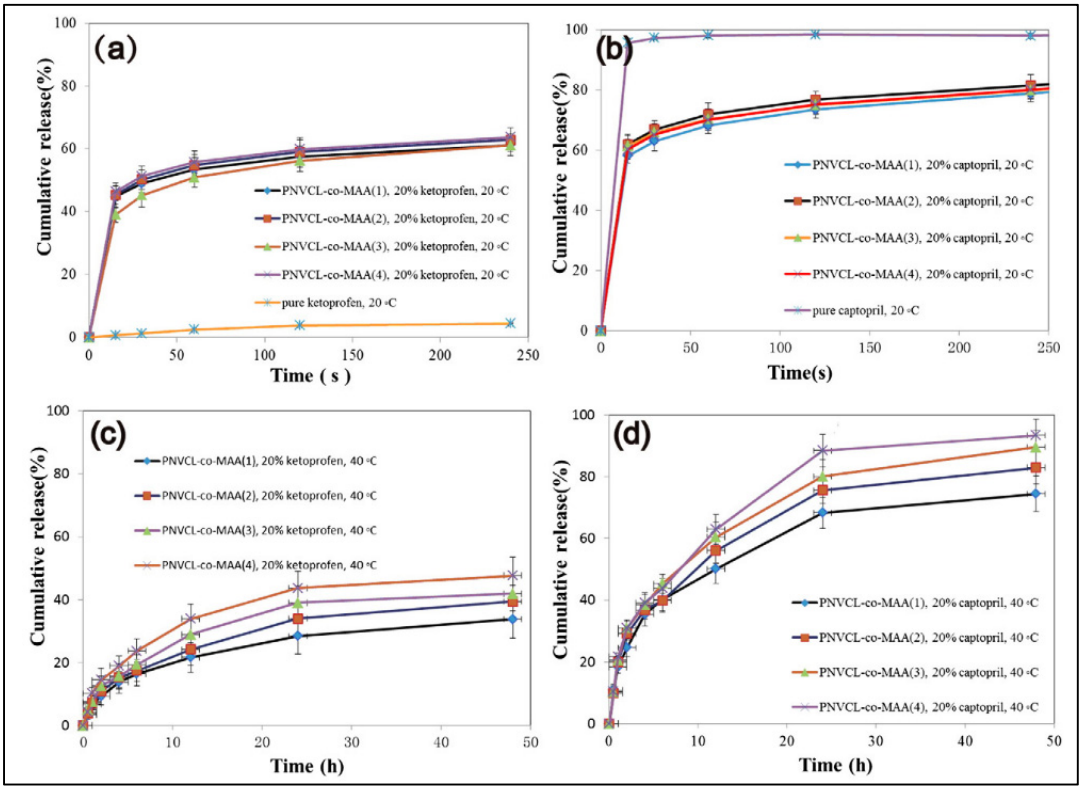

Figure 1.17 Drug release profile patterns for (a) ketoprofen at 20°C, (b) captopril at 20°C, (c) ketoprofen at 40°C, and (d) captopril at 40°C from the Poly(NVCL-*co*-MAA) fibers.
Adapted from Liu et al. (2016, p.587)

For the problem of stability of the fiber morphology in contact with water after the electrospun of thermosensitive polymers, in the case of PNVCL, this problem could be solved by changing the homopolymer by a copolymer obtained by the copolymerization of NVCL with Methyl methacrylate (MMA). In their study Yu et al. shows that the Poly(NVCL-*co*-MMA) copolymer membrane could keep the fibers morphology in contract with water compared to PNVCL membrane which totally dissolved in water (Figure 1.18 a and c). In the synthesis of Poly(NVCL-*co*-MMA), 2% of MBA crosslinker and varied amounts of MMA (the amount of MMA was a variant in proportion to PNVCL that ranging from 5% to 30%) were added, when the reaction time of the synthesis of PNVCL reached 12 h (Yu et al., 2015).

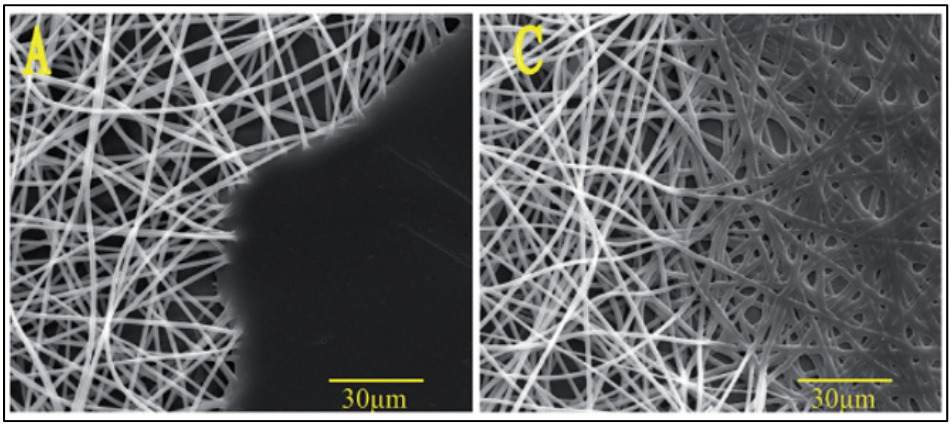

Figure 1.18 Morphology of nonwoven mats with partially dripping of a drop of water; (A) pure PVCL; (C) Poly(NVCL-*co*-MMA) (MMA to NVCL of 20%).
Adapted from Yu et al. (2015, p.64947)

The improvement of the fibers morphology stability in contact with water also results in better and stable drug release especially at temperature below the LCST (25ºC) (Figure 1.19).

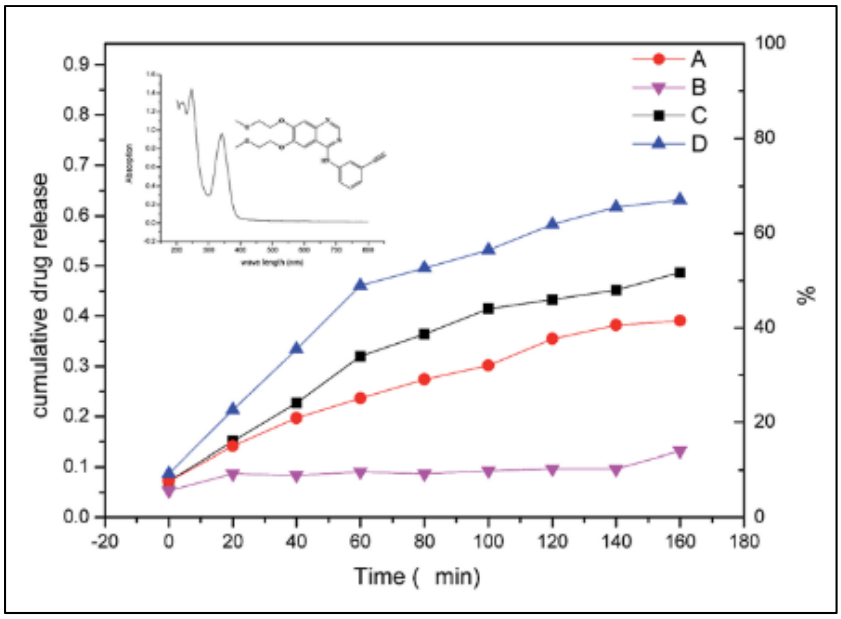

Figure 1.19 (A) Erlotinib release loaded Poly(NVCL-*co*-MMA) nanofiber at 25ºC; (B) drug release of Erlotinib loaded Poly(NVCL-*co*-MMA) nanofiber at 39ºC; Adapted from Yu et al. (2015, p.64948)

In their research, Huang et al. demonstrated that using PNIPAm based copolymer; poly(NIPAAm-*co*-N-methylolacrylamide) (PNN) also help the electrospun scaffolds to retain their fibrous structures after being soaked in water (Figure 1.20).

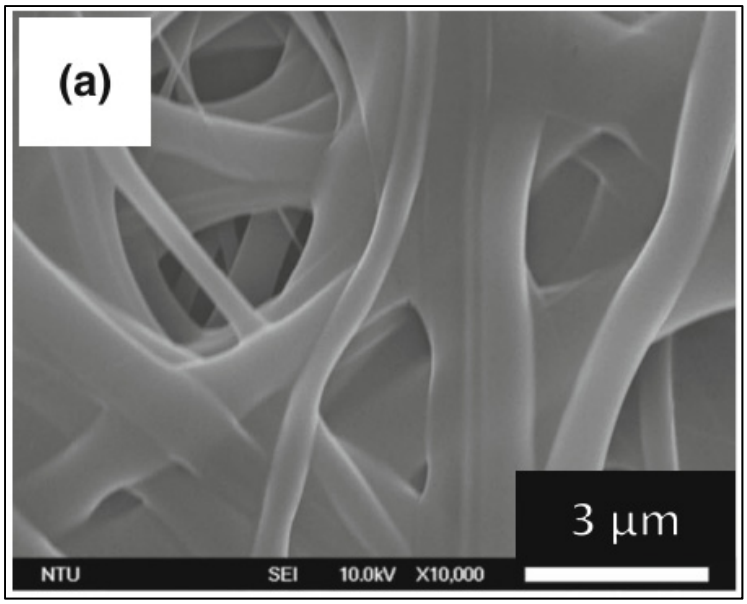

Figure 1.20 The SEM images of the soaked scaffolds of pure PNN
Taken from Huang et al. (2014, p. 2505)

In addition, electrospun PNN in blend with chitosan result to manufacture of nanofibers sensitive to both temperature and *pH* and achieve prolonged doxycycline hyclate (an antibiotic used to treat a variety of infections) release at different temperatures and *pH* values (Figure 1.21) (C. H. Huang et al., 2014).

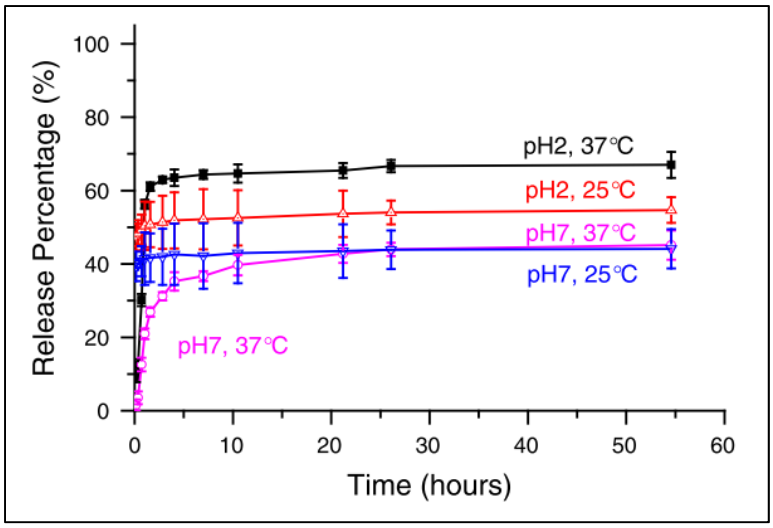

Figure 1.21 Drug release profiles of doxycycline hyclate from the PNN/Chitosan scaffold in aqueous solutions at different temperatures and pH
Taken from Huang et al. (2014, p. 2508)

1.7 Conclusion

This doctoral project concerns the development of new thermo and *pH*-sensitive fibrous scaffolds by electrospinning to be used as a drug delivery system.

Despite extensive research in the field of electrospinning of thermosensitive polymers for drug release control applications, except that these applications have several limitations, and the goal of this project is to overcome these limitations to produce a drug delivery system with morphology close to the morphology of human tissues and able to control the release of various types of drugs under the effect of changes in temperature and *pH*.

CHAPITRE 2

OBJECTIVES

2.1 General objective

The general objective of this thesis is to develop a new fibrous Drug Delivery System using the electrospinning process and based on thermo-and *pH*-sensitive polymers, in order to encapsulate hydrophobic, ketoprofen, and hydrophilic, caffeine, drug models and ensure a better control of their release under the effect of temperature and *pH*.

To achieve this objective, three steps are put in place to meet three sub-objectives.

2.2 First objective

Objective: Design and optimize the electrospinning of thermosensitive polymer (PNVCL) fiber structures and evaluate their potential as a drug delivery system, able to encapsulate and control the release of hydrophobic drugs (ketoprofen).

Operational objectives:

- Optimize the electrospinning of PNVCL and PNVCL blended with a hydrophobic polymer (PCL) by controlling the solution and the process parameters.
- Determine the effect of PNVCL electrospinning and its blend on the LCST temperature and the hydrophilicity of the electrospun membranes.
- Encapsulate 10%wt of ketoprofen in the fibers and evaluate its entrapment efficiency.
- Analyze the ketoprofen release profiles using independent and model-dependent (curve fitting) methods and determine the mechanism of its release.

2.3 Second objective

Objective: Assess the potential of a thermo-and *pH*-sensitive copolymer based on PNVCL as an electrospun drug delivery system, able to improve the stability of the fiber morphology in water and control the release of hydrophobic drugs (ketoprofen).

Operational objectives:

- Optimize the electrospinning of the thermo-and *pH*-sensitive copolymers Poly(NVCL-*co*-AA) with two molar mass fractions by controlling the solution and the process parameters.
- Encapsulate three ketoprofen concentrations and determine their effect on the fibers morphology, the LCST temperature, and the hydrophilicity of the electrospun membranes.
- Study the copolymer-ketoprofen interaction and the drug crystallinity once encapsulated in the fibers.
- Evaluate the cytotoxicity of the different obtained fibers by cell viability assays (MTT) and mouse embryonic fibroblasts cell lines (MEF cells).
- Measure the ketoprofen encapsulation efficiency and analyze its release profiles using independent and model-dependent (curve fitting) methods in different temperature and *pH* conditions.

2.4 Third objective

Objective: Assess the potential of a thermo-and *pH*-sensitive copolymer based on PNVCL as an electrospun drug delivery system, able to improve the stability of the fiber morphology in water and control the release of hydrophilic drug model (Caffeine).

Operational objectives:

- Optimize the electrospinning of the thermo-and *pH*-sensitive copolymer Poly(NVCL-*co*-AA) with two molar mass fractions by controlling the solution and the process parameters.
- Encapsulate two caffeine concentrations and determine their effect on the fibers morphology and the LCST temperature of the electrospun membranes.
- Study the copolymer-caffeine interaction and the caffeine crystallinity once encapsulated in the fibers.
- Evaluate the cytotoxicity of the different obtained fibers by cell viability assays (MTT) and mouse embryonic fibroblasts cell lines (MEF cells).
- Measure the caffeine encapsulation efficiency and analyze its release profiles using independent and model-dependent (curve fitting) methods in different temperature and *pH* conditions.

CHAPITRE 3

DESIGN AND CHARACTERIZATION OF PNVCL-BASED NANOFIBERS AND EVALUATION OF THEIR POTENTIAL APPLICATIONS AS SCAFFOLDS FOR SURFACE DRUG DELIVERY OF HYDROPHOBIC DRUGS

Marwa Sta,[1] Graziele Aguiar,[1,2] Abilio A. J. Forni,[2] Simone F. Medeiros,[2] Amilton M. Santos,[2] Nicole R. Demarquette*[1]

[1] Department of Mechanical Engineering, École de Technologie Superieure (ÉTS) 1100 rue Notre-Dame Ouest, Montréal, Québec, Canada H3C1K3
[2] Department of Chemical Engineering, Escola de Engenharia de Lorena, Universidade de São Paulo, , USP, Lorena, SP, Brazil

Paper published in Journal of Applied Polymer Science, December 2019

3.1 Chapter outline

This first published article responds to the first step to attend the objective of the doctoral project; optimizing the electrospinning of the PNVCL and of the PNVCL blended with a hydrophobic polymer by controlling the solution and the parameters of the process. The study of the effects of fiber mixtures and morphology on the release of ketoprofen, a hydrophobic drug, is also part of this article. Finally, the ketoprofen release behavior was analyzed using independent and model-dependent approaches.

3.2 Abstract

In this work, nanofiber scaffolds for surface drug delivery applications were obtained by electrospinning poly(N-vinylcaprolactam) (PNVCL) and its blends with poly(ε-caprolactone) and poly(N-vinylcaprolactam)-b-poly(ε-caprolactone). The process parameters to obtain smooth and beadless PNVCL fibers were optimized. The average fibers diameter was less

than 1 μm, and it was determined by scanning electron microscopy analyses. Their affinity toward water was evaluated by measuring the contact angle with water. The ketoprofen release behavior from the fibers was analyzed using independent and model-dependent approaches. The low values of the release exponent ($n<0.5$) obtained for 20 and 42ºC, indicating a Fickian diffusion mechanism for all formulations. Dissolution efficiencies (DEs) revealed the effect of polymer composition, methodology used in the electrospinning process, and temperature on the release rate of ketoprofen. PNVCL/poly(N-vinylcaprolactam)-b-poly(ε-caprolactone)-based nanofibers showed greater ability to control the in vitro release of ketoprofen, in view of reduced kinetic constant and DE, making this material promising system for controlling release of hydrophobic drugs.

Keywords: Drug delivery systems; Fibers; Stimuli-sensitive polymers.

3.3 Introduction

Electrospinning is a technique that can be used to produce micro- to nano-sized polymer fibers (Beachley & Wen, 2010; Bhardwaj & Kundu, 2010; Persano et al., 2013). Basically, an electrical field is applied to a polymer solution or melt that is fed at a continuous low volumetric flow rate through a metallic emitter. Due to a balance between electrostatic forces and surface tension, the polymer solution or melt is projected on a grounded surface in the form of fibers that form a mesh with a structure that depends on the type of the collector used. The obtained polymeric nonwoven structures can then be employed in several applications such as filtration membranes (Xiaohu Li et al., 2015; Huang et al., 2003), wound- healing tissue (Pawar et al., 2015), medical prostheses (Sell et al., 2009), scaffolds for tissue regeneration(W.-J. Li et al., 2007), and drug delivery (Heyu et al., 2018; Zavgorodnya et al., 2017; L. Liu et al., 2016; Zamani et al., 2013; Kenawy et al., 2009), among others. In the latter case, drugs are entrapped in the fibers electrospinning polymer solutions to which the drug was previously added. The rate at which the entrapped drug will

be delivered will then depend on the mesh and fiber morphology as well as on the affinity between the drug and the polymer (H. Jiang et al., 2005).

Smart or stimulus-responsive polymers have recently attracted lots of attention of academics and scientific community due to the interesting properties they present (J. Liu et al., 2014; Kumar et al., 2007). Basically, this type of polymer has the ability of changing its properties in response to environmental changes. These can be temperature, pH values, light, and electrical or magnetic field (S.F. Medeiros et al., 2011). Thermoresponsive polymers, which can change conformation, once in solution, upon a change of temperature, are probably the most suitable for biomedical applications. This is especially the case when this change of conformation occurs at temperatures close to the physiological temperature (Shengtong & Peiyi, 2011). Some of these thermosensitive polymers consist, for example, of a hydrophobic–hydrophilic balanced chain structure, which changes conformation, once in aqueous solution, according to the temperature. Below a specific temperature known as "Lower Critical Solution Temperature" [LCST] (J. Liu et al., 2014; Shengtong & Peiyi, 2011), the polymer is in an extended conformation; above this temperature, the polymer collapses. At temperatures below the LCST, the polymer is hydrophilic, whereas it becomes hydrophobic at temperatures above the LCST, turning these polymers extremely interesting candidates for drug delivery applications. Research for the development of thermosensitive polymers has led to the synthesis of polymers such as Poly(N-ethylacrylamide), poly(N-acrylopiperidine), poly(N-isopropylacrylamide) (PNIPAM), and poly(N-vinylcaprolactam) (PNVCL) to name a few (S.F. Medeiros et al., 2011). PNVCL, which presents an LCST around 32^{o}C (J. Liu et al., 2014), is an interesting thermosensitive polymer as differently from most smart polymers; it is nonionic, water soluble, and nontoxic compared with other thermosensitive polymers like PNIPAM, making it a good candidate for drug delivery applications (Vihola et al., 2005). Besides, it can be blended with other biocompatible and bio- degradable polymers in order to control its hydrophilicity LCST and processability (Wu et al., 2014). In this work, PNVCL as well as PNVCL/poly(ε-caprolactone) (PCL) and PNVCL/poly(N-vinylcaprolactam)-b-poly(ε-caprolactone) (PNVCL-b-PCL) blends were

electrospun to obtain membranes to be used in drug delivery applications. Both these polymers were chosen due to their biocompatibility, which was previously reported in our group (Medeiros et al., 2016; Medeiros et al., 2017). Due to its long degradation time, biocompatibility, and biodegradability, PCL was extensively used in medical application such as bone regeneration, drug delivery, and tissue engineering (Qin & Wu, 2012; Romeo et al., 2007). It is also known to be an easy polymer to electrospun. The objective of this work was therefore to study the electrospinability of PNVCL and blends of PNVCL/PCL and PNVCL/ PNVCL-b-PCL in order to control the fibers and mesh morphologies, and to investigate the possibility of encapsulating a and releasing drug using the obtained fibers and the effect between making a blend or a block copolymer with PCL in the degree of drug release. In addition, the effect of blending and electrospinning on the LCST and the hydrophobicity of the obtained meshes were evaluated.

3.4 Experimental

3.4.1 Materials

The polymers used in this study, PNVCL, PCL, and PNVCL-b-PCL, were synthesized and characterized as described below. For PNVCL syntheses, we used N-vinylcaprolactam monomer (NVCL, 98%, Sigma-Aldrich, São Paulo, Brazil, distilled at 110ºC under vacuum), 2,20-azobisisobutyronitrile initiator (AIBN, 99%, kindly supplied by BASF, purified by recrystallization in ethanol), and standard internal trioxane (99%, Sigma-Aldrich, São Paulo, Brazil), without further purification. The polymerization was carried out in 1,4-dioxane (99.8%, Sigma-Aldrich, São Paulo, Brazil, distilled over $LiAlH_4$ under vacuum). Finally, chloroform-d (99.8%, Sigma-Aldrich, São Paulo, Brazil) was used for determination of the monomer conversion by ^{1}HNMR analyses. For the synthesis of PCL, we used ε-caprolactone monomer (CL, 99%, Sigma-Aldrich, São Paulo, Brazil), pentanol initiator (98%, Merck, São Paulo, Brazil), tin ethanoate catalyst ($Sn[EH]_2$, 99%, Sigma-Aldrich, São Paulo, Brazil), and the solvent toluene (99,5% Synth, São Paulo, Brazil), all used as received. PNVCL-b-PCL

was synthesized using ring opening polymerization from hydroxyl-terminated PNVCL-OH, which was obtained using NVCL, AIBN, mercaptoethanol (98%, Synth, São Paulo, Brazil, as received), and 1,4-dioxane. For the synthesis of the block copolymer, we used $Sn(EH)_2$ as catalyst and toluene as solvent. All reagents were used as received. Distilled water, ethanol, and chloroform (CF) from Sigma Aldrich were used as solvents during the electrospinning process.

3.4.2 Methods

Synthesis and Characterization of PNVCL, PCL, and PNVCL-b-PCL. PNVCL was synthesized via free-radical polymerization, as previously described by Medeiros et al.(Medeiros et al., 2010) Appropriated amount of NVCL was dissolved in 100 mL of 1,4-dioxane and flushed with N2 for 20 min at a moderate gas flow rate. A solution of AIBN in 20 mL of the solvent was also prepared and flushed for 10 min. When the temperature reached 70ºC, the polymerization was initiated through the addition of the AIBN solution to the polymerization medium. The reaction was carried out in a 250- and 100-mL, respectively, glass double-wall reactor under nitrogen atmosphere. The experimental conditions are listed in Table 3.1.

Table 3.1 Experimental Conditions Used for the Synthesis of PNVCL and PCL

Run	**Monomer**	**[Mon]: [Initiator](mol)**	**[Mon]: [CTA](mol)**	**[Mon]: [Catalyst](mol)**
R1	NVCL	1: 0.015	1: 0.02	-
R2	E-CL	1: 0.02	-	1: 0.03

PCL was synthesized via ring-opening polymerization, by adding the monomer (ε-CL), the initiator pentanol, and the catalyst $Sn(EH)_2$ at the ratio listed in Table 3.1, in 20 mL of

toluene. The reaction mixture was purged with N_2 for 20 min and then heated at 100ºC in an oil bath for 12 h.

The block copolymer PCL-b-PNVCL was synthesized by ring-opening polymerization of ε-caprolactone, following the methodology suggested by Wu et al. (Wu et al., 2014) in 2014. For this synthesis, a hydroxyl-terminated PNVCL-OH was required, and for its preparation, 15 g of NVCL and 0.45 g of mercaptoethanol were dissolved in 140 mL of 1,4-dioxane. The reaction medium was degassed with N_2 for a period of 20 min, and when the temperature reached 70ºC, 0.15 g of AIBN was added. The reaction was carried out for a period of 5 h in a jacketed glass reactor. The obtained material was then precipitated in ice-cold hexane and dried under vacuum for 24 h at 35ºC. For the synthesis of PCL-b-PNVCL, the previously synthesized PNVCL-OH and the monomer ε-CL were dissolved in 40 mL of toluene at a molar proportion equivalent to 1:68. The concentration of Sn(EH)2 tin etanoate catalyst was set at 1% relative to the molar ratio of the monomer. Thereafter, the medium was degassed with N2 and heated to the temperature of 105ºC. The reactions happened for a period of 32 h. The copolymers were precipitated twice in ice cold ethyl ether and dried under vacuum for 24 h at 35ºC (1).

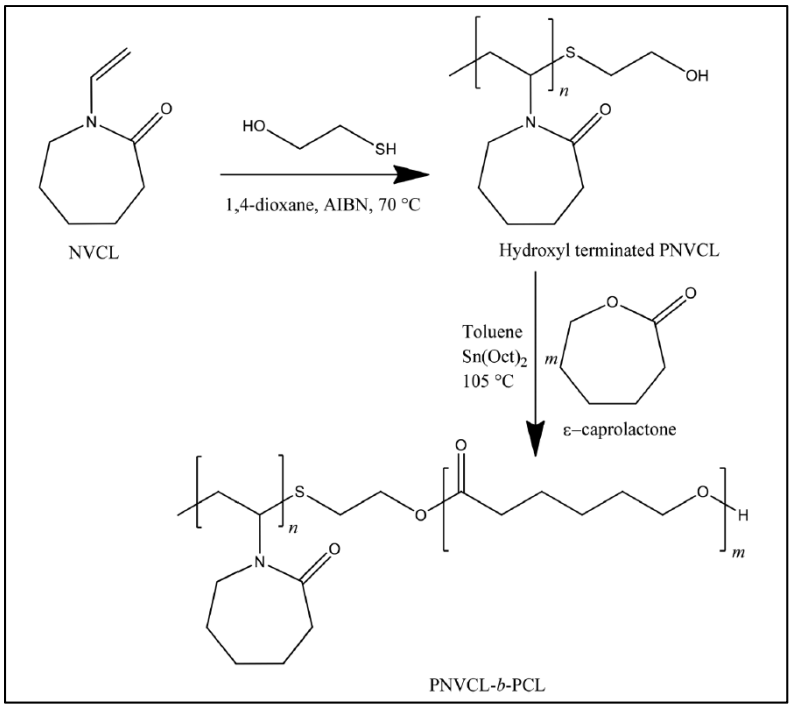

Figure 3.1 Synthesis of PCL-b-PNVCL block copolymer via ring opening polymerization from hydroxyl terminated PNVC

Electrospinning. The electrospinning device used in the present work consisted basically of three elements: (1) a 10-mL syringe, with a stainless steel needle, containing the polymer solutions, assembled on a digital syringe pump (PHD Ultra 4400, Harvard Apparatus) to control the flow rate of delivered solution, (2) a high-voltage power supply SL40*150 (Spellman) used to charge the needle, and (3) a collector consisting of an aluminum paper covered metallic plate. This device was used to electrospun PNVCL, PNVCL/PCL, PNVCL/PCL-b-PNVCL blends, and polymers solutions containing ketoprofen as follows.

PNVCL. Aqueous and ethanol PNVCL solutions with concentrations varying from 15 to 45-wt % polymer were prepared dissolving PNVCL powder in distilled water and ethanol, respectively, using a magnetic stirrer for 4 h.

The influence of processing parameters on the electrospinability, regularity, and size of the fiber was evaluated. Electric field was varied from 66 to 166 kV/m while keeping the flow rate at 33 μL/min and the working distance between the needle and the collector at 15 cm, and flow rate was varied from 5 to 50 μL/min while keeping the electric field at 100 kV/m and working distance at 15 cm. Different distances between the syringe tip and the collector, 10 and 25 cm, were also evaluated while keeping the electric field and the flow rate at 100 kV/m and at 33 μL/min, respectively.

PNVCL/PCL. 75/25 PNVCL/PCL blends were electrospun in four different forms:

As suspensions of that obtained after synthesizing PCL in aqueous solutions of PNVCL: for that, 1.5 g of PNVCL was dissolved in a homogeneous suspension of PCL prepared by dispersing 0.5 g of the polymer in 2.8 mL of distilled water at room temperature (21ºC) for 3 h on a stirrer.

As suspensions of electrosprayed PCL in aqueous solutions of PNVCL: for that, an electrosprayed PCL powder was obtained by electrospraying 1 g of PCL in 3 mL of acetone with 100 kV/m as an electric field, 50 μL/min flow rate and 15 cm working distance. 1.5 g of PNVCL was dissolved in a homogeneous suspension of PCL electrosprayed powder prepared by dispersing 0.5 g of obtained PCL in 2.8 mL of distilled water at room temperature (21ºC) for 3 h on a stirrer.

As aqueous suspension of PNVCL/PCL blend previously obtained by solution blending in CF: for that, 2 g of the mixture 75/25 PNVCL/PCL was dissolved in 3 mL of CF. After drying for 48 h, the mixture was fragmented and dispersed in 2.8 mL of distilled water at room temperature (21ºC) for 6 h on a stirrer.

As CF solution of the PNVCL/PCL blend: for that, 1.5 g of PNVCL and 0.5 g of PCL were dissolved in 2 mL of CF at room temperature (21ºC) for 30 min on a stirrer. CF was chosen as a solvent for the fourth blend, because CF is a good solvent to dissolve both PNVCL and PCL.

All blends contained 25-wt % PCL. All solutions to be electrospun contained 42-wt % solid. The resulting suspensions and solutions were electrospun into 18-gauge stainless steel

needle. The processing parameters used for electrospinning were 100-kV/m electric field, 33-μL/min flow rate, and 15-cm working distance.

PNVCL/PNVCL-b-PCL. Solutions in a mixture of ethanol/tetrahydrofuran (1:1.2) containing 42 wt % of 75/25, 50/50, 25/75, and 0/100 of PNVCL/PNVCL-b-PCL blends were also electrospun.

The resulting solutions were electrospun into 21-gauge stainless steel needle. The processing parameters used for electrospinning were 100-kV/m electric field voltage, 20-μL/min flow rate, and 15-cm working distance.

Ketoprofen entrapment. Solutions containing 10% ketoprofen and 42 wt % PNVCL, 42 wt % 75/25 PNVCL/PCL, and 42 wt % 25/75 PNVCL/PNVCL-b-PCL blends were obtained. Ethanol and ethanol/tetrahydrofuran (depending of the polymer blend) were used as a solvent to enable the incorporation of ketoprofen within the fibers as it is not soluble in water. The solutions were prepared as follows:

PNVCL/Ketoprofen: 2 g of PNVCL and 0.2 g of ketoprofen were dissolved in 3.5 mL of ethanol at room temperature (23ºC) for 1 h using a magnetic stirrer.

PNVCL/PCL/Ketoprofen: for that, two homogeneous solutions of blend were prepared, one using as obtained after synthesis PCL and the other one using electrosprayed PCL. 1.5 g of PNVCL, 0.4 g of PCL, and 0.2 g of ketoprofen was dissolved in 3.5 mL of ethanol at room temperature (23ºC) for 1 h on a stirrer.

PNVCL/PNVCL-b-PCL/Ketoprofen: 0.4 g of PNVCL, 1.5 g of PNVCL-b-PCL, and 0.2 g of ketoprofen were dissolved in 3.5 mL of ethanol/tetrahydrofuran (1:1.2) at room temperature (23ºC) for 1 h on a magnetic stirrer.

The resulting solutions were electrospun into a 21-gauge stainless steel needle. The processing parameters used for electrospinning were 100 kV/m electric field, 33 μL/min flow rate, and 15 cm working distance.

3.5 Characterization

The polymers were characterized in terms of chemical composition by nuclear magnetic resonance (^{1}H NMR) in a Varian Oxford instrument operating at a frequency of 300 MHz. Thermal analyses were performed using a Shimadzu differential scanning calorimetry (DSC) DGT-60 instrument. The temperature ranged from −10 to 200ºC with a controlled heating of 10ºC/min. The instrument was calibrated using indium as standard. The weight of each sample was approximately 5–10 mg. The polymer molar masses were determined by size-exclusion chromatography. Dried samples were diluted in THF at a concentration of 5 mg/mL, and filtrated through a 0.45-mm pore-size PTFE membrane before analysis. The separation was carried out using a modular system comprising a 1515 Isocratic HPLC Pump (Waters) and an autosampler 717Plus (Waters).

Three columns [two PLgel 5 μm Mixed C (300 × 7.5 mm2) and one PLgel 5 μm 500 Å (300 × 7.5 mm2)] thermostated at 40ºC were used with THF as an eluent at a flow rate of 1 mL/min. The setup was equipped with Waters 2414 refractive index (RI) detector. The average molar mass (number-average molar mass, M_n, and weight-average molar mass, Mw) and the dispersity ($Đ = M_w/M_n$) were derived from the RI signal by a calibration curve based on poly(methyl methacrylate) standards (Sigma-Aldrich). The thermal sensitivity of PNVCL homopolymer was evaluated by UV–visible analyses at 570 nm, using Genesys 10 Series spectrophotometers. The polymer concentration in solution was 5 mg/mL. The light intensity through the solution was measured as a function of temperature. The transmittance measurements were performed from 28 to 42ºC with an increase of 1ºC. The transition temperature (LCST) was defined as the temperature in which the transmittance is 50% of the initial value obtained at room temperature. In order to understand the parameters controlling the electrospinning process related to the materials, the cinematic viscosities and surface tension of the different PNVCL solutions were measured using an Ubbelohde viscometer (Cannon Instrument Company, Zeitfuchs cross-ARM Viscometer) with 0.1061 and 1.037 cSt/s constant for the sizes 4 and 6, respectively, and a pendant drop apparatus equipped the DROPFIT software (UMR 5257).

The electrospun fibers were characterized by scanning electron microscopy. After being coated with gold, the membranes were observed using a scanning electron microscope (SEM; Hitachi S3600N). The diameter of the fibers was evaluated using the Image J software. The size of the PCL particles in the fibers formed using suspensions 1, 2, and 3 and solution 4 were evaluated using an ultrahigh resolution SEM (HITACHI SU 9000) using cross-sectional cut.

The LCST of the materials was evaluated by DSC using a Perkin Elmer differential calorimeter (Pyris 1) at a heating rate of 10ºC/min for PNVCL and PNVCL/PCL samples with distilled water. The results obtained were shown to be independent of the polymer concentration as had already been observed by Laukkanen et al.(Laukkanen et al., 2004)

The contact angles formed by water drops on the electrospun membranes were evaluated using a contact angle goniometer (optical tensiometer model VCA optima [AST Products, INC]).

Drug Entrapment and Release

The evaluation of drug entrapment efficiency (EE) was performed using a UV–visible spectrophotometer (Genesys 10 Series) at a wavelength of 255 nm: 1.5 mg of the nanofibers was dissolved in 2 mL of ethanol by magnetic stirring during 48 h and the obtained solution was 20 times diluted and then analyzed. The EE was calculated according to the feed ratio of the actual to theoretical drug content in the nanofibers [see eq. (3.1)]:

$$\text{EE (\%)} = \left(\frac{W_d}{W_t}\right) \times 100 \qquad (3.1)$$

Where W_d represents the real amount of ketoprofen, which was determined into fibers and W_t is the weight of ketoprofen used for the preparation of fibers mat.

Release studies were made as follows: the fibers containing ketoprofen (1–2 mg) were gently fixed on a glass carrier and placed in 40 mL of phosphate buffer saline (pH 7.4) used as a dissolution medium. The samples were magnetically stirred at 100 rpm and temperatures of

20 and 42ºC. Aliquots (3 mL) were removed at suitable intervals from the dissolution vessel and immediately assayed spectrometrically at 255 nm. The removed samples were replaced by fresh phosphate buffer. The released ketoprofen concentration was quantified using UV–visible spectrophotometer from a standard curve. The means of two determinations was used to calculate the drug release from each of the formulations.

Methods Used to Compare Ketoprofen Release Profiles from PNVCL, PNVCL/PCL, PNVCL- Eletrosprayed PCL, and PNVCL/PNVCL-b-PCL

Drug release profiles were analyzed using independent [dissolution efficiency (DE)] and model-dependent (curve-fitting) approaches. KinetDS was used to fit the release curves to the Korsmeyer–Peppas mathematical model (Table 3.2). (Singhvi & Singh, 2011) The accuracy and prediction ability of the mathematical model were analyzed by the calculation of coefficient of determination (R^2), Akaikes's information criterion (AIC), and root-mean square error (RMSE), described in Table 3.2. DE values were also obtained via the software KinetDS,(Mendyk et al., 2012) (Table 3.2).

Table 3.2 Independent and Dependent Kinetic Model Applied to Analyze the Drug Release Data Approach

Approach	Method	Equation
Model-dependent	Empirical R^2	$R^2_{emp} = 1 - \frac{\sum_{i=1}^{n}(yi_{obs} - yi_{pred})^2}{\sum_{i=1}^{n}(yi_{obs} - y_{AV})^2}$
	Akaike information criterion	$AIC = (2\times K) + n \times \left[\ln\left(\sum_{i=1}^{n}(yi_{obs} - yi_{pred})^2\right)\right]$
	Root-mean-squared error	$RMSE = \sqrt{\frac{\sum_{i=1}^{n}(yi_{obs} - yi_{pred})^2}{n}}$
Model-independent	Dissolution Efficiency	$DE = \left(\frac{\int_0^t Mtdt}{Mt_{max}\times t}\right) \times 100$

Mt is the amount of drug released in time t; K is the release constant incorporating structural and geometric characteristics of the drug-dosage form; n is the diffusional exponent indicating the drug-release mechanism; Mt_{max} is the maximum amount of drug released (=100%)

3.6 Results and discussion

3.6.1 Synthesis of PNVCL and PCL Homopolymers and PNVCL-b- PCL Copolymer

In this work, PNVCL, PCL, and block copolymers PNVCL-b- PCL were synthesized aiming to elaborate polymeric nanofibers based on the polymers alone and their blends. Table 3.3 presents the data of average molar masses (number-average molar mass, M_n, and weight-average molar mass, M_w) and the dispersity ($Đ = M_w/M_n$), obtained for each polymer. The thermoresponsive PNVCL presented LCST at 34ºC, determined by transmittance measurements of the polymer aqueous solution as a function of temperature in UV–visible analyses (curve not shown).

Table 3.3 Number-Average Molar Mass (M_n), Weight-Average Molar Mass (M_w) and Dispersity ($Đ = M_w/M_n$), Obtained for PNVCL, PCL, and PNVCL-b-PCL

Polymer	**M_n (g/mol)**	**M_w (g/mol)**	**$Đ = M_w/M_n$**
PNVCL	37 000	62 900	1.7
PCL	10 000	15 000	1.5
PNVCL-b-PCL	9951	11 150	1.12

The ^{1}H NMR spectra of pure PNVCL and PCL samples, after purification, are displayed in Figure 3.2(a,b), respectively. In the PNVCL spectrum shown in Figure 3.2(a), peaks at δ = 4.40 ppm (1H ─HCN─ at the position ‘a’), δ = 3.20 (2H, ─NCH_2, ‘c’), δ = 2.50 (2H, ─$COCH_2$, ‘g’), and δ = 0.80–2.00 (6H, ─CH2─ of caprolactam rings and 2H, ─CH2─ of repeated chains, “b,”“d,” and “f”) are observed. The peak of the vinyl group protons at δ = 7.35 ppm was not detected, indicating complete conversion. With respect to PCL, it is possible to observe in Figure 3.2 (b) the multiplets at δ = 1.25, δ = 1.37, and δ = 1.65 ppm (“m,”“n,” and “l,” respectively) and the triplet at δ = 2.31 (“k”). These peaks are related to

the PCL aliphatic chain, in agreement with the literature. The triplet at 3.70 ppm (“o”) refers to the protons in CH_2 attached to the end hydroxyl group. Furthermore, the peak at $\delta = 4.27$ (“p”) indicates the protons in CH2 attached to oxygen. All other unidentified peaks may refer to the residual catalyst $Sn(EH)_2$. The ^1H NMR spectrum obtained for the precursor (PNVCL-OH) for the block copolymer PNVCL-b-PCL [Figure 3.2 (c)] is quite similar to that presented in Figure 3.2(a), with the exception of the protons related to the hydroxyl termination of the chains, which in this case could be observed at 3.65 ppm. Finally, the 1H NMR spectrum performed for the block copolymer PNVCL-b-PCL, shown in Figure 1(d), confirms the presence of the second PCL block, incorporated to the starting chain, that is, the macroinitiator PNVCL-OH. The displaced peaks corresponding to protons in PCL chains (“j” to “n”) could be observed together with the main peaks from PNVCL chains (“a”to “i”). In addition, the peak “j” at 3.65 ppm in Figure 3.2 (c) could not be observed indicating the incorporation of the second block in PNVCL chains.

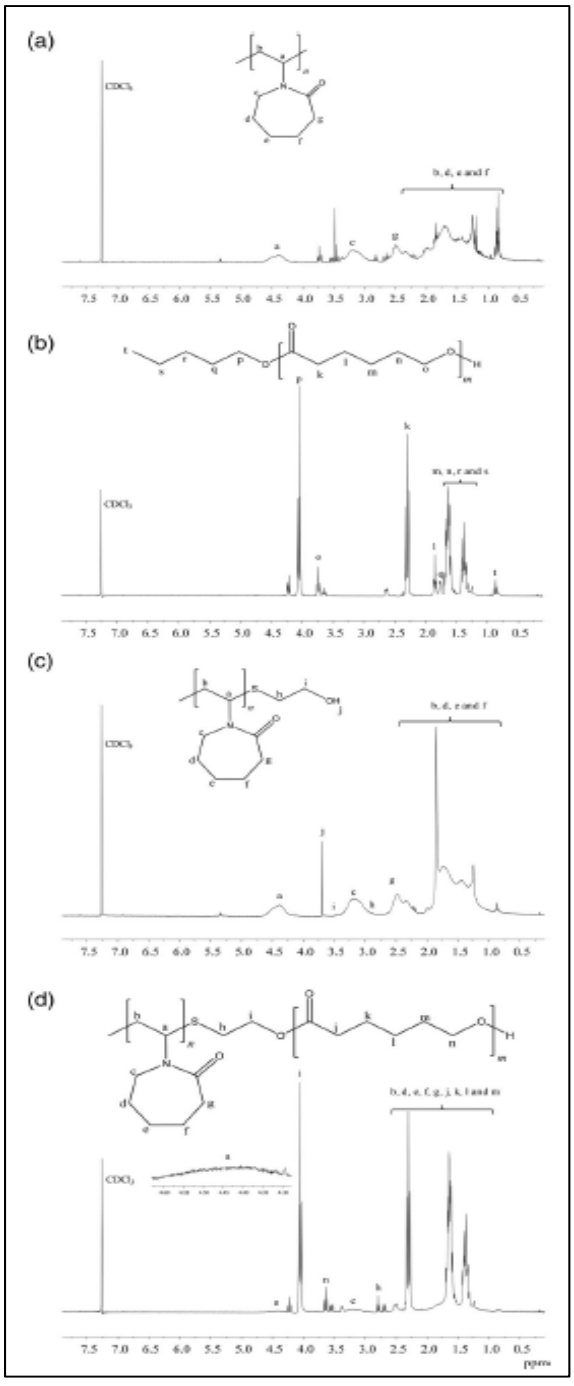

Figure 3.2 ^{1}H NMR spectra of PNVCL (a), PCL (b), the precursor PNVCLOH (c), and PNVCL-b-PCL (d)

3.6.2 Optimization of PNVCL Electrospinning

Table 3.4 Solution Properties of PNVCL Aqueous and Ethanol Solutions with Different Concentrations Mass

Mass molar	Solvent	Concentration (w/v) (%)	Viscosity (cSt)	Surface tension (mN/m)	Dielectric constant (ε)
37 000	Distilled water	0 20 30 35 45	0.953 47.5 277 626 870	72.4 50 47 45 37.5	80.1 - - - -
	Ethanol	0 20 30 35 42	1.5 56 256 382 575	22 28 23.5 21 20	24.5 - - - -

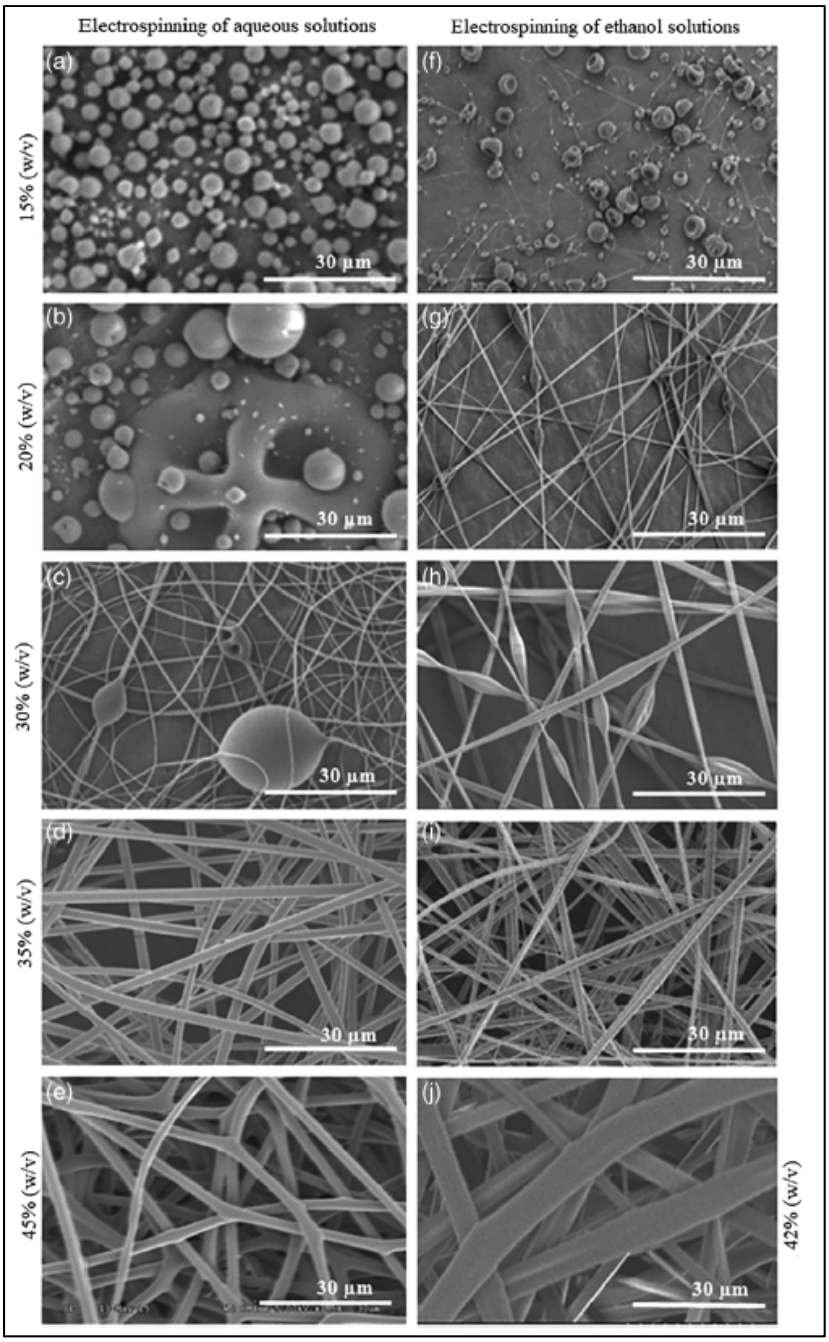

Figure 3.3 Scanning electron microscopy images of fibers morphology as a function of increasing solution concentration with distilled water (a–e) and ethanol (f–j) as solvents

Table 3.4 presents the viscosity and surface tension values for different PNVCL solutions prepared for electrospinning with distilled water and ethanol as solvents and Figure 3.3 shows the typical morphology of the resulting fibers. It can be seen that the morphology of the material electrospun varies according to the solution concentration with distilled water and ethanol. For PNVCL concentration below 30 wt %, only particles were obtained, most likely due to the lack of entanglements between the polymers chains originated by the low viscosities of the solutions. The electrospinning of the 30 wt % solution leads to the formation of fibers with beads. This morphology corresponds to an intermediate stage between electrospraying and electrospinning. For these solution concentrations, the polymer chains most likely present sufficient entanglements to result in the formation of fibers. However, due to a large value of surface tension, the jet contracts during the flight resulting in the formation of beads. For a PNVCL concentration of 35%, it seems that the chain entanglements were sufficient enough to oppose the surface tension and pearl formation. For PNVCL concentration above 35%, the membrane loses its fiber morphology and connected ribbons appear. This type of morphology can be explained by the high viscosity of the polymer solution, which reduces sol- vent evaporation during electrospinning increasing the diameter of the fibers. Similar observations were made for different polymers (Gupta et al., 2005)(Sarabi-Mianeji et al., 2015) and were explained by different analytical models describing the effect of material properties on electrospinning (Simko Jirí ; Lukás, David, 2014).

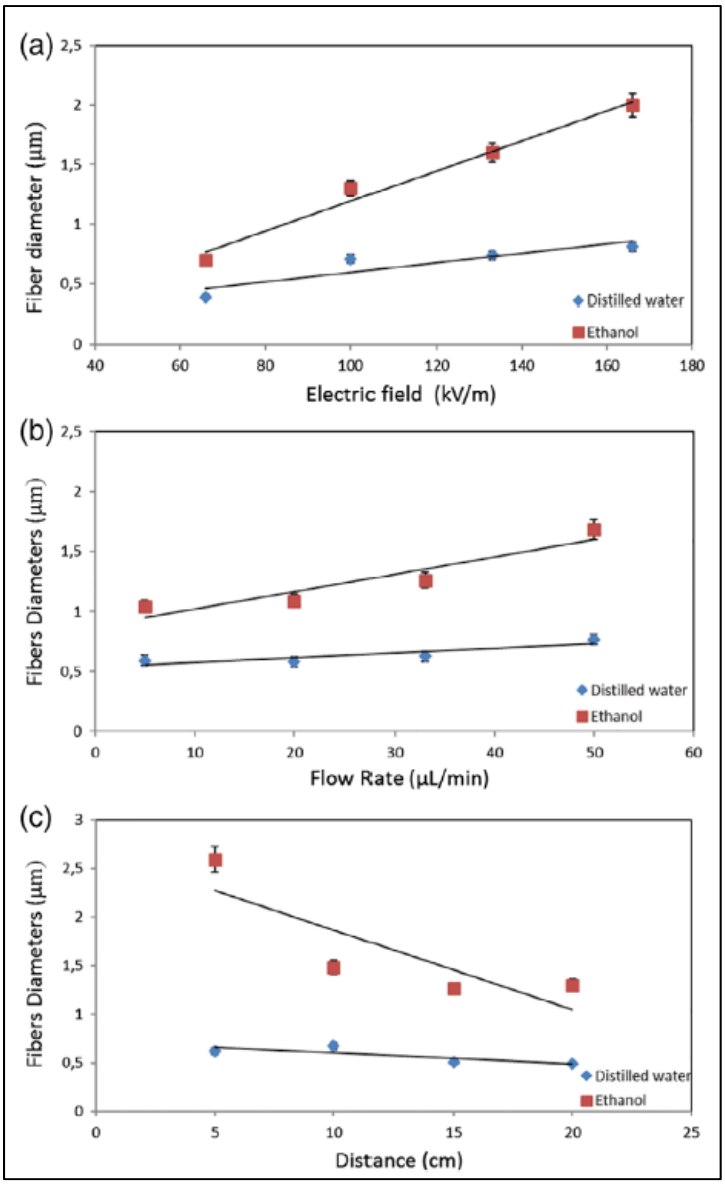

Figure 3.4 Average fibers diameter as a function of the (a) electric field with 33 µL/min flow rate and 15 cm capillary-collector distance for aqueous and ethanol PNVCL solutions, (b) flow rate with 100 kV/m electric field and 15 cm capillary-collector distance for aqueous and ethanol PNVCL solutions, and (c) working Distance with 100 kV/m electric field and 33 µL/min flow rate for aqueous and ethanol PNVCL solutions

Figure 3.4(a–c) presents the effect of electric field (with a flow rate of 33 μL/min flow rate and a capillary-collector distance of 15 cm), flow rate (with an applied electric field of 100 kV/m and a capillary-collector distance of 15 cm), and distance between the needle and the collector (with an applied electric field of 100 kV/m and a flow rate of 33 mL/min) on the fiber diameters, respectively. It can be seen that the fiber diameter increases proportionally with increasing the electric field and the flow rate. However, it decreases with the increasing needle collector distance. Upon increase of flow rate, the amount of polymer to be stretched is higher resulting in fibers with larger diameters.

Similar results have been observed by Zhang et al.(C. Zhang et al., 2005) for PVA polymer fibers and Sarabi-Mianeji et al.(Sarabi-Mianeji et al., 2015) for PCL polymers fibers; in their studies, they show that fiber diameter increased with the applied electrical field and the flow rate. On the other hand, an increase in the needle collector distance will result in more time for the solvent to evaporate and consequently a smaller diameter of fibers.

The average diameter of fibers electrospun from ethanol solutions was about twice thicker than the average diameter of fibers electrospun from aqueous solutions. This could be explained by the different viscosities of polymer solutions made by different solvents (ethanol and distilled water) at the same concentration. Furthermore, the higher dielectric constant of 80.1 for water, compared to 24.5 for ethanol, increased the elongation force on the jet, stretching the fibers and resulting in the formation of thinner fibers(Haider et al., 2015)(Kanani S. Hajir, 2011).

3.6.3 Electrospinning of PNVCL/PCL Blends

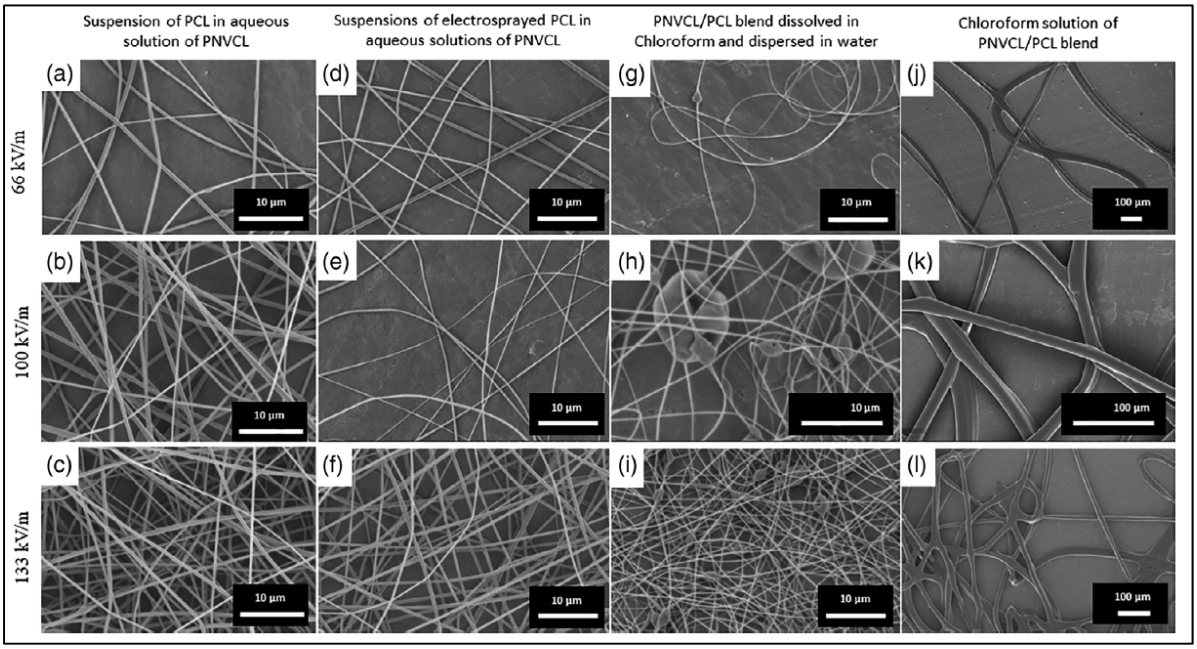

Figure 3.5 Scanning electron microscopy morphology of the four PNVCL/PCL blend fiber mats with 66 kV/m; 100- and 133-kV/m electric field, 33-µL/min flow rate, and 15-cm capillary-collector distance

Since electric field was the parameter that affected the most the diameter of the PNVCL fibers, its influence on the blend fiber diameter and morphology was evaluated. Figure 3.5 displays the morphology of the different blend mats for different electric fields. It can be seen that for better electrospinability, a high electric field, 133 kV/m, must be applied to these four blends

[Figures 3.5(c,f,i, and j)]. When CF was used as a solvent (Figure 3.5(j–l)], the mats presented fused fibers and higher diameter fibers ~10 µm when compared with the other blends. This probably originates from the higher volatility of CF when compared with the one of water and from the much higher dielectric constant of water when compared with the one of CF (80.1 vs 4.8) (Luo et al., 2012). The electrospinning of the aqueous suspension of PNVCL/PCL blend previously obtained by solution blending in CF also did not result in nice

and homogeneous fibers. Dissolving the PNVCL/PCL blend in water did not result in a homogeneous suspension when adding PCL particles in PNVCL aqueous solution (blend one and two). The use of this suspension induced syringe blockage during the electrospinning process resulting in the appearance of beads within the fibers [see Figure 3.5(h)]. Similar behavior was observed by Sant et al.36 who electrospun PCL PGS blends.

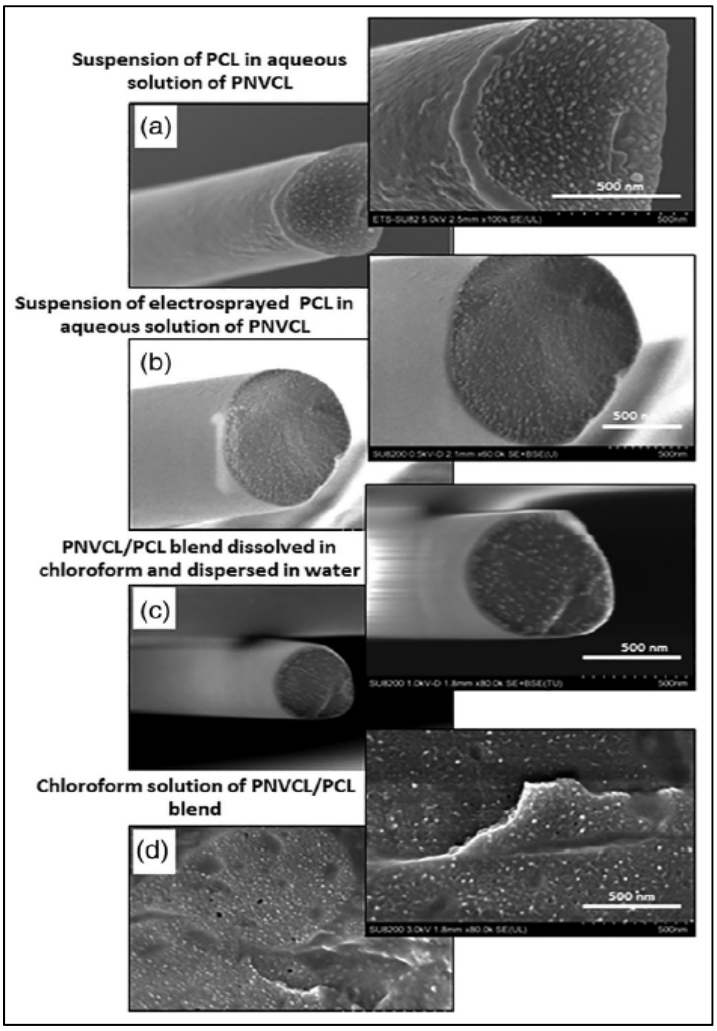

Figure 3.6 Scanning electron microscopy images of the four PNVCL/PCL blend cross-sectional fibers electrospinned with 100-kV/m electric field, 33-μL/min flow rate, and 15-cm capillary-collector distance.

Table 3.5 Average Fibers Diameters and Particle Size of the Four PNVCL/PCL Blend Fibers Mats

Fibers	**PNVCL/water**	**Suspension of PCL in aqueous solution of PNVCL**	**Suspension of electrosprayed PCL in aqueous solution of PNVCL**	**PNVCL/PCL blend dissolved in chloroform and dispersed in water**	**Chloroform solution of PNVCL/PCL blend**
Fibers diameters (μm)	0.6	0.9	1	0.730	10
Average particles size (nm)	-	20	14	17	16

Figure 3.6 shows the cross sections of the four PNVCL/PCL blend fibers. Table 3.5 reports the diameters of the electrospun fibers as well as the average PCL particle size. Both were evaluated using the ImageJ software. The addition of PCL to the blends resulted in an increase in fiber diameters. Whether PCL was added as obtained after synthesis or in an electrosprayed form did not seem to have an influence on the fiber diameter. However, the average size of the PCL particles within the fibers is smaller when the PCL was electrosprayed.

Table 3.6 LCST Measurements of PNVCL/PCL Blend with Different Fibers Mat

Fibers	**PNVCL/water**	**Suspension of PCL in aqueous solution of PNVCL**	**Suspension of electrosprayed PCL in aqueous solution of PNVCL**	**PNVCL/PCL blend dissolved in chloroform and dispersed in water**	**Chloroform solution of PNVCL/PCL blend**
LCST Temperature (°C)	38	36	36.5	36.5	36

Table 3.6 presents the LCST of the PNVCL and PNVCL/PCL blend fiber mats in distilled water as measured by DSC following the procedures reported in the experimental section. Upon addition of PCL, the LCST of PNVCL decreases in 2ºC. These results are in good agreement with the results of Wu et al. who observed that the copolymerization of PNVCL to PCL resulted in a decrease of LCST of PNVCL. They also observed that an increase of PCL block length resulted in a greater decrease of LCST. The decrease of LCST can be explained by the hydrophobicity of PCL. The mixture of PNVCL with a hydrophobic polymer like PCL makes it more hydrophobic, decreasing therefore the transition temperature between the hydrophilic state and the hydrophobic state. However, the addition of PCL to PNVCL did not result in an increase of the value of contact angle formed by drops of water on the surface of the membranes. Smooth and homogeneous fibers were observed only when using the PCL suspensions within PNVCL solutions and the ethanol solution. Therefore, only PNVCL fibers and the mats obtained using those two aqueous suspensions were tested for drug delivery.

3.6.4 Electrospinning of PNVCL/PNVCL-b-PCL Blends

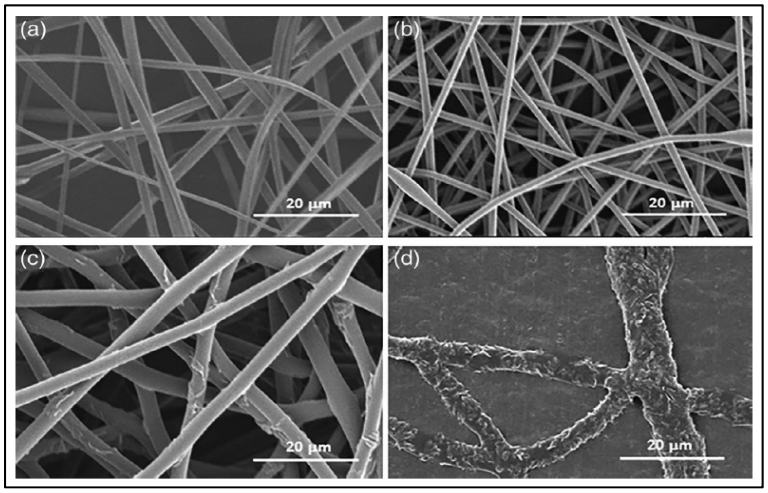

Figure 3.7 Scanning electron microscopy morphology of the four PNVCL/ PNVCL-b-PCL blend fibers mats with (a) 75/25, (b) 50/50, (c) 25/75, and(d) 0/100 blend ratios.

Figure 3.7 shows the scanning electron microscopy images of the resulting fibers obtained from the electrospinning of PNVCL/PNVCL-b-PCL polymer solutions using a mixture of ethanol/tetrahydrofuran (1:1.2) with different block copolymer ratios. It can be seen that it was possible to obtain homogenous, continuous, and bead-free fibers, after the addition of block copolymer PNVCL-b-PCL to blends in concentrations of up to 50% in respect of total mass of polymer (Figure 3.7 (a,b). By increasing the concentration of the block copolymers to 75% [Figure 3.7(c)], the fiber surface dramatically changed and some roughness appeared, resulting from the formation of polymer clusters at the nanofiber surface, which in turn originated from the increased hydrophobicity of the polymer mixtures. On the other hand, the electrospinning of PNVCL/PNVCL-b-PCL blend with the 0/100 ratio did not result in nice and homogeneous fibers, as observed in Figure 3.7 (d). The appearance of roughness in the nanofibers can be attributed to the significant increase in the hydrophilicity of the blend, with the increase of the amphiphilic block copolymer PNVCL-b-PCL. In general, the fibers diameters were less than 1 μm, as can be observed in Figure 3.7. In native skin, extracellular matrix components are composed of nonwoven collagen fibers approximately 50–500 nm in diameter. In spite of the extensive study regarding different materials for wound healing, there is no consensus regarding the duration and the ideal fiber diameter for this application. It is known that the material must mimic the properties of the natural fibers belonging to the skin. Additionally, an optimal wound matrix should be durable, such that it can provide long-lasting support of wound healing, by withstanding mechanical forces while maintaining flexibility. The fact that the fibers obtained in this study had a diameter similar to those of the natural components of the skin is an indication that these materials will be well tolerated when in contact with the surface of the skin. However, there is a lack in the literature regarding the rate of in vivo degradation of materials based on the polymers evaluated herein.

Table 3.7 LCST Measurements of PNVCL/PNVCL-b-PCL Blends Ratios with Different Fibers Mat

Fibers	PNVCL/water	PNVCL/PNVCL-*b*-PCL 75/25 blend ratio	PNVCL/PNVCL-b-PCL 50/50 blend ratios	PNVCL/PNVCL-b-PCL 25/75 blend ratios
LCST Temperature (°C)	35	35	33.5	31

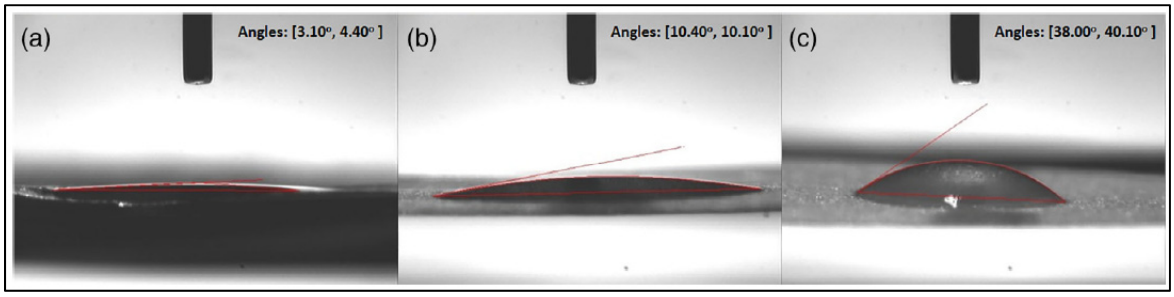

Figure 3.8 Water contact angle measurements of fiber with different ratios of PNVCL/PNVCL-b-PCL: (a) 75/25, (b) 50/50, and (c) 25/75

Table 3.7 presents the LCST of the PNVCL and PNVCL/PNVCL-b-PCL blend fiber mats in ethanol and ethanol/tetrahydrofuran (1:1.2) mixture as measured by DSC. Upon addition of PNVCL-b-PCL block copolymers, the LCST of PNVCL decreases from 35 to 33.5°C and 31°C. These results were expected from the previous result of the PNVCL/PCL blends (Table 3.5). It can be seen that increasing of PCL or the block copolymers PNVCL-b-PCL resulted in a greater decrease of LCST (Wu et al., 2014). The increase in hydrophobicity of blends formed by PNVCL/PNVCL-b-PCL as a function of increasing the amount of the block copolymer PNVCL-b-PCL in the nanofibers preparation can be confirmed by the contact angle measurements, as shown in Figure 3.8. The addition of PNVCL-b-PCL block copolymer resulted in an increase in the value of the contact angle formed by drops of water on the surface of the membranes [Figure 3.8(c)] especially for the ratio 25/75 PNVCL/PNVCL-b-PCL. This increased hydrophobicity was also responsible for the

formation of agglomerates on the surface of the fibers, promoting the appearance of a rougher surface, as shown in Figure 3.8(c), in comparison with those formed from less hydrophobic blends. In view of the more hydrophobic property of 25/75 PNVCL/PNVCL-b-PCL nanofibers, they were tested for evaluating the ketoprofen encapsulation and in vitro controlled release.

3.6.5 Ketoprofen Entrapment and Release

Table 3.8 Ketoprofen Entrapment into PNVCL Electrospun Fibers Mats

Ketoprofen fibers mat	EE (%)
PNVCL/Ket	99.6
PNVCL/PCL/Ket	87.7
PNVCL/electrosprayed PCL/Ket	95.4
PNVCL/PNVC-b-PCL/Ket	99.6

Table 3.8 presents the ketoprofen entrapment in the PNVCL, PNVCL/PCL, and PNVCL/PNVCL-b-PCL fibers mats. It can be seen that the EE for the three samples is above 85%. These mean that the amount of ketoprofen present in the PNVCL, PNVCL/PCL, and PNVCL/PNVCL-b-PCL fibers was nearly the total amount used during the formulations; therefore, the electrospun fibers may be considered as potential carriers for drugs.

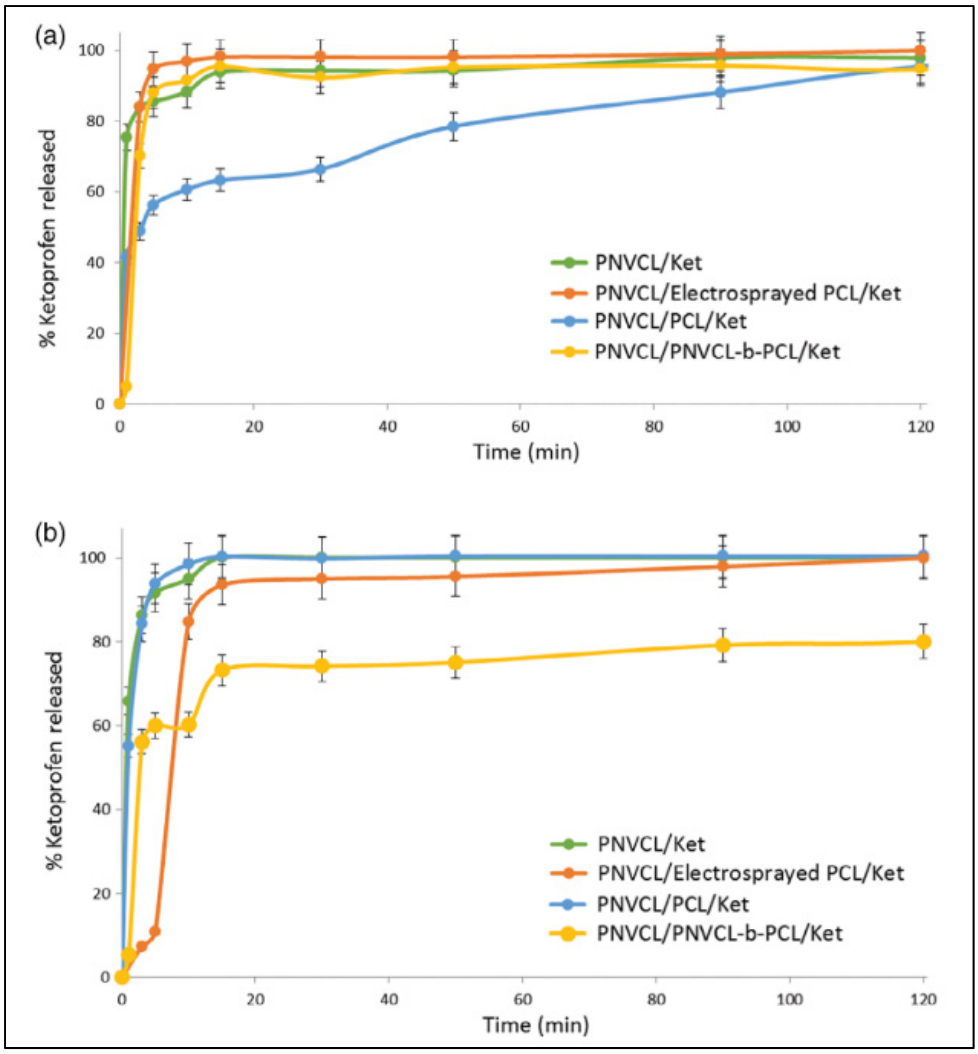

Figure 3.9 Drug release profile of ketoprofen through PNVCL, PNVCL/PCL, and PNVCL/PNVCL-b-PCL fibers mats at 20ºC (a) and 42ºC (b)

Table 3.9 Results of Curve Fitting And Kinetic Analysis of Ketoprofen Release Data from PNVCL Electrospun Fibers Mats Using the Korshmeyer–Peppas Model and Dissolution Efficiency (DE) Obtained via Independent Model Analysis

Curve fitting parameters	20ºC				42ºC			
	PNVCL /Ket	PNVCL /PCL/ Ket	PNVCL/ electrosprayed PCL/Ket	PNVCL /PNVCL-b-PCL/Ket	PNVCL /Ket	PNVCL /PCL/ Ket	PNVCL/ electrosprayed PCL/Ket	PNVCL/ PNVCL-b-PCL/ Ket
R^2	0.9695	0.9761	0.9691	0.9819	0.9706	0.9718	0.9918	0.9828
RMSE	5.4842	2.4933	6.8851	18.6498	7.1451	9.2326	22.6017	2.3727
AIC	64.0634	45.2977	65.6131	85.5426	66.3544	71.4807	89.3864	77.3357
k(min^{-1})	72.4415	40.3572	76.8497	53.0750	73.9081	71.9547	25.6395	37.5914
n	0.0760	0.1723	0.0730	0.1545 0.0813	0.0813	0.0882	0.3179	0.1778
DE	94.4544	77.6533	98.6316	93.25 98.4779 84	98.4779	98.4982	91.2796	74.0761

Figure 3.9(a,b) shows ketoprofen release as a function of time for the different fiber mats studied in this work at 20 and 42ºC. Table 3.9 presents the DEs during 120 min as the quantitative interpretation of the values obtained in the dissolution assays is easier using DE to describe the release profiles. For PNVCL/Ketoprofen fiber mat, a percentage greater than 60% drug was released during the first minute of assay at both 20 and 42ºC. The release curves for these two temperatures are quite similar at both temperatures, indicating that the thermosensitive character of the PNVCL did not have an effect on the release rate of the ketoprofen. Only a small increase in the rate of dissolution of the drug was observed, as DE varied from 94.4544 to 98.4779 when the temperature increased from 20 to 42ºC, respectively. This result may indicate that there was no sufficient interaction between PNVCL chains and ketoprofen at the moment of fiber preparation to benefit from the thermosensitive effect of the PNVCL during the dissolution rate of the drug in the aqueous

medium. Upon addition of PCL in a blend or copolymer form, a decrease in the rate of release of ketoprofen was observed as evidenced by the curves shown in Figures 3.8(a,b) and the DE values listed in Table 3.9: 77.65 and 93.26 for PNVCL/PCL/Ket and PNVCL/PNVCL-b-PCL/Ket fibers at 20ºC. At 42ºC, the ketoprofen dissolution rate from the PNVCL/PCL blends was quite similar to that from the PNVCL/Ket. However, in comparison with DE for blends at 20ºC, a considerable increase was observed indicating that when physical mixtures of these polymers are used, the thermosensitive effect of the PNVCL becomes evident. For the blends of PNVCL and PNVCL-b-PCL, the reduction in the dissolution rate of ketoprofen, compared with bare PNVCL, was visible even at 42ºC, due to the presence of PNVCL on both the surface and the core of the fibers, in which ketoprofen is preferentially buried; DE reduced from 98.50 to 74.08. An opposite behavior was observed when the blends formed by PNVCL and electrosprayed PCL were used. It was expected that this system would also exhibit a slower ketoprofen release rate than the one of nanofibers containing only by PNVCL and ketoprofen. However, at 20ºC, DE values of 94.46 and 98.63 were obtained for PNVCL/Ket and PNVCL/electrosprayed PCL/Ket, respectively, as shown in Table 3.9. It appears that when the electrospinning process was performed in the presence of PCL preformed particles, the drug remained at the interface between PCL and the upper layer of PNVCL, resulting in a fast release upon the dissolution of PNVCL chains at 20ºC. The ability of PCL nanofibers to delay the in vitro release of ketoprofen has been reported in the literature; Basar et al. (Basar et al., 2017) performed comparative release studies between the single PCL electrospun mat and the binary PCL/gelatin electrospun mat and found that the second mat totally suppressed the burst release of Ketoprofen and it exhibited a continuous and sustained drug release for >100 h (~4 days), while PCL fibers mat exhibited a burst release profile that reached a plateau after approximately only 12 min time at which it released ~90% of the drug. The release of ketoprofen from PNVCL-*co*-MAA nanofibers at different temperatures was previously evaluated by Liu et al. The results showed that slow release over several hours was observed at 40ºC (above the LCST of PNVCL-*co*-MAA), while the drug exhibited a burst release of several seconds at 20ºC (below the LCST). To the best of our knowledge, it is the first time that the release of ketoprofen from nanofibers

formed by physically blending PNVCL and PCL or PCL-*b*-PNVCL block copolymer is evaluated, and the results shown in this study reveal that the nanofibers containing the block copolymer may become potential systems for the encapsulation and controlled release of ketoprofen or other similar drugs.

3.6.6 Curve Fitting and Drug Release Mechanism

To determine the mechanism of drug release, the cumulative drug (until 120 min) release from the PNVCL-based nanofibers was fitted in the Korsmeyer–Peppas model. Nonlinear regressions were applied for cumulative dissolved drug. In this model, the kinetic constant (k) incorporates structural and geometric characteristics of the polymer system, and the release exponent (n) characterizes the mechanism of drug release [eq. (1) and Table 3.2]. These parameters as well as the coefficient of determination (R^2), RMSE, and Akaike's information criterion (AIC) values were determined using the KinetDS software. The data obtained from Korsmeyer–Peppas model for dissolution experiments performed using PNVCL electrospun fibers mats at different temperatures are listed in Table 3.9. It can be observed that the drug release mechanism is well described mathematically by the Korsmeyer–Peppas equation, considering the values of R^2, AIC, and RMSE. Korsmeyer–Peppas model is used to analyze the release of pharmaceutical polymeric dosage forms, when the release mechanism is not well known or when more than one type of release phenomenon could be involved (Sheng et al., 2006). Peppas used the value of n to characterize the different release mechanisms, reaching values of n up to 0.5 for diffusion (Fick model) and values of n higher between 0.5 and 1, and 0 in a flat system, for the transfer of mass according to a non-Fickian model. In this work, the low values of the release exponent ($n < 0.5$) for both 20 and 42°C indicate a Fickian diffusion mechanism for al formulations, i.e., polymer relaxation followed by the diffusion of ketoprofen. The variation in the release rate of ketoprofen (k) with increasing temperature from 20 to 42°C presents a different behavior as a function of the polymers used in the preparation of the drug-containing nanofibers.

When only PNVCL was used in the preparation of the ketoprofen-containing nanofibers, there is an insignificant, within experimental error, increase of k with the increase in temperature from 25 to 42ºC, that is, the value of k determined for the release assay at 20ºC was 72.4415 min^{-1}, whereas it was 73.9081 min^{-1} for the release assay at 42ºC. What can be confirmed from these results is that, at the moment of nanofibers fabrication, there was not enough interaction between the PNVCL chains and the ketoprofen, and as a consequence, the drug easily detached from the polymer when the fibers were placed in aqueous medium. Because of their solubility at 20ºC and even at 42ºC, that is, above the LCST of PNVCL, the chains of PNVCL precipitated separately and the drug molecules dissolved in the medium. Thus, it was not possible to benefit from the thermal sensitivity of PNVCL on the dissolution of ketoprofen in aqueous medium. For the PNVCL/PCL blends containing ketoprofen, the rate of drug release increased considerably with increasing temperature, as evidenced by an increase of k from 40.36 to 71.48 min^{-1}, when the temperature increased from 20 to 42ºC. This fact leads us to believe that at the moment of fiber formation, the ketoprofen was buried mostly in nanofibers core, together with PCL, while PNVCL chains remained mostly on the fibers surface. Thus, the increase in temperature caused the compression of PNVCL chains in some regions of the surface, causing the formation of pores in other regions, thereby allowing the drug molecules to diffuse into the dissolution medium. For the nanofibers based on the blends of PNVCL/electrosprayed PCL, the increase in temperature from 20 to 42ºC caused a considerable decrease in the release ketoprofen rate, as evidenced by the reduction of k from 76.85 to 25.64 min^{-1}. For these nanofibers, previously electrosprayed PCL particles were used for a second electrospinning process, this time at the presence of PNVCL and ketoprofen. The drug probably remained at the interface between the previously formed PCL-based hydrophobic particles and the hydrophilic layer formed by the PNVCL. Once the system was placed at 20ºC, PNVCL solubilized rapidly and ketoprofen was released. However, at 42ºC, that is, above the LCST of PNVCL, the outer layer of this polymer shrinked, forming a barrier for the passage of ketoprofen. The dosing efficiency, in turn, decreased from 98.63 to 91.28 with the increase of temperature from 20 to 42ºC. Finally, for the nanofibers prepared with the PNVCL blends with PNVCL-b-PCL block copolymers

containing ketoprofen, increasing the temperature from 20 to 42ºC caused a slight reduction in the rate of drug release, as evidenced by the decrease of k from 53.15 to 37.59 min^{-1} and DE from 93.60 to 74.08. When pure and hydrophilic PNVCL were physically linked with the amphiphilic copolymers based on PNVCL, the chains of the thermosensitive polymer remained distributed more homogeneously at both the core and the surface of the nanofibers, thereby favoring the polymer–polymer interactions with increasing temperature and reducing the diffusion of ketoprofen. In general, it can be seen here that using block copolymer PNVCL-b-PCL presents more stable and long-time ketoprofen release from the fibers.

3.7 Conclusion

Promising thermo-responsive drug delivery systems based on the blends of PNVCL with PCL or PNVCL-b-PCL block copolymer were developed in this work using solution electrospinning. Several processing parameters and formulation were tested. The morphology of the electrospun membrane obtained could be controlled by the process parameters such as the electric field, flow rate, and distance between the needle and the collector as well as by the composition of the blends electrospun. The addition of PCL or PNVCL- b-PCL block to PNVCL presented a direct effect on the LCST, hydrophobicity of the membrane, and water contact angle formed by drops of water on the surface of the membrane. When ketoprofen, a hydrophobic drug, was added to the polymer solutions to be electrospun, membranes with entrapped drug were obtained. The drug entrapment was dependent on the polymers used in nanofiber preparations and PNVCL/PNVCL-b-PCL based nanofibers showed the highest EE value. The morphology of the PCL/PNVCL blends was shown to control the drug release. The addition of PNVCL-b-PCL block copolymer to PNVCL slowed and prolonged the in vitro release. The results reported here provide good evidence that the systems developed enable the adjustment of drug release kinetics, varying the type and ratio of concentration of polymers used in the blends, and should be tested for other drugs showing different affinities with the polymers.

3.8 Acknowledgments

The authors wish to thank the Natural Sciences and Engineering Research Council of Canada (NSERC), the University Mission of Tunisia in North America (MUTAN) and the Fundação de Amparo a Pesquisa do Estado de São Paulo (FAPESP), Brazil for the financial support.

CHAPITRE 4

ELECTROSPUN POLY(NVCL-*CO*-AA) FIBERS AS POTENTIAL THERMO-AND *PH*-SENSITIVE AGENTS FOR CONTROLLED RELEASE OF HYDROPHOBIC DRUGS

Marwa Sta,[1] Dayane B. Tada,[2] Simone F. Medeiros,[3] Amilton M. Santos,[3] Nicole R. Demarquette*

[1]Department of Mechanical Engineering, École de Technologie Superieure
1100 rue Notre-Dame Ouest, Montréal, Québec, Canada H3C1K3
[2]Laboratory of Nanomaterials and Nanotoxicology, Universidade Federal de São Paulo
Rua Talim, 300 São José dos Campos, São Paulo, Brazil
[3] Department of Chemical Engineering, Escola de Engenharia de Lorena,Universidade de São Paulo, USP, Lorena, SP, Brazil

Paper submitted for publication, April 2021

4.1 Chapter outline

The goal of this second article is to respond to the second steps of the doctorate; Optimizing the electrospinning of two molar mass fractions a thermo-and *pH*-sensitive copolymer based on PNVCL in mixture with different concentrations of ketoprofen, hydrophobic drug. Following the results of the first article and research carried out, it has been shown that the use of a thermo-and *pH*-sensitive copolymer helps to stabilize the morphology of electrospun fibers in contact with water. In this article emphasis is placed on the interaction between the copolymer and the drug and its effect on the release of ketoprofen.

4.2 Abstract

Electrospun nanofibrous membranes have been widely investigated for many biomedical applications such as self-healing, wound dressing/healing, drug delivery and tissue

engineering. In this study, poly(N-vinylcaprolactam-*co*-acrylic acid) (Poly(NVCL-*co*-AA)) containing 20 and 30 mol% AA, were used to prepare thermo-and-*pH*-sensitive fibers containing a hydrophobic drug, ketoprofen, via electrospinning. Ketoprofen entrapment efficiency was assessed via UV-visible spectroscopy and revealed high values. The interaction drug/copolymer was investigated by (FTIR), which indicated the drug entrapment into the fibers. The crystallinity of the ketoprofen-loaded fibers evaluated via (DSC) confirmed the presence of ketoprofen in its amorphous phase. Cytotoxicity of ketoprofen-loaded fibers was evaluated by cell viability assays using MTT. The results showed that the copolymer was not cytotoxic at a low ketoprofen concentration. The ketoprofen release profile was analyzed using independent and model-dependent approaches and showed slow-release rates at high temperature. The study of the drug release mechanism showed that the Korsmeyer–Peppas model fits to the release behavior. These findings may expand poly(NVCL-*co*-AA) application making them promising candidates for temperature and pH responsive drug delivery systems.

Keywords: Themo-sensitive, *pH*-sensitive, Electrospinning, Fibers, Controlled release, Drug delivery

4.3 Introduction

Electrospinning of fibers has gained a lot of attention in several research areas especially for applications such as wound-healing tissue (Pawar et al., 2015), scaffolds for tissue regeneration (Sill & Recum, 2008), and drug delivery agents (Deepak et al., 2018)(Milla et al., 2018)(Riccitiello et al., 2018)(L. Liu et al., 2016). This technique enables rapid production of micro- to nano-sized fibers from a wide range of polymers (Haider et al., 2015)(Goh et al., 2013)(Islam et al., 2019). In addition, electrospinning may result in porous fibers, which are very useful as drug delivery systems (Rezabeigi et al., 2017) for providing a high drug-incorporation ratio and enhanced fluidity of body fluids throughout the matrix. Therefore, electrospun fibers are widely used for the delivery of different pharmaceutical

ingredients due to their high surface area, which promotes the controlled released of drugs from these fibers at a defined rate over a defined period (Islam et al., 2019). When those electrospun fibers are used for drug delivery, different strategies can be adopted for the inclusion of drugs into the fibers. This can be achieved by mixing the drug in a polymer solution used as a supply for the electrospinning process, by confining the drug in the core of a fiber obtained by coaxial electrospinning, by encapsulating the drug in nanostructures such as the one created by the phase separation technique (Rezabeigi et al., 2018)(Rezabeigi et al., 2017)(Rezabeigi & Demarquette, 2019), or by fixing the Drug on the surface of the fiber (Yuan Gao et al., 2014). One of the most widely studied drugs for topical wound healing application is phenytoin, well known by its ability to regulate collagenase activity, bacterial colonization, and the formation of a wound exudate. However, some interesting studies reveal the potential of polymeric fiber to modify the dissolution and release properties of other commonly administrated anti-inflammatory agents (NSAIA) such as ketoprofen (E. R. Kenawy et al., 2007)(Mutlu et al., 2018)(Qu et al., 2013). The analgesic and antipyretic properties of this hydrophobic nonsteroidal drug justify their use for everyday illnesses with properties that are widely used to evaluate drug delivery systems. In addition, due to its low molecular weight, high permeability and short plasma elimination half-life (2–3), ketoprofen is an appropriate drug for transdermal controlled delivery (Arshad et al., 2018).

Concerning the matrices, a large variety of natural or synthetic polymers can be used to produce electrospun fibers in the pursuit of medical fabrics in wound dressing. Poly(ε-caprolactone) (Mutlu et al., 2018), poly(vinyl alcohol) (E. R. Kenawy et al., 2007) and cellulose acetate (Qu et al., 2013). Stimulus-responsive polymers, which are able to change their properties in response to temperature, pH or other stimuli, have received lots of attention for drug delivery over the last decade (James et al., 2014)(Chakraborty et al., 2018). In particular, thermo-responsive or thermosensitive polymers are of particular interest, in view of their conformation change, upon a change of temperature. According to their thermosensitive behavior, these polymers can be classified into two categories: polymers exhibiting lower critical solution temperature (LCST) and upper critical solution temperature

(UCST) (J. Liu et al., 2014)(S.F. Medeiros et al., 2011). For polymers exhibiting LCST the polymer chains change from a soluble state to a collapsed state at a certain temperature (Ward & Georgiou, 2011). Some polymers such as poly(N-vinylcaprolactam) (PNVCL) are of particular interest as their LCST is around 32^{O}C, being close to the physiological temperature (J. Liu et al., 2014). Also, PNVCL is a very interesting candidate for drug delivery applications (Simone F. Medeiros et al., 2017)(Marwa Sta et al., 2020) since it is nonionic, water soluble, and nontoxic, compared to other thermosensitive polymers like PNIPAM (Vihola et al., 2005)(Simone F. Medeiros et al., 2010). Furthermore, it is possible to improve the functionality of PNVCL by incorporating other polymeric segments, such as poly(acrylic acid) (PAA) segments, into the PNVCL backbone to obtain a thermo and *pH*-sensitivity copolymer; poly(N-vinylcaprolactam-*co*-acrylic acid) (Poly(NVCL-*co*-AA)) (Simone F. Medeiros et al., 2017). This PNVCL based copolymers can change, quickly and reversibly, its conformation, once in aqueous solution, upon a change of temperature and pH simultaneously (Simone F. Medeiros et al., 2017).

In this work, thermo-and-pH-sensitive poly(N-vinylcaprolactam-co-acrylic acid) (Poly(NVCL-co-AA)) containing 20 and 30 mol% AA, respectively, were used to prepare electrospun fibers. In addition, ketoprofen was introduced in different concentrations to obtain ultrafine membranes to be used as carriers for drug delivery. The ketoprofen was used as a hydrophobic and highly crystalline drug model, but the results showed that the versatile nanofibers can be applied to entrap and deliver various biological agents long-term to local tissues at the wound site. The copolymer matrices not only provide physical protection to the wound, but they also have the capacity to incorporate a large variety of drugs, which have limited dissolution, reducing their action on the diseased area. The effects of copolymer composition and the drug concentration on the LCST, the hydrophobicity, the cytotoxicity, and the ketoprofen release rate from the fibers, were evaluated. The originality of the present work, mainly comparing it with the work previously published by Liu et al. (L. Liu et al., 2016), lies in the study of the difference in the copolymer segment lengths which are sensitive to temperature and to pH, allowing a better control of drug delivery. In addition, our study presents a detailed optimization of the electrospinning process parameters, in order to

obtain fibers with reduced diameter and homogeneous morphology. The effect of the copolymers on the biocompatibility of ketoprofen is clear by observing the cell viability data, which show that, in general, this parameter increased with drug entrapment in polymer fibers.

4.4 Experimental

4.4.1 Materials

Poly(NVCL-co-AA) (80:20) and poly(NVCL-co-AA) (70:30), previously obtained in our research group were used throughout this work. The properties of poly(NVCL-co-AA) (80:20) is reported in details by Medeiros et al (2017) [24]. Briefly, the molar mass (Mn) and dispersity (Đ) were 6640 g/mol and 1.58, respectively. The content of AA in the poly(NVCL-co-AA) copolymers, determined by titration and 1H NMR, was equivalent to 17 mol%, which is near the percentage used in the feed (20 mol%) (data not shown). Finally, the LCST obtained for polymer linear chains via UV-vis was 39°C (spectrum not shown). For poly(NVCL-co-AA) (70:30) the molar mass (Mn) and dispersity (Đ) were 6247 g/mol and 1.59, respectively. The content of AA in the poly(NVCL-co-AA) copolymers was 28 mol% and the LCST was 40°C (spectra not shown). For both copolymers, 1H NMR spectra (not shown) were used to analyze NVCL and AA conversion, and it was observed that NVCL was totally consumed after 3h into the reaction. 1H NMR also revealed the absence of a peak corresponding to the vinylic proton of the AA molecule after 15 min of copolymerization. Crystalline ketoprofen, a hydrophobic drug, was kindly supplied by Sanofi (Brazil) and used as received. Ethanol and N,N-Dimethylformamide (DMF) from Sigma Aldrich were used to obtain the solutions to be electrospun.

4.4.2 Nanofibers preparation and ketoprofen entrapment

The ketoprofen/copolymer electrospun solutions were prepared by adding 0%, 10%, 30 % and 50% ketoprofen to the copolymer dissolved in a mixture of ethanol and DMF at a ratio of 50:50 (v:v), using a magnetic stirrer for 1 hour, to obtain a homogeneous solution with 45wt% concentration in the case of Poly(NVCL-*co*-AA) (80:20) and 35wt% in the case of Poly(NVCL-*co*-AA) (70:30). Once obtained the solutions were electrospun in a vertical electrospinning machine (Bionicia FluidNatek L100). The processing parameters used for electrospinning were 100 kV/m electric field, 2 mL/h flow rate, 10 cm working distance, 21°C electrospinning temperature and 35% to 40% humidity.

4.4.3 Solution characterization

Before electrospinning, the kinematic viscosity and the surface tension of the electrospun solutions were measured using an Ubbelohde viscometer (Cannon Instrument Company, Zeitfuchs cross-ARM Viscometer), with 1.100 cSt/s constant for the range 200 to 1000 cSt and a pendant drop apparatus equipped DROPFIT software (UMR 5257) respectively.

4.4.4 Membrane Characterization

The electrospun fibers were then characterized by scanning electron microscopy. After being coated with gold, the membranes were observed using a SEM (Hitachi S3600N). An ultra-high Resolution Scanning Electron Microscope (SEM) (HITACHI SU8230) was used to verify the presence of drug particles on the surface of the poly(NVCL-*co*-AA) fibers with 0%, 10%, 30 % and 50% ketoprofen concentrations. The diameter of the fibers was evaluated using the Image J software.

To verify the drug trapping in the fibers and the presence of drug/polymer interaction, Fourier transform Infrared spectrometer (FTIR) spectra were collected on FTIR Perkin Elmer spectrometer by using 1 cm^2 of the fiber's membrane. Scans were taken over 3500–1500

cm^{-1} with a resolution of 2 cm^{-1} and an average of 32 scans. The Crystallinity and LCST of the materials were evaluated by Differential Scanning Calorimetry (DSC) (Perkin Elmer, Pyris 1), from 10ºC to 110ºC at a heating rate of 15 ºC/min under a nitrogen atmosphere and with distilled water for the LCST measurement. Wide-angle X-ray diffraction (XRD) measurements were performed on a Panalytical X'pert pro X-ray diffractometer equipped with a copper, CuKα, tube at 45 kV and 35 mA. Scans were performed in the 2theta range of 10–70°. The wettability of the electrospun mats were measured using a contact angle goniometer (optical tensiometer model VCA optima [AST Products, INC]) and by evaluating the contact angles formed by distilled water drops on the electrospun membranes 5s after a single water drop contacts the membranes surface.

4.4.5 Drug Entrapment

The evaluation of drug entrapment efficiency (EE) was performed using a UV–visible spectrophotometer (Varian Cary 300 Bio) at a wavelength of 260 nm. Two mg of ketoprofen-loaded membranes were dissolved in 40 ml of a basic solution (pH 10) under magnetic stirring during 48h. The obtained solution was then analysed. The EE was calculated as the ratio of the amount measured by UV-visible spectrum, W_d , over the actual amount used for the preparation of fibers mat, W_t, eq. (4.1) (Pawar et al., 2015):

$$EE(\%) = \left(\frac{W_d}{W_t}\right) \times 100 \quad (4.1)$$

4.4.6 Cell viability assays

The fibers cytotoxicity was evaluated by an indirect method against mouse embryonic fibroblasts (MEF) cells by using the cell viability assay known as MTT assay. Firstly, membranes were cut using pliers-paper-punch, with a 6 mm diameter. The samples extracts were prepared by incubation of the membranes in the culture medium. The cut membranes

were placed in a 48-well plate, with 5 pieces (D = 6mm) of each sample in each well. The coverage was that recommended by ISO 10993-12 (1,4 cm^2/mL). To each well, 1 mL of Dulbecco's Modified Eagle Medium (DMEM) supplemented with 20% fetal bovine serum (FBS) was added and incubated for 24 hours at 37°C and 5% CO_2 in a humid atmosphere. After that period, the medium that was in contact with the samples was filtered using 0.22 µm Millipore syringe filters. The obtained filtrate is called sample extract and was used to assess the cytotoxicity of the samples by the indirect method. In a 96-well plate, 150 µL of DMEM 20% FBS were added to each well. Then, 100 µL of the cell suspension at 105 cells/mL in DMEM 20% FBS were added in order to achieve a concentration of 104 cells per well. The plate was incubated at 37°C and 5% CO_2 in a humid atmosphere during 24h. After 24h, the DMEM was removed and 100 µL of phosphate buffer saline solution (PBS) was added to each well for washing. The PBS was immediately replaced by the membrane extract (200 µL per well) resulting in a total of 4 wells per extract of each type of membrane. The cells incubated without extracts was considered as a negative control group, the cells incubated with 20% DMSO (v/v) was considered as the positive control group. The plate, containing the extract of each type of membrane, the positive control, and the negative control group, was incubated for 24h at 37°C and 5% CO_2 in a humid atmosphere. Afterwards, the culture medium was removed from the wells and the cells were washed with 100 µL of PBS, which was immediately replaced by 100 µL of 3-(4,5- dimethylthiazol-2-yl)-2,5-diphenyltetrazolium bromide, referred to as MTT, solution at 0.5 mg/mL prepared in PBS and incubated for 3h at 37°C and 5% CO_2 in a humid atmosphere. After this period, the MTT solutions were carefully removed, so that the formazan salt could be preserved inside the well, followed by the addition of 100 µL of dimethyl sulfoxide (DMSO) to solubilize the salt. Finally, absorbance was measured approximately 30 minutes after the DMSO addition, at a wavelength of 540 nm in the Microplates Reader – Hybrid Multidetection Synergy H1, preceded by 3 minutes of plate stirring (410 cpm). The negative control group represented 100% of cell viability and the samples cell viability was calculated as the ratio between absorbance of the sample and that of the negative control group. All the samples were done in four replicates, and the results are presented as average values and standard deviations.

4.4.7 In vitro drug release study

Release studies for the two copolymers with loadings of 10, 30 and 50% ketoprofen were made as follows: 10 mg of the membrane was placed in 40 mL of phosphate buffer saline (pH 7.4) or acidic medium (pH 1.2) used as a dissolution medium. The samples were magnetically stirred at 100 rpm and at temperatures of 25ºC and 42ºC. Then, at suitable intervals, aliquots of 3 mL were removed from the dissolution vessel (replaced by a fresh one) and immediately analyzed with UV-visible spectrophotometer (Varian Cary 3 used to quantify the released ketoprofen concentration, and the average of two determinations was used to calculate the drug release from each of the formulations.

4.4.8 Analysis of Drug Release Profiles

To understand the release mechanisms and to compare the ketoprofen release profile of the different poly(NVCL-*co*-AA) fibers mats, independent [dissolution efficiency (DE)] and model-dependent (curve-fitting) approaches were used. KinetDS, free open-source software, was used to calculate the DE and to fit the release curves to the Korsmeyer–Peppas mathematical model [Table 4.1](Singhvi & Singh, 2011). Same software was also used to analyze the accuracy and prediction ability of the mathematical model by the calculation of the coefficient of determination (R^2), Akaikes's information criterion (AIC), and root mean-square error (RMSE) [Table 4.1] (Mendyk et al., 2012).

Table 4.1 Independent and Dependent Kinetic Model Applied to Analyze the Drug Release Data Approach

Approach	Method	Equation
Model-dependent	Empirical R^2	$R^2_{emp}= 1- \frac{\sum_{i=1}^{n}(yi_{obs}-yi_{pred})^2}{\sum_{i=1}^{n}(yi_{obs}-y_{AV})^2}$
	Akaike information criterion	$AIC= (2\times K) + n \times \left[\ln\left(\sum_{i=1}^{n}(yi_{obs} - yi_{pred})^2\right)\right]$
	Root-mean-squared error	$RMSE= \sqrt{\frac{\sum_{i=1}^{n}(yi_{obs}-yi_{pred})^2}{n}}$
Model-independent	Dissolution Efficiency	$DE= \left(\frac{\int_0^t Mtdt}{Mt_{max}\times t}\right) \times 100$

Mt is the amount of drug released in time t; K is the release constant incorporating structural and geometric characteristics of the drug-dosage form; n is the diffusional exponent indicating the drug-release mechanism; Mt_{max} is the maximum amount of drug released (=100%)

4.5 Results and discussion

4.5.1 Preparation of fibers containing ketoprofen

Polymer solutions containing ketoprofen at different concentrations had their viscosity, and surface tension evaluated prior to electrospinning. The values are listed in Table 4.2. Polymer solutions without ketoprofen were also prepared for both Poly(NVCL-*co*-AA) (80:20) and Poly(NVCL-*co*-AA) (70:30).

Table 4.2 Properties of Poly(NVCL-*co*-AA) (80:20) and Poly(NVCL-*co*-AA) (70:30) solutions with different ketoprofen concentrations

Ketoprofen Concentration (wt)	**Poly(NVCL-*co*-AA) (80:20)**		**Poly(NVCL-*co*-AA) (70:30)**	
	Viscosit (cSt)	Surface tension (mN/m)	Viscosit (cSt)	Surface tension (mN/m)
0%	840	9.9	550	12
10%	720	14.5	510	17.5
30%	570	15	470	18
50%	940	17	580	19

Then, fibers mats were electrospun from both copolymers Poly(NVCL-*co*-AA) (80:20) and Poly(NVCL-*co*-AA) (70:30) solutions containing different ketoprofen concentrations. The average fiber diameters in Figure 4.1 were obtained via Image J software from the cross-section SEM images of the fibers shown in Figures 4.2 and 4.3.

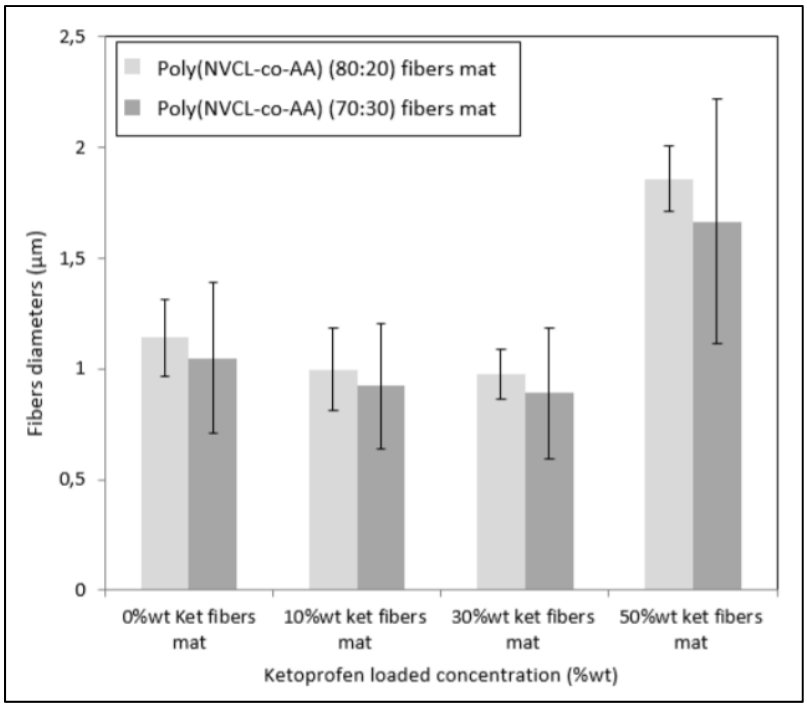

Figure 4.1 Average fibers diameter as a function of copolymer type and ketoprofen concentrations added to the fibers

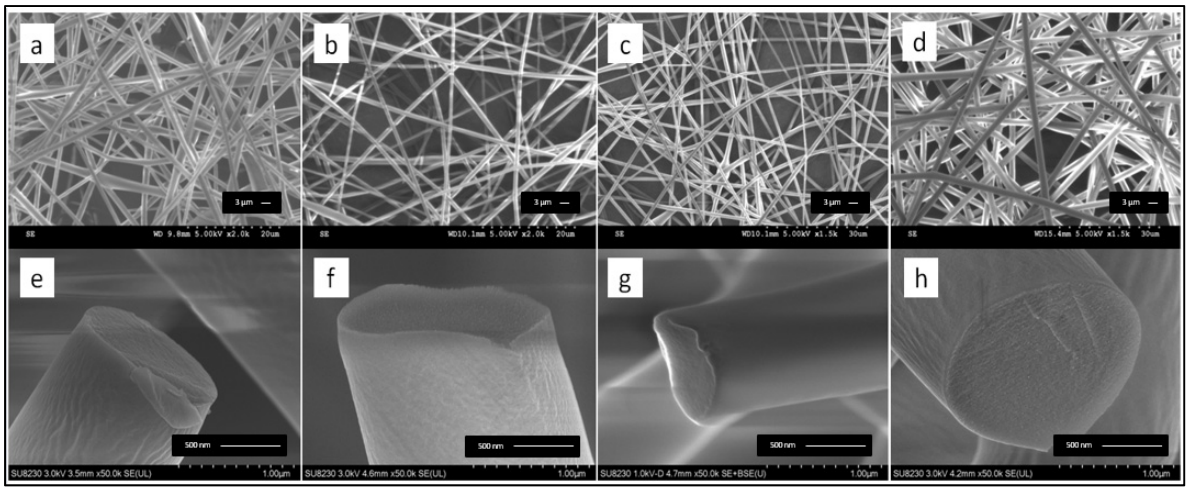

Figure 4.2 SEM images of Poly(NVCL-*co*-AA) (80:20) fibers with different ketoprofen concentrations: (a, e) pure poly(NVCL-*co*-AA) fibers, (b, f) poly(NVCL-*co*-AA) fibers with 10% ketoprofen, (c, g) poly(NVCL-*co*-AA) fibers with 30% ketoprofen and (d, h) poly(NVCLco-AA) fibers with 50% ketoprofen

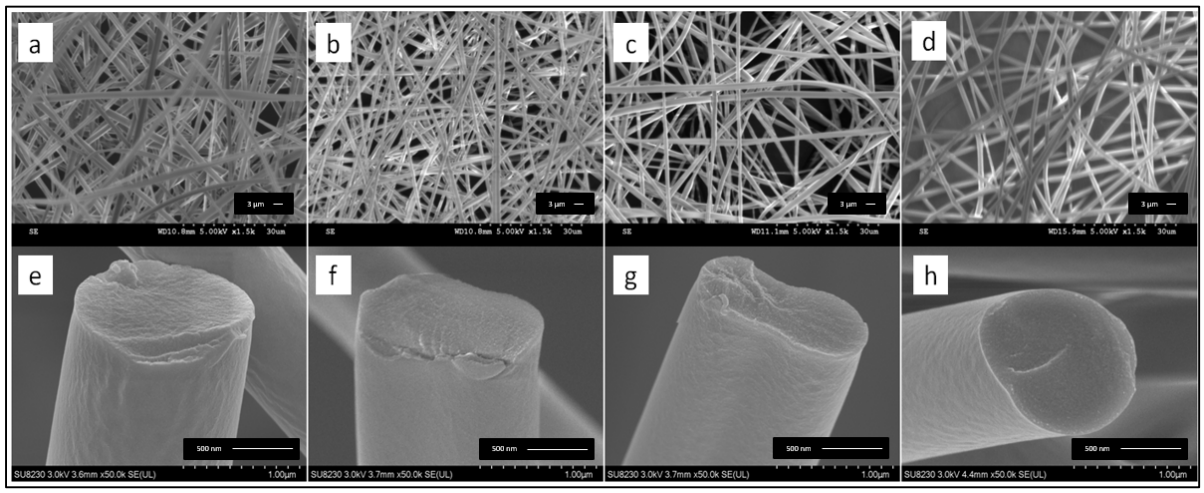

Figure 4.3 SEM images of Poly(NVCL-*co*-AA) (70:30) fibers with different ketoprofen concentrations: (a, e) pure poly(NVCL-*co*-AA) fibers, (b, f) poly(NVCL-*co*-AA) fibers with 10% ketoprofen, (c, g) poly(NVCL-*co*-AA) fibers with 30% ketoprofen (d, h) and poly(NVCL-co-AA) fibers with 50% ketoprofen

It can be seen that the copolymer and copolymer drug-loaded membranes yield beadless cylindrical fibers with smooth surface morphology and uniform diameter distribution. Ultra-high resolution SEM images (Figure 4.2 and 4.3, e-h) of the cross-section ketoprofen-loaded

fibers seem to indicate that no drug crystals were observed on the surface. This can indicate that the drug was well incorporated and dispersed into the fiber matrices. A slight difference of the mean fibers diameters was observed between the Poly(NVCL-co-AA) (80:20) and the Poly(NVCL-co-AA) (70:30) fibers mat. This slight difference can be related to the difference of electrospun solutions viscosity, varying from 570 to 940 cSt for Poly(NVCL-*co*-AA) (80:20), compared to Poly(NVCL-*co*-AA) (70:30), varying from 470 to 580 cSt. Increasing the loading amount of ketoprofen from 0%wt to 10%wt and 30%wt, the solution viscosity of Poly(NVCL-*co*-AA) (80:20) decreased (from 840 to 570 cSt) while its surface tension increased from 9.9 to 15 mN/m. This phenomenon can be attributed to the plasticizer effect of the ketoprofen for the copolymer chains decreasing the solution viscosity. A similar effect was reported in the research of Reda et al. using Eudragit fibers(Reda et al., 2017). In their research Reda shows that increasing the ketoprofen loading, the Eudragit fiber diameter decreased significantly as a consequence of a significant decrease in viscosity after adding the drug (Reda et al., 2017). Generally, the addition of ketoprofen which is a hydrophobic non-polar drug in the copolymer solution should decrease the surface tension. Such a behaviour was not observed in the present work. Indeed increasing the loading amount of ketoprofen from 0%wt to 30%wt resulted in an increase of surface tension of Poly(NVCL-*co*-AA) (80:20) and Poly(NVCL-*co*-AA) (70:30) solutions. This can be explained by the encapsulation of the non-polar hydrophobic ketoprofen by the hydrophilic part of the copolymers.

As the ketoprofen content increased to 50%wt from 30%wt, the average diameter of Poly(NVCL-co-AA) (80:20) ketoprofen loaded fibers increased as much as 1.85 ± 0.14 µm from 0.97 ± 0.11 µm, this can be attributed to the increase in viscosity of the electrospun solution (increases from 570 to 940 cSt). A similar effect was also observed with Park and Lee. In their paper Park reports that increasing the ketoprofen content to 3% from 0%, the average diameter of PLA/ketoprofen fibers decreased to as much as 1,530 nm from 2,747 nm, then, increased again to 1.765 nm with 8% of ketoprofen (Park & Lee, 2011). The sudden increase of the Poly(NVCL-co-AA) (80:20) solution viscosity with 50%wt

ketoprofen may indicate that the drug amount has reached saturation in the solution, which can significantly decrease the mobility of the macromolecules, and as a consequence increase the solution viscosity. The same phenomenon was also observed for Poly(NVCL-*co*-AA) (70:30) ketoprofen loading fibers.

4.5.2 Analysis of drug/polymer interaction

Fourier transform infrared (FTIR) analysis, differential scanning calorimeter (DSC) analysis, X-ray diffraction (XRD), and LCST measurements were also performed to verify drug trapping in fibers and the presence of drug/polymer interaction

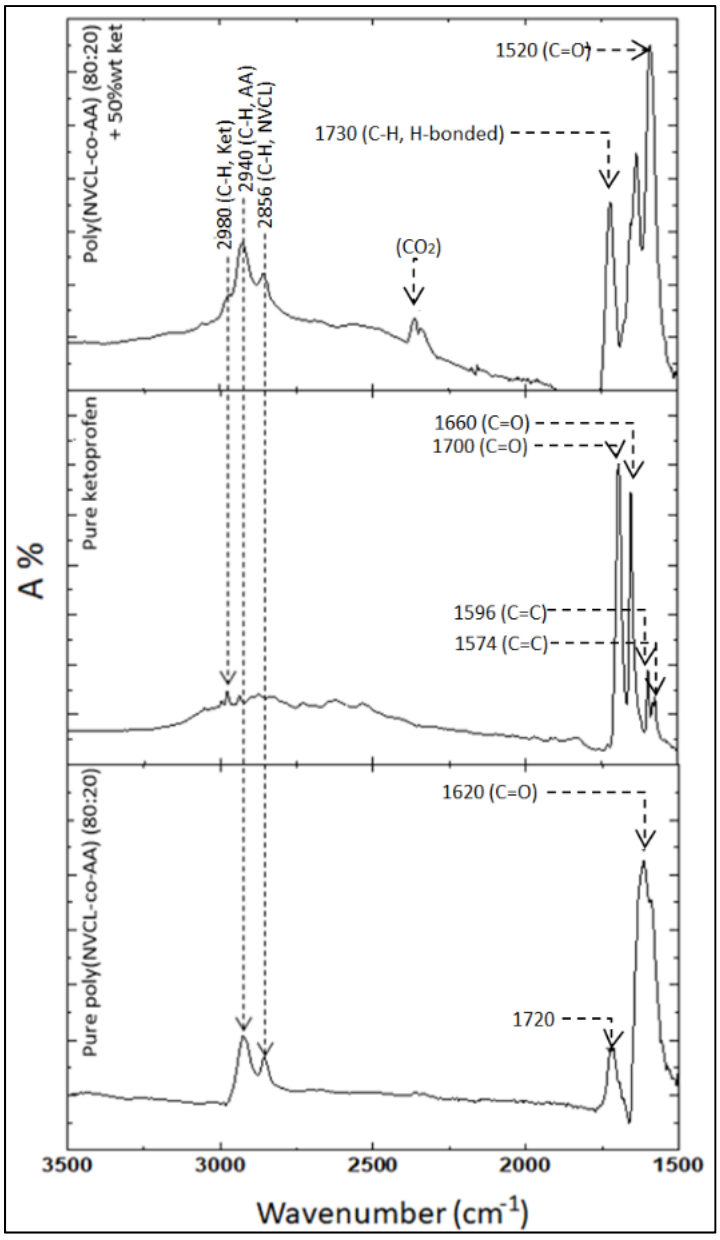

Figure 4.4 FTIR spectra of pure Poly(NVCL-*co*-AA) (80:20), pure ketoprofen and Poly(NVCL-*co*-AA) (80:20) with 50%wt ketoprofen

Figure 4.4 shows the FTIR spectra of pure Poly(NVCL-*co*-AA) (80:20), pure ketoprofen ,and 50%wt ketoprofen-loaded Poly(NVCL-*co*-AA) (80:20) fibers. Pure ketoprofen infrared

spectra present two characteristic peaks at 1660 cm^{-1} and 1700 cm^{-1} corresponding to (C=O) stretching bands. Peaks at 2980 and 2878 cm^{-1} indicating stretching vibrations of methyl (C–H) groups and peaks at 1596 and 1574 cm^{-1} can be attributed to (C=C) stretching of the aromatic ring (Yanshan Gao et al., 2017).

The spectra of Poly(NVCL-*co*-AA) (80:20) present absorption at 2940 cm^{-1} and 2856 cm^{-1} related to the aliphatic (-C–H) band of AA and NVCL respectively. The spectra of Poly(NVCL-*co*-AA) (80:20) fibers loading 50%wt ketoprofen show the absence of ketoprofen typical absorption peaks (1700 cm^{-1}). These missing peaks indicate the formation of hydrogen bonding between the polymer and ketoprofen molecules (1730 cm^{-1}). By interacting with the copolymer, ketoprofen molecules were less favorable to arrange in a regular way and to form a crystalline network (X. Wang et al., 2015)(J. Liu et al., 2014). The shift of carbonyl stretching band of Poly(NVCL-*co*-AA) from 1620 cm^{-1} to 1520 cm^{-1} and the disappearance of the stretching vibration of ketone group (1660 cm^{-1}) in pure ketoprofen can also be explained by the presence of molecular interaction between ketoprofen molecule and copolymer matrix. These findings demonstrate that there is good affinity between the drug and the carrier polymer. A small doublet was also seen at 2350 cm^{-1} and this is due to CO_2 molecules in the atmosphere (Park & Lee, 2011). Similar spectra were obtained with other ketoprofen concentrations and Poly(NVCL-*co*-AA) (70:30) loading fibers.

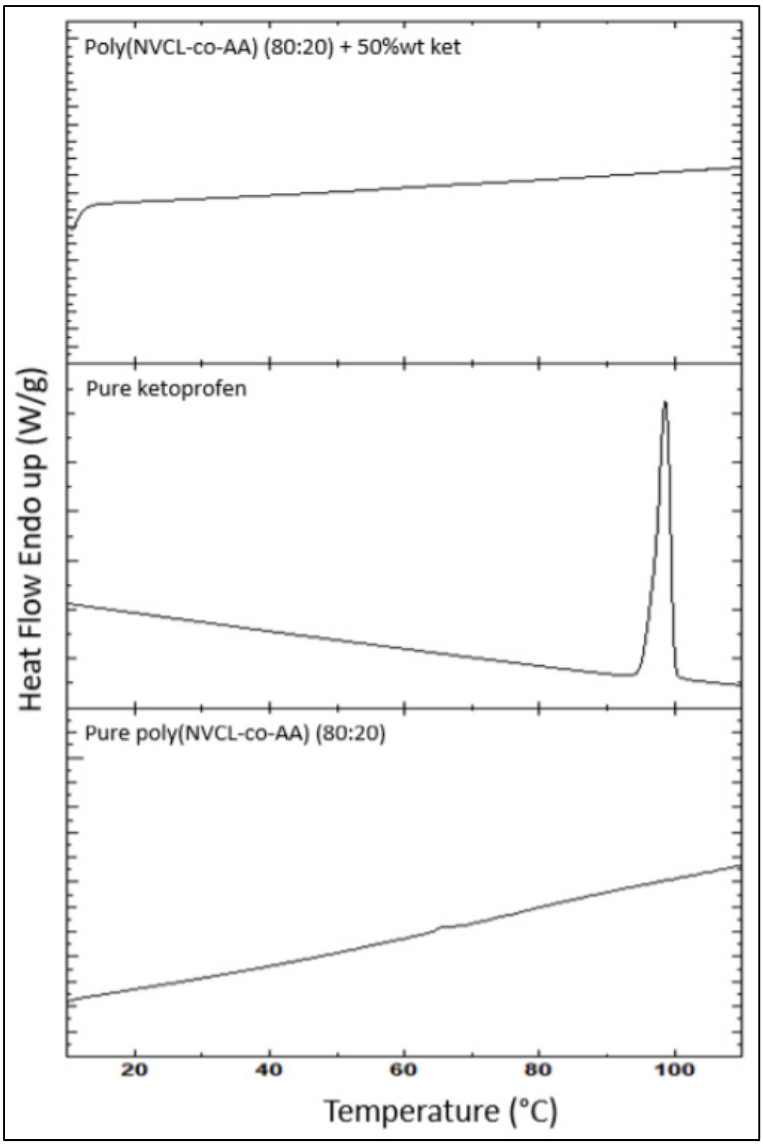

Figure 4.5 DSC curves of pure Poly(NVCL-*co*-AA) (80:20), pure ketoprofen and Poly(NVCL-*co*-AA) (80:20) fibers with 50%wt ketoprofen

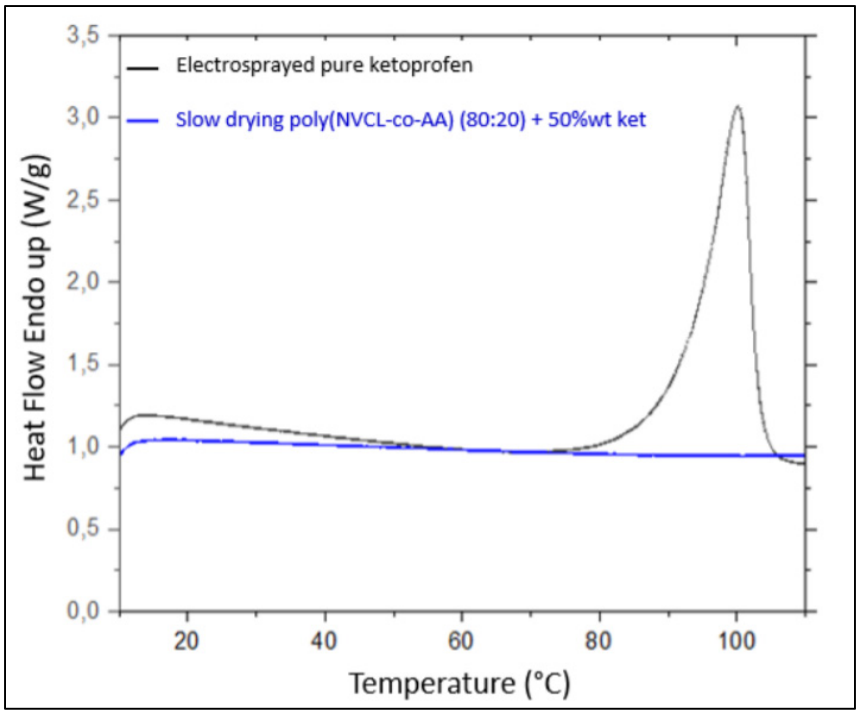

Figure 4.6 DSC curves of electro-sprayed pure Ketoprofen and slow drying Poly(NVCL-*co*-AA) (80:20) with 50%wt ketoprofen solution

Figure 4.5 shows the DSC thermograms of pure poly(NVCL-*co*-AA) powder, pure ketoprofen and the ketoprofen loaded fibers. Because poly(NVCL-*co*-AA) is an amorphous copolymer, its DSC curve did not show any phase transitions or endothermic response in the studied temperature range. Conversely, the DSC curve of the pure ketoprofen manifests an endothermic response at 98ºC corresponding to a fusion peak. DSC thermograms of the ketoprofen-loaded fibers did not show any fusion peak of the drug, which indicates that ketoprofen, was converted into an amorphous state during the electrospinning process. This can be explained by two hypotheses: one related to the electrospinning process and the high volatility of the solvents used and one related to the interaction between the drug and the copolymer, which may have prevented and slowed down the crystallization of ketoprofen. To confirm these hypotheses, DSC tests of slow drying of the ketoprofen/ poly(NVCL-*co*-AA) solution and ketoprofen electrospray powder were done. Figure 4.6 shows the DSC curves of

electro-sprayed pure Ketoprofen and slow drying Poly(NVCL-*co*-AA) (80:20) with 50%wt ketoprofen solution. The result of this test shows that the melting peak of ketoprofen disappeared even without electrospinning, which can confirm the interaction between the drug and the copolymer. This is in contrast to what is often mentioned in literature that the decline and the demise of ketoprofen's crystallinity, when encapsulated in fibers, is due to the electrospinning process and the volatility of the solvents (H. Li, Sang, et al., 2018)(H. Li, Sang, et al., 2018)(Seif et al., 2015). Maintaining the melting peak of electrosprayed ketoprofen powder shows that the electrospinning process or electrospray process is not the main and factor responsible for the decline in the drug crystallinity. Similar results were also obtained with other ketoprofen concentrations and Poly(NVCL-*co*-AA) (70:30) loaded fibers DSC curves.

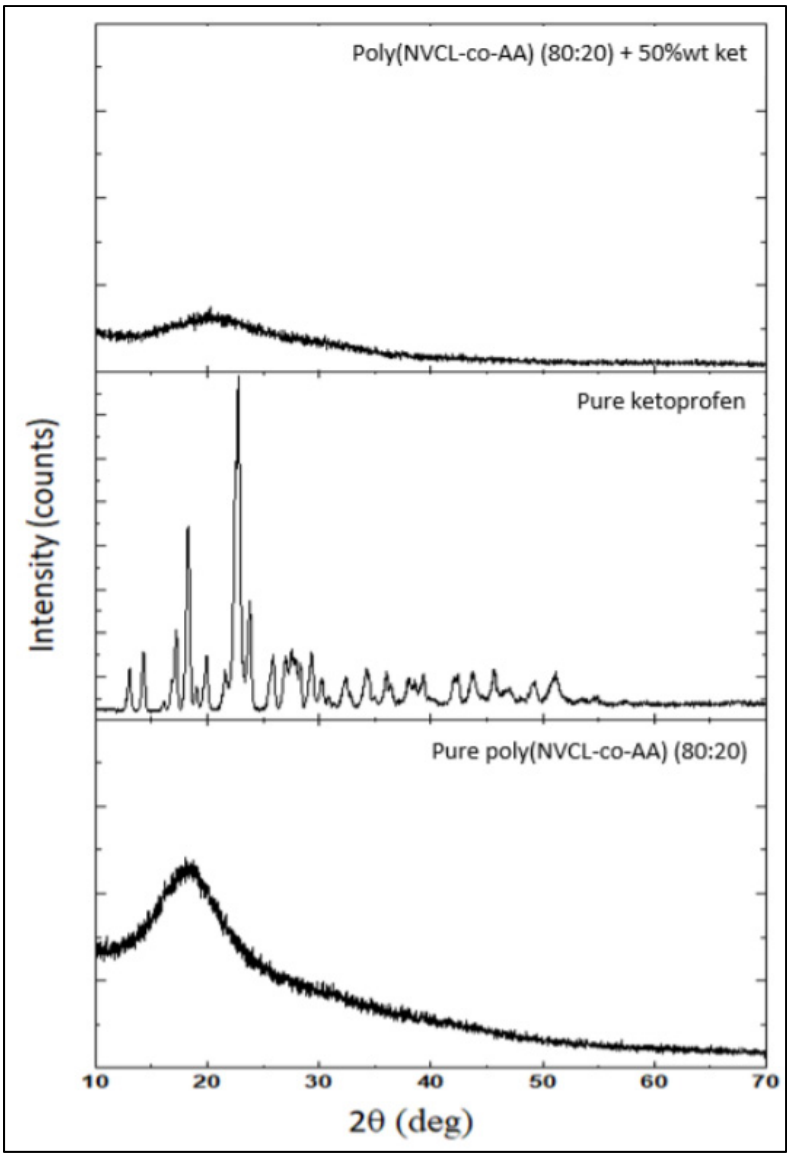

Figure 4.7 XRD patterns of pure Poly(NVCL-*co*-AA) (80:20), pure ketoprofen and Poly(NVCL-*co*-AA) (80:20) fibers with 50%wt ketoprofen

Figure 4.7 shows the XRD patterns of pure Poly(NVCL-*co*-AA) powder, pure ketoprofen and the ketoprofen-loaded fibers. X-ray diffraction of the pure ketoprofen shows numerous distinct reflections of the pure drugs which confirm the crystallinity of the pure drug. The pattern of amorphous Poly(NVCL-*co*-AA) (80:20) and Poly(NVCL-*co*-AA) (70:30) was

characterized by the absence of any diffraction peaks which confirm the non-crystallinity of the copolymers. Ketoprofen-loaded fibers patterns shows characteristic humps of amorphous forms in place of the ketoprofen characteristic reflections. Similar to the DSC results, the XRD results demonstrated that ketoprofen existed in amorphous forms in the Drug-loaded fibers.

Table 4.3 LCST Measurements of Poly(NVCL-*co*-AA) (80:20) and Poly(NVCL-*co*-AA) (70:30) with different ketoprofen concentration Fibers Mat

Copolymer	**Poly(NVCL-*co*-AA) (80:20)**				**Poly(NVCL-*co*-AA) (70:30)**			
Ketoprofen Concentration (wt)	0%	10%	30%	50%	0%	10%	30%	50%
LCST (ºC)	39	39	36	36	40	39	36	35

Table 4.3 presents the LCST of Poly(NVCL-*co*-AA) (80:20) and Poly(NVCL-*co*-AA) (70:30) with 0%wt, 10%wt, 30%wt and 50%wt ketoprofen concentration fibers mats. The LCST of the fibers mats was measured in distilled water by DSC. Increasing the ketoprofen concentration from 10% to 50% results in the decrease of loaded poly(NVCL-*co*-AA) fibers mats LCST from 39ºC to 35ºC. The decrease of the LCST can be explained by the hydrophobicity of ketoprofen. Mixing the poly(NVCL-*co*-AA) copolymers with a hydrophobic drug like ketoprofen makes it more hydrophobic, therefore, decreasing the transition temperature between the hydrophilic state and the hydrophobic state. In view of these results, the remarkable decrease in LCST confirms the copolymer drug interaction already seen by DSC and XRD.

4.5.3 Electrospun mats wettability

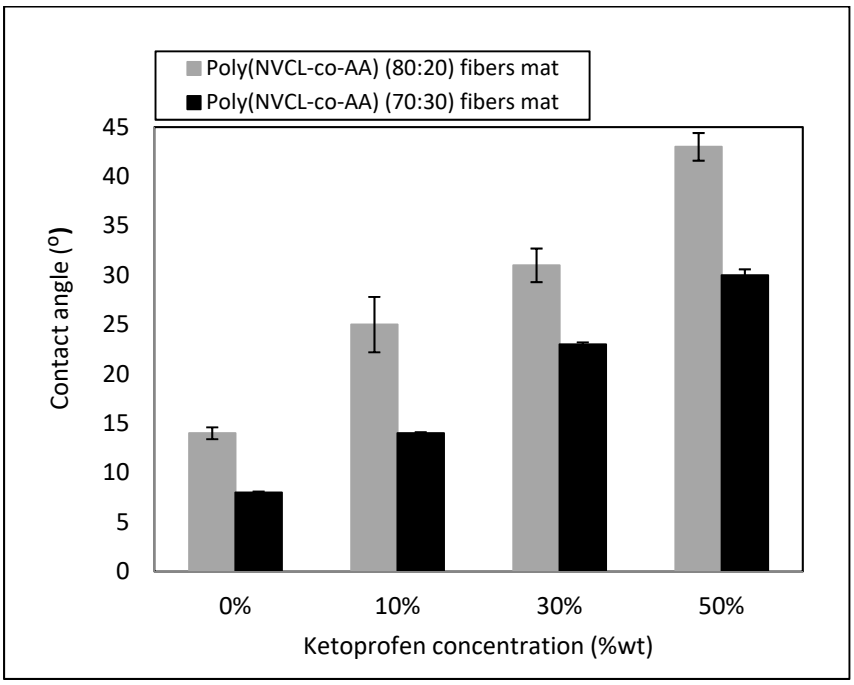

Figure 4.8 Average contact angle on electrospun Poly(NVCL-*co*-AA) (80:20) and Poly(NVCL-*co*-AA) (70:30) with different ketoprofen concentration fibers mat

Figure 4.8 presents the contact angle variation of a distilled water drop in pure Poly(NVCL-*co*-AA) (80:20), Poly(NVCL-co-AA) (70:30) fibers mats, and ketoprofen loaded fibers mats. The contact angle measurements show that the addition of the hydrophobic ketoprofen leads to an increase in the contact angle value formed by water drops on the surface of the membranes Poly(NVCL-*co*-AA) (80:20) and Poly(NVCL-*co*-AA) (70:30) especially with 50%wt concentration. This is in good agreement with the LCST results, the hydrophilicity of the membrane decreases as a function of increasing the ketoprofen concentration. However, the contact angle of the poly(NVCL-*co*-AA) with 50%wt of ketoprofen was 43° ± 1.4° for Poly(NVCL-*co*-AA) (80:20) and 30 ± 0.6° for Poly(NVCL-*co*-AA) (70:30), which is less than 90°. This confirms the hydrophilic nature of the membranes in spite of the non-solubility of the copolymers in water. The hydrogen bonding between the amide groups from

PNVCL segments and the non-ionized carboxylic groups from PAA segments makes the poly(NVCL-*co*-AA) copolymers non-soluble in water (Medeiros et al., 2017), but that does not reduce its wettability, which is critical in the biomedical field and specially in tissue engineering applications (Santana-melo et al., 2017).

4.5.4 Cell viability and cytotoxicity assays

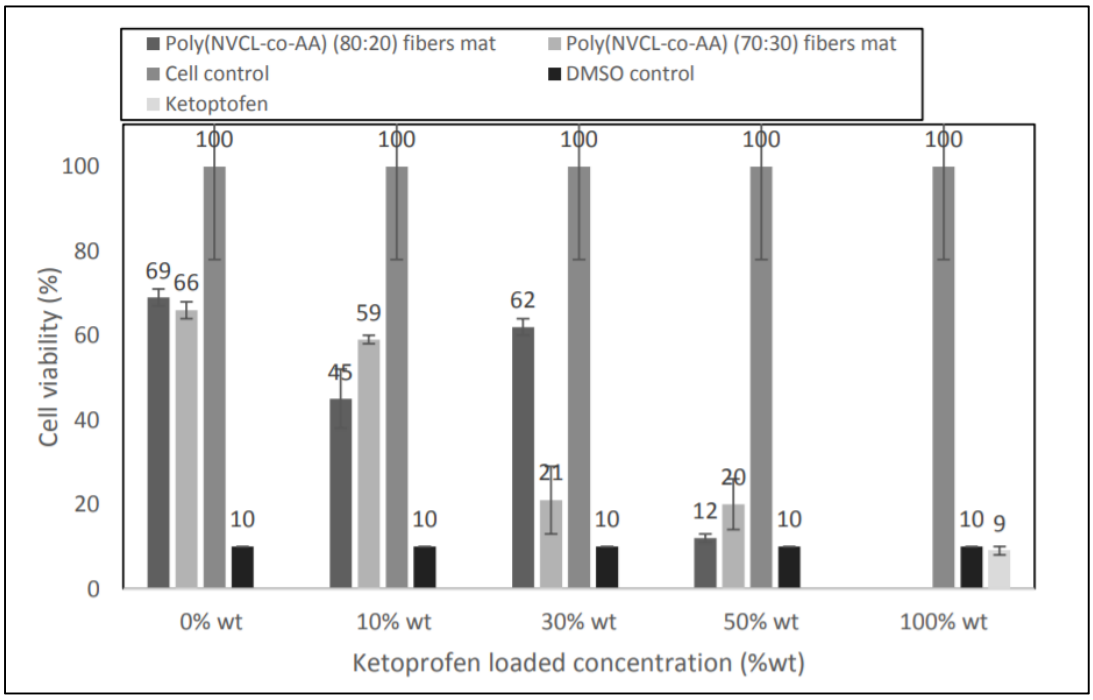

Figure 4.9 Cell viability of MEF cells incubated with Poly(NVCL-*co*-AA) (80:20) and Poly(NVCL-*co*-AA) (70:30) at different ketoprofen concentrations

Figure 4.9 shows the MTT cell viability performed for poly(NVCL-*co*-AA) fibers mat with 0%, 10%, 30% and 50%wt ketoprofen. It was observed that cell viability decreases with increasing the ketoprofen concentration. The cell viability percentage varies from 66% to 20% for Poly(NVCL-*co*-AA) (70:30) fibers mat, and little higher, from 69% to 12% for Poly(NVCL-*co*-AA) (80:20) fibers mat. These results can be explained by the high

cytotoxicity of the ketoprofen (9% of cell viability) and the percentage of AA in the copolymers. As expected, the cytotoxicity of Poly(NVCL-*co*-AA) (70:30) fibers mat without ket was higher than the cytotoxicity of Poly(NVCL-*co*-AA) (80:20) fibers mat without ket, and is due to the high proportion of the acrylic acid monomer (30 mol%) in the Poly(NVCL-*co*-AA) (70:30) compared to the Poly(NVCL-*co*-AA) (80:20) (20 mol%) (Medeiros et al., 2017). At the ketoprofen concentration of 10% wt with the copolymer Poly(NVCL-*co*-AA) (70:30) and 30% wt with the copolymer Poly(NVCL-*co*-AA) (80:20), the fibers mat could be considered as non-cytotoxic since the cell viability of MEF cells incubated with this sample for 48h was above 50%. Thus, these results suggest that the Poly(NVCL-*co*-AA) (80:20) and Poly(NVCL-*co*-AA) (70:30) fibers mat loaded with ketoprofen have considerable potential as a drug carrier.

4.5.5 Ketoprofen Entrapment and Release

Table 4.4 Ketoprofen Entrapment into poly(NVCL-*co*-AA) Electrospun Fibers Mats

Ketoprofen fibers mat		**EE (%)**
Poly(NVCL-*co*-AA) (80:20)	10% ketoprofen	100
	30% ketoprofen	96.4
	50% ketoprofen	94.5
Poly(NVCL-*co*-AA) (70:30)	10% ketoprofen	100
	30% ketoprofen	98
	50% ketoprofen	91

Table 4.4 presents the ketoprofen entrapment in the poly(NVCL-*co*-AA) containing 10, 30 and 50%wt ketoprofen. It can be seen that, for both copolymers sample the EE values were above 90%. With 10%wt ketoprofen loading, 100% of the drug was successfully encapsulated. However, increasing ketoprofen concentration results in decreased entrapment, which may be related to a limit concentration of ketoprofen within the fibers, exceeding of which results in excess of the drug remaining in suspension. These results confirm the use of electrospun fibers as a potential drug carrier as the amount of ketoprofen used during

formulations is almost totally encapsulated in the poly (NVCL-*co*-AA) fibers after electrospinning.

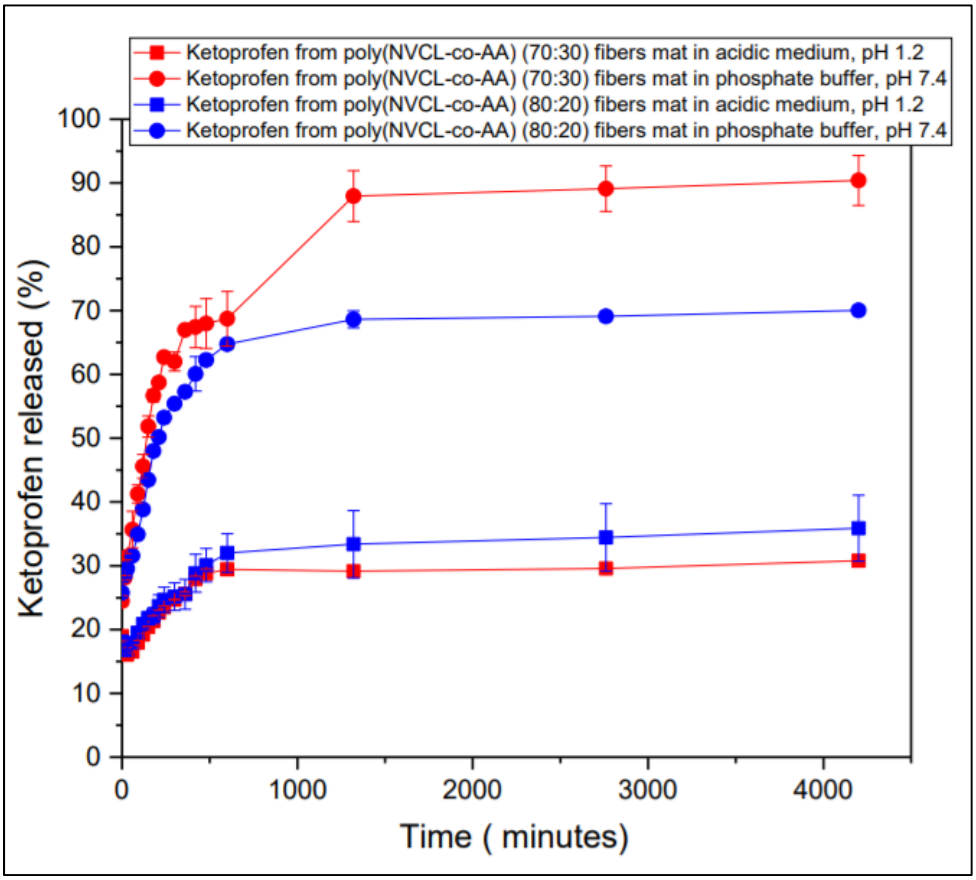

Figure 4.10a In vitro release profile of 10% wt ketoprofen from Poly(NVCL-*co*-AA) (80:20) and Poly(NVCL-*co*-AA) (70:30) fibers mats at 25°C in acidic medium, pH 1.2 and in phosphate buffer, pH 7.4

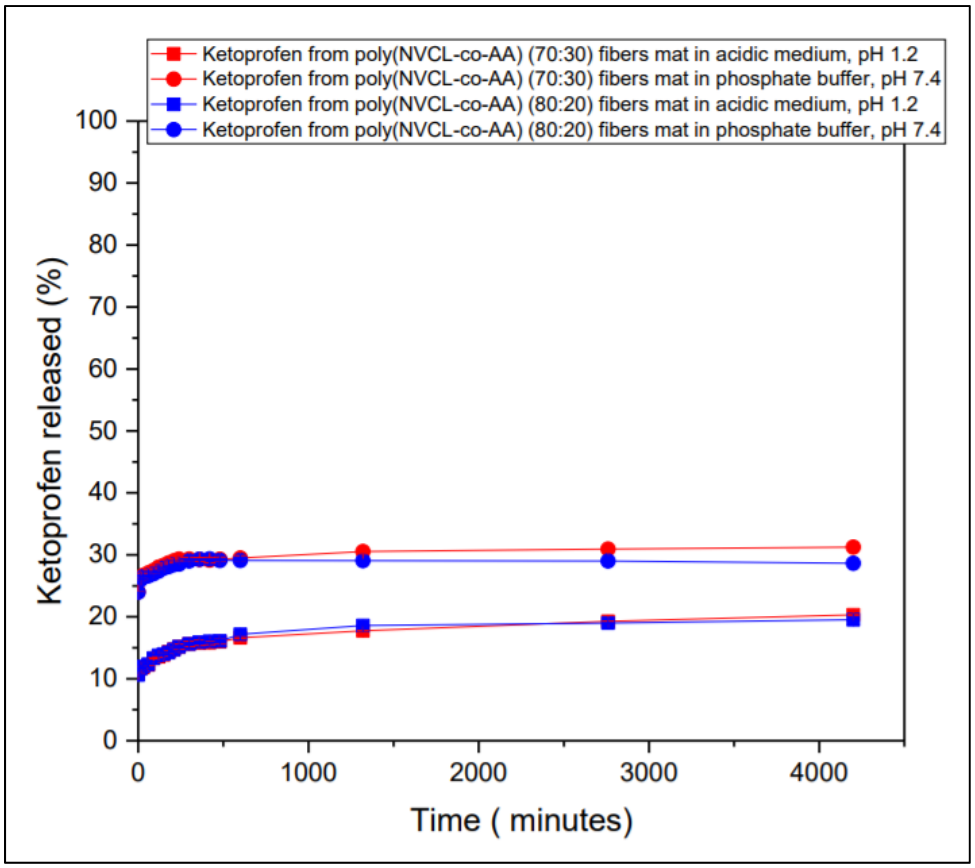

Figure 4.10b In vitro release profile of 10% wt ketoprofen from Poly(NVCL-*co*-AA) (80:20) and Poly(NVCL-*co*-AA) (70:30) fibers mats at 42ºC in acidic medium, pH 1.2 and in phosphate buffer, pH 7.4

Figure 4.10 (a,b) shows the ketoprofen in vitro release profiles as a function of time for two different poly(NVCL-*co*-AA) proportion fiber mats obtained in acidic medium (pH 1.2) and PBS (pH 7.4). The lines are just a guide for the eye. For each pH, two different temperatures were evaluated, 25ºC and 42ºC. Table 4.5 presents the quantitative interpretation of the values obtained in the dissolution assays using dissolution efficiency (DE) obtained after 4200 min to describe the release profiles. It can be observed that increasing pH from 1.2 (acidic medium) to 7.4 (PBS) generates an increase of the ketoprofen release rate from both Poly(NVCL-*co*-AA) (80:20) and Poly(NVCL-*co*-AA) (70:30) fibers mats. At 25ºC, the release rate increases from $DE_{4200} \cong 33\%$ at pH 1.2 to $DE_{4200} \cong 65\%$ at pH 7.4 for

Poly(NVCL-*co*-AA) (80:20), and from $DE_{4200} \cong 28\%$ at pH 1.2 to $DE_{4200} \cong 80\%$ for Poly(NVCL-*co*-AA) (70:30). The same behavior was observed at 42ºC, although to a lesser extent than at temperatures below LCST, confirming the positive effect of increasing the pH on the acceleration of the ketoprofen release from the fibers. Medeiros et al. (Medeiros et al., 2017) also studied the effect of pH on ketoprofen release from poly(NVCL-*co*-AA) spray-dried microparticles. The authors compared the release of ketoprofen from PNVCL and poly(NVCL-*co*-AA) spray-dried microparticles and concluded that pH was an important parameter governing the drug diffusion from the microparticles to the release medium mainly for poly(NVCL-*co*-AA) microparticles. In view the acidic nature of ketoprofen, pH also influences the water solubility of this drug (Medeiros et al., 2017). In general, insignificant difference in the release rate of ketoprofen from the two copolymers could be observed at the same temperature and pH conditions, as evidenced in Table 4.5. In addition to the pH, temperature is the parameter that most controls the diffusion of drugs from the poly(NVCL-*co*-AA) fibers into the release medium. It can be seen that ketoprofen release from both Poly(NVCL-*co*-AA) (80:20) and Poly(NVCL-*co*-AA) (70:30) fibers mats decreased when the temperature increased from 25ºC ($DE_{4200} \cong 80\%$) to 42ºC ($DE_{4200} \cong 30\%$) in pH 1.2 and 7.4 (Figure 4.10 (a,b), Table 4.5). Beside the temperature and the pH, the concentration of ketoprofen entrapped in the fibers also plays an important role in the drug release profile. It can be seen that the drug release decreases according to the increase of ketoprofen concentration in the fibers mat. At 42°C and pH 1.2, DE values of 18% were obtained for both copolymer Poly(NVCL-*co*-AA) (70:30) and Poly(NVCL-*co*-AA) (80:20) containing 10%wt of ketoprofen, 8% and 9% for copolymers Poly(NVCL-*co*-AA) (70:30) and Poly(NVCL-*co*-AA) (80:20) containing 30%wt of ketoprofen respectively and finally, 4% and 7% for copolymers Poly(NVCL-*co*-AA) (70:30) and Poly(NVCL-*co*-AA) (80:20) containing 50%wt of ketoprofen respectively. This remarkable decrease can be justified by the strong hydrophobicity of pure ketoprofen even at high temperature. Similar result was also reported by Medeiros et al. (2017), as the authors obtained a very low dissolution efficiency value ($DE_{240} \cong 2\%$) of ketoprofen released from poly(NVCL-*co*-AA)

microparticles with a ratio of (1:1) copolymer/drug, compared to the proportion of (2:1)(Medeiros et al., 2017).

4.5.6 Curve Fitting and Drug Release Mechanism

Table 4.5 Results of Curve Fitting and Kinetic Analysis of 10%wt Ketoprofen Release Data from Poly(NVCL-*co*-AA) (80:20) and Poly(NVCL-*co*-AA) (70:30) Electrospun Fibers Mats Using the Korsmeyer–Peppas Model and Dissolution Efficiency (DE) Obtained via Independent Model Analysis

Curve fitting parameters	**Poly(NVCL-*co*-AA) (80:20)**				**Poly(NVCL-*co*-AA) (70:30)**			
	25°C		**42°C**		**25°C**		**42°C**	
	pH 1.2	**pH 7.4**	**pH 1.2**	**pH 7.4**	**pH 1.2**	**pH 7.4**	**pH 1.2**	**pH 7.4**
R^2	0.93	0.92	0.97	0.90	0.92	0.93	0.98	0.69
RMSE	1.70	4.48	0.38	0.45	1.42	5.84	0.28	0.27
AIC	70.26	69.84	20.07	16.78	46.46	104.85	8.48	7.61
k (min^{-1})	9.96	16.77	8.46	23.68	10.03	15.89	8.32	23.99
n	0.16	0.18	0.10	0.03	0.14	0.23	0.11	0.03
DE	32.84	65.34	18.24	29.49	28.41	79.61	18.18	30.39

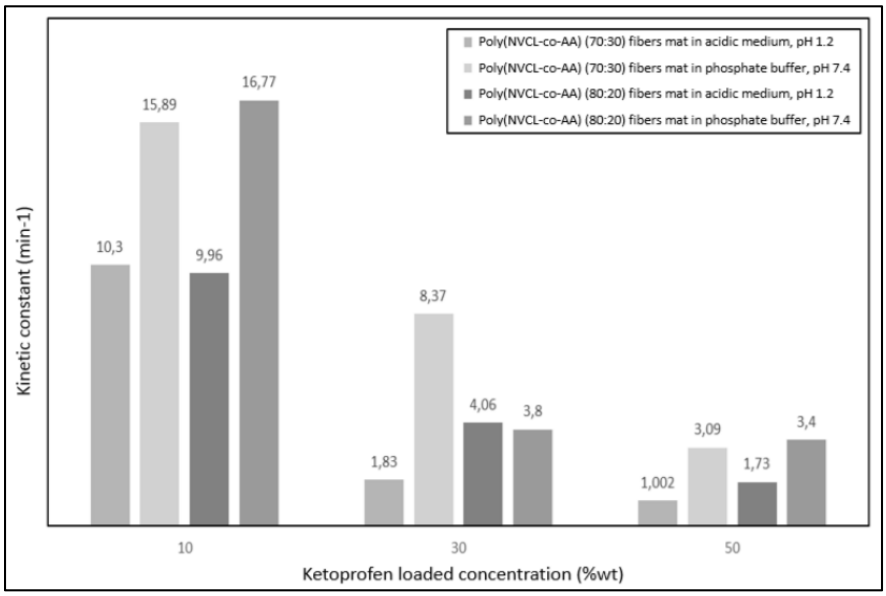

Figure 4.11a Kinetic constant of from Poly(NVCL-*co*-AA) (80:20) and Poly(NVCL-*co*-AA) (70:30) Electrospun Fibers Mats at 25°C in acidic medium, pH 1.2 and in phosphate buffer, pH 7.4

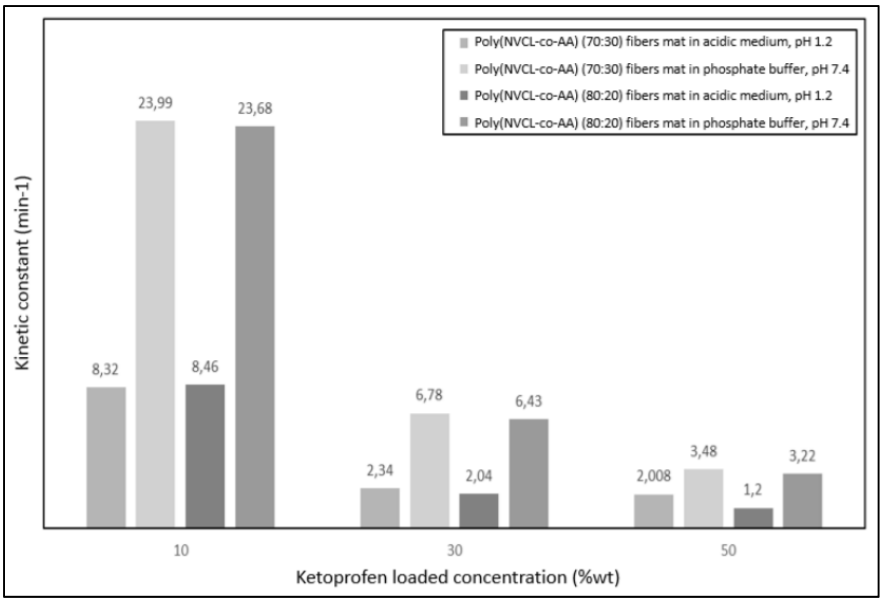

Figure 4.11b Kinetic constant of from Poly(NVCL-*co*-AA) (80:20) and Poly(NVCL-*co*-AA) (70:30) Electrospun Fibers Mats at 42ºC in acidic medium, pH 1.2 and in phosphate buffer, pH 7.4

Table 4.5 presents the coefficient of determination (R^2), root-mean-square error (RMSE), Akaike's information criterion (AIC), kinetic constant (k), which incorporates structural and geometric characteristics of the polymer system, and also the release exponent (n), which characterizes the mechanism of drug release. All these parameters were obtained from Kinet DS software by fitting the cumulative ketoprofen (until 4200 min) release to the Korsmeyer–Peppas (Table 4.1) model for dissolution experiments performed using poly(NVCL-*co*-AA) fibers mats at different temperatures, pH, polymer type and drug concentration to determine the mechanism of drug release. Figure 4.11(a,b) shows the kinetic constant (K) values as a function of ketoprofen loading concentration in poly(NVCL-*co*-AA) fiber mats obtained in acidic medium (pH 1.2) and PBS (pH 7.4). For each pH, two different temperatures were evaluated, 25°C and 42°C. Nonlinear regressions were applied for cumulative dissolved drug. The R^2 value close to unity indicates that the Korsmeyer–Peppas model is best adapted for the release kinetics of the poly(NVCL-*co*-AA) fibers mats containing respectively 20 and

30 mol% AA. The release exponent (n) characterizes the different release mechanisms, when the value n is higher than 0.5, this indicates that the diffusion of the release mechanism follows a non-Fick pattern (anomalous diffusion). And when value of n is less than 0.5 and close to 0 (flat system), this indicates that the release behavior resembles Fickian model (Sheng et al., 2006). For both temperature (25° and 42°C) and pH (1.2 and 7.4) values, the release exponent is less than 0.5; this indicates a Fickian diffusion mechanism for all formulations loading 10%, 30% and 50%wt of ketoprofen. In PBS (pH 7.4) and 42°C, the n values are exceedingly small, which implies that the approach to final equilibrium is extremely fast. In acidic medium, the release rate of ketoprofen (k) increased as the temperature decreased from 42°C to 25°C, and this can be explained by the increase of drug diffusion when temperature decreased (figure 4.11-a,b). Below LCST (25°C) and at pH 1.2, hydrogen bonds were formed between lactam seven-membered-ring of thermo-sensitive part of molecular chains and water molecules. This causes a strong hydrophilicity of the poly(NVCL-*co*-AA) fibers mats. As a result, copolymer molecular chain will relax and extend allowing free movement of drug which explains the higher release rates. Contrarily, above the LCST (25°C) poly(NVCL-*co*-AA) fibers mats display strong hydrophobicity. At this temperature and due to the vibration of a water molecule, hydrogen bonds are destroyed, and polymer-polymer interactions appear and as results the copolymers chain collapse, thus limiting the drug movement. In this case, drug release follows sustained release rate. However, in PBS, the release rate of ketoprofen (k) increased as the temperature increased from 25°C to 42°C, and this can be explained by the swelling of the PAA chain in pH 7.4. Even at temperatures above the LCST, varying from acidic medium to PBS medium, the PAA segments change from an agglomerated state to a swollen state. The ionization of carboxyl groups from PAA segments in PBS (pH 7.4) causes the dissociation of the polymeric complex and the swelling of the fibers under the effect of the electrostatic repulsion, which favors the diffusion of ketoprofen molecules. The same result was also obtained using 30% and 50%wt of ketoprofen loading fibers mats under the same condition. It can be seen that for the four in vitro drug release conditions, a burst release occurred at the beginning of the test, which can be related to the dissolution of ketoprofen molecules located

on the surface of fibers. In this work, another factor that affects drug release is the portion of hydrophilic acrylic acid monomers in the poly(NVCL-*co*-AA). During the synthesis process of the poly(NVCL-*co*-AA) copolymer, the portion of hydrophilic groups and hydrophobic groups was changed by adjusting the amount of AA monomers. As a result, a faster drug release ($DE_{4200} \cong 30.5\%$) was obtained in PBS and 42°C from the Poly(NVCL-*co*-AA) (70:30), compared with the release of ketoprofen from Poly(NVCL-*co*-AA) (80:20) at the same conditions ($DE_{4200} \cong 29\%$). At 42°C, decreasing the lactam seven-membered-ring hydrophobic portion of NVCL and increasing of hydrophilic –COOH proportion of AA leads to increasing of hydrophilicity of Poly(NVCL-*co*-AA) (70:30) compared to Poly(NVCL-*co*-AA) (80:20). This copolymer hydrophilicity helps the water molecules to enter into the fibers and as consequence diffusion of the ketoprofen when the AA portion is favored by its swelling. A similar effect was observed by Lin et al. using poly(NVCL-*co*-MAA) fibers (L. Liu et al., 2016). In their research, Lin et al. show that the rate of drug release increases with increasing portions of MAA in the synthesized Poly(NVCL-*co*-MAA). In their research, Yang et al. also show that PNVCL based copolymer (poly(NVCL-*co*-MAA)) effectively controlled the drug release of hydrophobic drug such as Nifedipine and could keep for more than 150 min (Yang et al., 2020).

4.6 Conclusion

In this work, it was possible to obtain membranes with smooth and continuous fibers by electrospinning poly(NVCL-*co*-AA) solutions containing respectively 20 and 30 mol% AA and loading different ketoprofen concentrations. The control of the fibers diameters, the drug crystallinity, LCST and hydrophobicity were also possible by electrospinning the polymers with 10%, 30% and 50%wt of ketoprofen. The decline in crystallinity of ketoprofen, when encapsulated in fibers, was found to be related to the drug-copolymer interaction and not to the electrospinning process, which contrasts with what is often mentioned in the literature. The drug entrapment was dependent on the ketoprofen concentration in fiber preparations

and 10%wt ketoprofen loaded fibers showed the highest EE value (100%). The release of the encapsulated drug was studied at two temperatures above and below the lower critical solution temperature (LCST) and two pHs above and below the pKa. A slight difference in drug release rate was observed between Poly(NVCL-co-AA) (80:20) and Poly(NVCL-co-AA) (70:30) depending on the tested medium. The ketoprofen in vitro release profiles of the two copolymers show rapid drugs release at a temperature below LCST compared with temperatures above. Above LCST, ketoprofen release was significantly slower, especially in acidic medium (pH 1.2). The rate and extent of drug release are slower for high concentration ketoprofen loaded fibers than for those containing only 10%wt ketoprofen. The drug release profiles were found to be highly influenced by the environmental temperature and pH, the portion of hydrophilic groups and hydrophobic groups in the copolymer, and the concentration of drugs. The results shown in this study reveal that the fibers electrospun from thermo and *pH*-sensitive copolymers may become potential systems for the encapsulation and controlled release of ketoprofen or other similar hydrophobic drugs model and to be used as drug delivery system.

4.7 Acknowledgments

The authors are grateful to the financial supports from the Natural Sciences and Engineering Research Council of Canada (NSERC), the University Mission of Tunisia in North America (MUTAN) and the Fundação de Amparo a Pesquisa do Estado de São Paulo (FAPESP) of Brazil.

CHAPTER 5

HYDROPHILIC DRUG RELEASE OF ELECTROSPUN MEMBRANES MADE OUT OF THERMO AND *pH*-SENSITIVE POLYMERS

Marwa Sta,[1] Dayane B. Tada,[2] Simone F. Medeiros,[3] Amilton M. Santos,[3] Nicole R. Demarquette[1]

[1]Department of Mechanical Engineering, École de Technologie Superieure
1100 rue Notre-Dame Ouest, Montréal, Québec, Canada H3C1K3
[2]Laboratory of Nanomaterials and Nanotoxicology, Universidade Federal de São Paulo
Rua Talim, 300 São José dos Campos, São Paulo, Brazil
[3] Department of Chemical Engineering, Escola de Engenharia de Lorena,Universidade de São Paulo, USP, Lorena, SP, Brazil

Paper submitted for publication, October 2021

5.1 Chapter outline

The goal of this third article is to respond to the third steps of the doctorate; Optimizing the electrospinning of two molar mass fractions a thermo-and *pH*-sensitive copolymer based on PNVCL in mixture with two concentrations of caffeine, hydrophilic drug model. In this article emphasis is placed on the interaction between the copolymer and the drug and its effect on the release of caffeine.

5.2 Abstract:

Electrospun fibers of the thermo-and *pH*-sensitive poly(N-vinylcaprolactam-*co*-acrylic acid) (Poly(NVCL-*co*-AA) loaded with 10% and 30 wt% caffeine (Caf) were obtained by electrospinning and evaluated as potential drug delivery systems. Caffeine was used as a hydrophilic drug model, and poly(NVCL-*co*-AA) containing either 20 or 30 mol% AA was used as a carrier. The fibers morphology, as well as, their interaction with caffeine, were studied using different analytical techniques. The cytotoxicity of the different obtained fibers

was evaluated by cell viability assays using 3-(4,5-Dimethylthiazol-2-yl)-2,5-Diphenyltetrazolium Bromide (MTT) and mouse embryonic fibroblasts cell line (MEF cells). Caffeine release was studied at temperatures of 25 ºC and 42ºC and pH of 1.2 and 7.4. Beadless copolymer fibers with diameters ranging from 1µm to 2µm were obtained. The addition of caffeine, which was in crystalline form after being encapsulated in the fibers, resulted in an increase of fiber diameter. The obtained membranes were found to be not cytotoxic. The entrapment of caffeine was greater for the copolymer containing 30 mol% AA due to a greater affinity of AA to caffeine. At a pH of 1.2 and at both temperatures of 25ºC and 42ºC, as well as, at a pH of 7.4 and a temperature of 42ºC, a Fickian diffusion mechanism for all copolymer fiber mats was observed. At a pH of 7.4 and 25ºC the release profile showed a high rate and followed a zero order model, due to the fast dissolution of caffeine in water. These results indicated that thermo and *pH*-sensitive poly(NVCL-*co*-AA) are promising candidates for controlled release of hydrophilic drugs.

5.3 Introduction

Electrospun fiber scaffolds are widely used in biomedical applications, especially in tissue engineering (Pawar et al., 2015)(Goh et al., 2013)(Ardila Nelson; Arkoun ,Mounia; Heuzey,Marie-Claude; Ajji,Abdellah; Panchal,Chandra J., 2016)(Kim Jeong-Hyun; Lee, Mi Hee; Kwon,Byeong Ju; Park, Jong-Chul, 2012), and delivery of pharmaceutical compounds (Sta et al., 2020)(Immich et al., 2017)(Ghafoor et al., 2018)(Liu et al., 2016). Indeed, these scaffolds, can be obtained with a large variety of polymers, are flexible and consist of micro-to nano-size fibers (Islam et al., 2019)(Calderón & Zhao, 2014), therefore providing a large surface area. All these properties make them interesting candidates for drug delivery systems. Concomitantly, in drug delivery systems, polymer-drug affinity is very critical because it determines the possible drug-loading amount, the drug dispersion within the carrier, and the drug release rate. In the particular case of electrospun fibers, their drug encapsulation can be achieved using different techniques such as mixing the drug in the to be electrospun polymer solution, attaching the drug to the fibers surface,

confining the drug in the fibers core or encapsulating it in nanostructures (Goh et al., 2013)(Islam et al., 2019)(Rezabeigi et al., 2017).

Thermo-sensitive and *pH*-sensitive polymers are materials that have attracted particular attention as drug delivery systems over the last decade or so (James et al., 2014)(Chakraborty et al., 2018) as they can present a variable affinity to chemical substances, depending on their temperature and pH environment. Thermo-sensitive polymers undergo distinct water soluble/non-water-soluble phase transitions at a specific temperature: lower critical solution temperature (LCST), or upper critical solution temperature (UCST). Poly(N-vinylcaprolactam) (PNVCL) is one of these thermosensitive polymers with an LCST of 32º C (Cortez-Lemus & Licea-Claverie, 2016)(Ward & Georgiou, 2011)(Sta et al., 2020). Being a nontoxic polymer compared to other thermo-sensitive polymers such as poly(N-isopropylacrylamide) (PNIPAm), PNVCL is a potential candidate for drug delivery systems (Vihola A; Valtola, L; Tenhu, H; Hirvonen, J., 2005)(Simone F. Medeiros et al., 2010). In addition to temperature-sensitivity, *pH*-sensitivity can be an interesting stimulus to control drug release in drug delivery systems (Li et al., 2018)(Dai et al., 2008). Furthermore, having polymers sensitive to both temperature and pH is even more advantageous. In the particular case of PNVCL, this is possible by incorporating acrylic acid (AA) segments, into the thermo-sensitive backbone (PNVCL), to obtain a thermo-and *pH*-sensitive copolymer such as poly(N-vinylcaprolactam-*co*-acrylic acid) (poly(NVCL-*co*-AA)) (Simone F. Medeiros et al., 2017). These thermo- and *pH*-sensitive copolymers are able to change their conformation quickly and reversibly, once in water, under the effect of temperature and pH simultaneously (Medeiros et al., 2017).

In this work, electrospun thermo-and *pH*-sensitive membranes were prepared by electrospinning two different poly(NVCL-*co*-AA) copolymers containing 20 and 30 mol% AA, respectively. The fibers were loaded with caffeine. Caffeine (Caf) is a model hydrophilic drug, highly soluble in aqueous solutions (Gaspar & Ramos, 2016) (Ullrich et al., 2015a)

(Ullrich et al., 2015b) The objective of the work was to study the electrospinability of the two copolymers to which 10% and 30 wt% caffeine was added, and to characterize the obtained membranes by evaluating their capacity to be used for controlled drug release. For that, the electrospinability of the systems was optimized, the influence of caffeine addition on the LCST of the copolymer was evaluated, the cytotoxicity of the obtained membranes was verified, and the drug entrapment efficiency and release quantified.

5.4 Experimental

5.4.1 Material

The copolymers used in this study, Poly(N-vinylcaprolactam-*co*-acrylic acid) (Poly(NVCL-*co*-AA) containing 17 and 28 mol% AA, were previously obtained and characterized in our research group (Medeiros et al., 2017). For the sake of simplicity, they are referred to 20 and 30 mol% [poly(NVCL-*co*-AA) (70:30) and poly(NVCL-*co*-AA) (80:20)], which corresponds to the desired molar ratios of the monomers introduced in the syntheses. Caffeine, a crystalline hydrophilic substance, was obtained from Sigma-Aldrich. Ethanol and N,N-Dimethylformamide (DMF) were also supplied by Sigma-Aldrich and used as solvents for the electrospinning process.

Poly(NVCL-*co*-AA) (70:30) and poly(NVCL-*co*-AA) (80:20), named for the sake of simplicity $P_{(70:30)}$ and $P_{(80:20)}$ in the rest of the manuscript.

5.4.2 Method

5.4.2.1 Synthesis and characterizations of poly(N-vinylcaprolactam-*co*-acrylic acid) (poly(NVCL-*co*-AA))

The synthesis and characterization of the $P_{(70:30)}$ and $P_{(80:20)}$ were reported by Medeiros et al. (2017). In summary, an initial acrylic acid mol% of 20 and 30 with 80 and 70 mol% of

NVCL, was used to synthesize the copolymers $P_{(70:30)}$ and $P_{(80:20)}$, respectively. The final AA mol% was assessed via titration and the chemical composition of the copolymers was further confirmed by Hydrogen Nuclear Magnetic Resonance (^{1}H NMR)(Medeiros et al., 2017).

5.4.2.2 Caffeine Entrapment and Electrospinning

Caffeine suspensions were prepared by adding 10 wt% and 30 wt% of caffeine powder to a mixture of ethanol and DMF in a ratio of 50:50 (v:v). Then, $P_{(70:30)}$ or $P_{(80:20)}$ in a 35 wt% and 45 wt% concentration, respectively, was dissolved in homogeneous caffeine suspensions for 3 hours using a magnetic stirrer at room temperature (21°C).

The obtained suspensions were electrospun using a commercial electrospinning machine (L100), produced by Bioinicia, Spain. The processing parameters were optimized and found to be 100 kV/m electric field, 2 mL/h flow rate, and10 cm working distance. The humidity and the temperature during the electrospinning were set at values ranging from 35% to 40% and 21°C, respectively.

5.4.2.3 Characterization of Electrospun Suspension

The kinematic viscosity and surface tension of the electrospun suspensions were measured using an Ubbelohde viscometer (Cannon Instrument Company, Zeitfuchs cross-ARM Viscometer) with 1.100 cSt/s constant and a pendant drop apparatus equipped with DROPFIT software (UMR 5257), respectively.

5.4.3 Membrane Characterization

After being coated with gold, the obtained membranes were characterized by scanning electron microscopy (SEM, Hitachi S3600N). Poly(NVCL-*co*-AA) membranes loaded with 0wt%, 10wt% and 30wt% caffeine, were also characterized with Ultra-high Resolution SEM

(HITACHI SU8230) to verify the presence of caffeine particles at the surface of the fibers. The diameter of the fibers was then evaluated using the Image J software.

Fourier transform Infrared spectrometer (FTIR, Perkin Elmer spectrometer) was used to verify the presence of trapped caffeine in the fibers, and the indications of caffeine-copolymer interaction. The spectra were collected using 1 cm^2 of the fiber's membrane and scans were taken over 3500–1500 cm^{-1} with a resolution of 2 cm^{-1} and an average of 32 scans.

Differential Scanning Calorimetry (DSC, Perkin Elmer differential calorimeter (Pyris 1)) was used to evaluate the crystallinity and LCST of the poly(NVCL-*co*-AA), and the caffeine loaded poly(NVCL-*co*-AA) membranes. The simples were heated from 10ºC to 110ºC at a heating rate of 15ºC/min under nitrogen atmosphere. Distilled water was used for the LCST measurement.

Wide-angle X-ray diffraction (XRD) measurements were performed on a Panalytical X'pert Pro X-ray diffractometer equipped with copper, CuKα, tube at 45 kV and 35 mA. Scans were performed in the 2θ range of 10–70°.

5.4.4 Cell viability assay

The membrane cytotoxicity was evaluated carrying out viability assays of mouse embryonic fibroblasts (MEF) cells incubated in the presence of the membranes. After cells incubation with copolymers membranes loaded with 0, 10 or 30wt% of caffeine, cell viability was measured using 3-(4,5-Dimethylthiazol-2-yl)-2,5-Diphenyltetrazolium Bromide referred to as (MTT) .

150 µL Dulbecco's Modified Eagle Medium (DMEM) containing 20% fetal bovine serum (FBS), followed by 100 µL of DMEM containing a cell suspension at 10^5 cells/mL were added to each well of a 96-well plate to achieve a final concentration of 10^4 cells per well. Then, the 96-well plate was incubated at 37 °C in a 5% CO_2 humid atmosphere during 24h. After 24h, the DMEM was removed using a micro-pipette, leaving the cells in the wells. 100 µL of phosphate buffer saline solution (PBS) was added to each well to rinse the cells.

Immediately PBS was removed using a micro-pipette and replaced by 250 µL of fresh culture medium (DMEM containing 20% FBS).

After that, membranes to be tested cut into 6 mm diameter round-shaped samples needed to meet the ISO 10993-12 (1.4 cm^2/mL) standard, were placed in contact with the cells inside each well. For comparison, a group of cells was incubated with an aqueous solution of caffeine at 1.5 mg/mL corresponding to the maximum caffeine concentration (30wt%) release. The plate containing the samples was then incubated again at 37 °C in a 5% CO_2 humid atmosphere during 24h. Afterwards, the culture medium was removed from the wells and the cells were washed with 100 µL of PBS, which was immediately replaced by 100 µL of MTT solution with a concentration of 0.5 mg/mL prepared in PBS. The plate containing the samples was then incubated again for 3h at 37 °C in a 5% CO_2 humid atmosphere. The MTT solutions were carefully withdrawn, so that the formazan salt could be preserved inside the well. 100 µL of dimethyl sulfoxide (DMSO) was then added to each well to solubilize the formazan salt and kept for 30 minutes.

Finally, the plate was stirred at 410 cycles per minute for 3 minutes and absorbance was measured at a wavelength of 540 nm in a Microplates Reader – (Hybrid Multidetection Synergy H1). Cells incubated in the absence of membrane samples were used as a negative control and cells incubated with 20% of DMSO were used as a positive control of cytotoxicity. Cell viability was calculated by using the average value of the absorbance at 540 nm of the negative control as 100 % viability. All the samples were used in four replicates and the cell viability values are presented as average values along with the standard deviation.

5.4.5 Caffeine Entrapment and Release

Two milligrams of caffeine-loaded membranes were dissolved in 40 ml of a basic solution pH 10 (aqueous solution of monosodium phosphate and sodium hydroxide) under magnetic stirring during 48h. The solutions were analysed as a function of time by UV-visible

spectroscopy (Varian Cary 300 Bio), using the characteristic absorption peak of caffeine at 273 nm.

The Encapsulation Efficiency (EE) was calculated as the ratio of the real amount measured by UV-visible spectrum, W_d, over the weight of caffeine used in the preparation of fibers mat, W_t, eq. (5.1):

$$EE\ (\%) = (W_d/W_t) \times 100 \quad (5.1)$$

5.4.6 In vitro Caffeine release study

The in-vitro release studies for 10 and 30 wt% caffeine loaded in $P_{(70:30)}$ and $P_{(80:20)}$ were made as follows:

First, the electrospun membrane (10 mg) was placed in the dissolution medium (40 mL) of phosphate buffer saline PBS (pH 7.4), or in an acidic medium of sodium chloride and hydrochloric acid in water (pH 1.2). The samples were then magnetically stirred at 100 rpm at two different temperatures: below the LCST at 25ºC and above the LCST 42ºC. Subsequently, aliquots of 3 mL were removed from the dissolution medium (at suitable intervals), and immediately replaced by a fresh ones, and analyzed with UV-visible spectroscopy (Varian Cary 300 Bio) at 273 nm. To quantify the released caffeine concentration and to calculate its release rate from each of the formulations, a calibration curve, and the average of two determinations were used respectively.

5.4.7 Caffeine Release Profiles

Two types of methods are commonly used to study the kinetics of controlled drug release from formulations: model-independent and model dependent. Model independent methods use a difference factor and a similarity factor to compare dissolution profiles and calculate the dissolution efficiency (DE). Model dependent methods describe the dissolution profile based on mathematical functions which are fitted to experimental data obtained from in vitro

drug release as a function of time (Table 5.1). Caffeine release profiles were analyzed using the independent [dissolution efficiency (DE)] and the model-dependent (curve-fitting) methods. KinetDS, free open-source software, was used to calculate the DE and to fit the release curves to several models. The Korsmeyer–Peppas model was found to give the best fit, eq (5.2) , eq (5.3), in Table 5.1 (Singhvi & Singh, 2011). KinetDS was used to analyze the accuracy and prediction ability of this model by calculating the coefficient of determination (R^2), the root mean-square error (RMSE), and the Akaikes's information criterion (AIC), eq (5.4), eq (5.5), in Table 5.1(Mendyk et al., 2012).

Table 5.1 Independent and Dependent Kinetic Model Applied to Analyze the Drug Release Data Approach

Approach	Method	Equation
Model-independent	Dissolution Efficiency (DE)	$DE = \left(\frac{\int_0^t Mtdt}{Mt_{max} \times t}\right) \times 100$ (5.2)
Model-dependent	Korsmeyer-Peppas	$\frac{M_t}{M_\infty} = k \times t^n$ (5.3)
	Best Model Criteria	$RMSE = \sqrt{\frac{\sum_{i=1}^{n}(yi_{obs} - yi_{pred})^2}{n}}$ (5.4) $AIC = (2 \times k) + n \times \left[\ln\left(\sum_{i=1}^{n}(yi_{obs} - yi_{pred})^2\right)\right]$ (5.5)

M_t is the amount of drug released in time t; k is the release constant incorporating structural and geometric characteristics of the drug-dosage form; n is the diffusional exponent indicating the drug-release mechanism; Mtmax is the maximum amount of drug released (=100%)

5.5 Results and discussion

5.5.1 Synthesis of Poly(NVCL-*co*-AA)

The synthesis and characterization of $P_{(80:20)}$ were done according to the method described in detail by Medeiros et al (2017). Briefly, the molar mass (*Mn*) and dispersity (*Đ*) were 6640 g/mol and 1.58, respectively. The content of AA in the poly(NVCL-*co*-AA) copolymer,

determined by titration and ^{1}H NMR, was found to be equal to 17 mol%, which is slightly below the percentage used in the feed (20 mol%). Finally, the LCST obtained via UV-vis was 39°C. For $P_{(70:30)}$ the molar mass (*Mn*) and dispersity (*Đ*) were 6247 g/mol and 1.59, respectively. For this copolymer the content of AA was found to be equal to 28 mol%, which is slightly below the percentage used in the feed (30 mol%), and the LCST was 40°C.

5.5.2 Preparation of caffeine containing fibers

5.5.2.1 Morphology and average diameters of the fibers

The viscosity, and surface tension of the polymer solutions containing caffeine in different concentrations were measured prior to electrospinning. The values are listed in Table 5.2. Polymer solutions without caffeine were also prepared for both poly(NVCL-*co*-AA) copolymers.

Table 5.2 Properties of $P_{(70:30)}$ and $P_{(80:20)}$ solutions with different Caffeine concentrations

Caffeine Concentration (wt)	**Poly(NVCL-*co*-AA) (70:30)**		**Poly(NVCL-*co*-AA) (80:20)**	
	Viscosity (cSt)	**Surface tension (mN/m)**	**Viscosity (cSt)**	**Surface tension (mN/m)**
0%	550	12	840	9.9
10%	590	9.8	860	13.3
30%	850	8.8	990	11.4

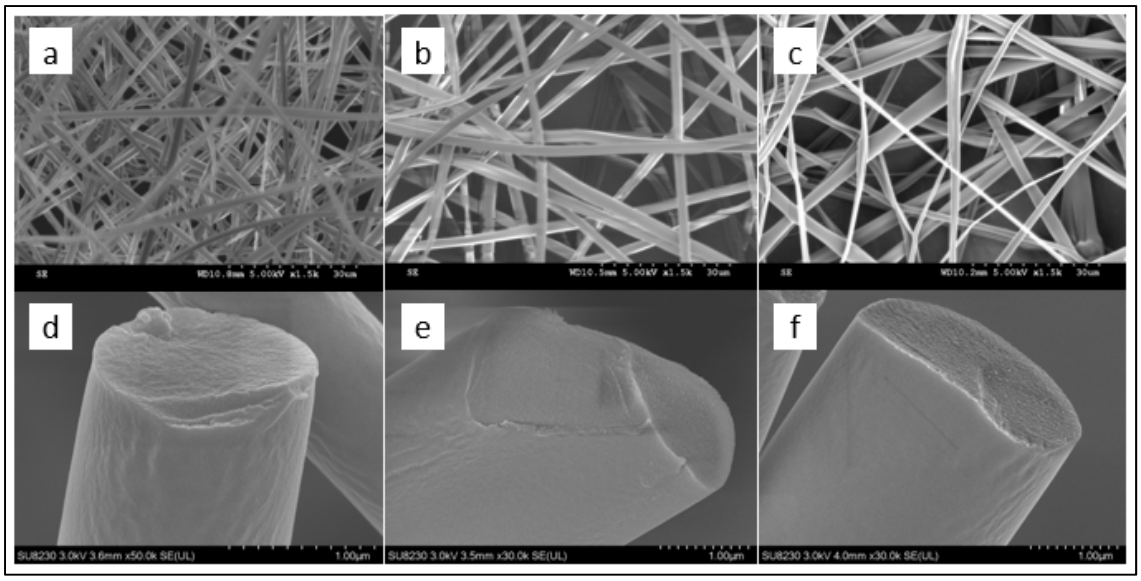

Figure 5.1 SEM images of $P_{(70:30)}$ fibers with different caffeine concentrations (a, d) Poly(NVCL-*co*-AA) fibers, (b, e) Poly(NVCL-*co*-AA) fibers with 10%wt caffeine, (c, f) Poly(NVCL-*co*-AA) fibers with 30wt% caffeine

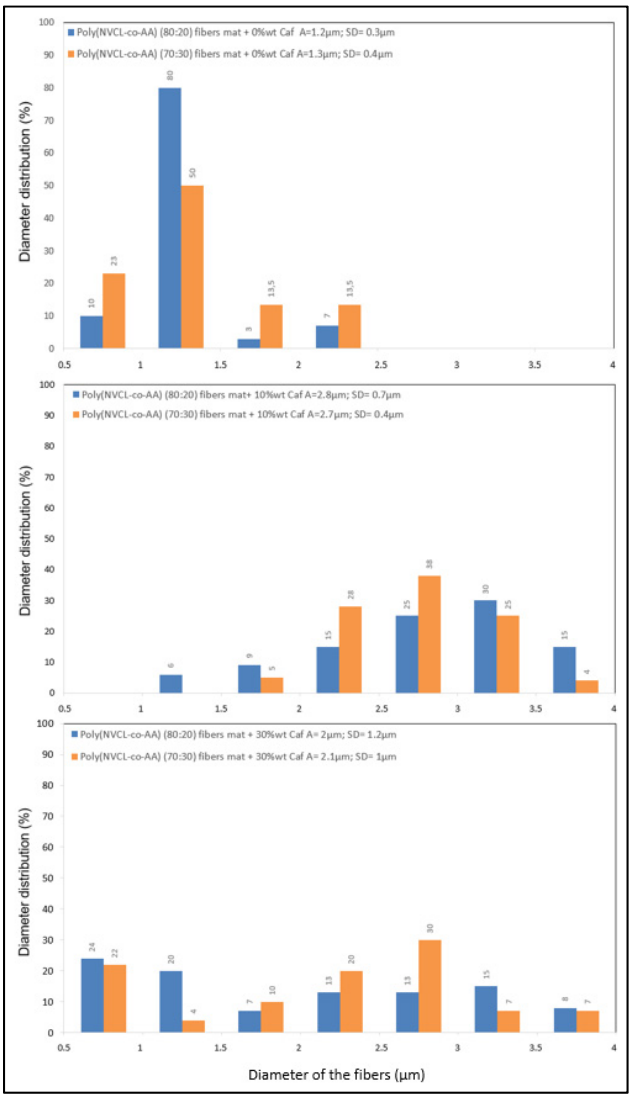

Figure 5.2 Fiber diameter distribution of $P_{(70:30)}$ and $P_{(80:20)}$ with 0 wt%, 10 wt% and 30 wt% caffeine loaded fibers concentrations

Figure 5.1 shows typical morphologies of $P_{(70:30)}$ electrospun fibers containing 0, 10 and 30wt% caffeine obtained in this work. Figure 5.2 reports the fiber diameter distribution for each type of fibers obtained.

It can be seen that electrospinning poly(NVCL-*co*-AA) without caffeine leads to beadless cylindrical fibers with a smooth surface morphology (Figure 5.1-a). In contrast, electrospinning poly(NVCL-*co*-AA) with caffeine leads to ribbon-like fibers. Ultra-high resolution SEM images (Figure 5.1, d-f) of the cross-section caffeine-loaded fibers seem to indicate the absence of caffeine crystals on the fiber surface. This indicates that the caffeine was, probably, incorporated inside the fiber matrix.

Incorporating caffeine into the fibers resulted in increasing the average fiber diameter from ~1µm to ~ 2µm (Figure 5.2). This was observed for both copolymers. This increase can be related to the increase of electrospun solutions viscosity, from 550 up to 850 cSt for $P_{(70:30)}$, and for $P_{(80:20)}$, from 840 up to 990 cSt, upon caffeine addition (Table 5.2). It can be observed (Figure 5.1) that increasing the loading amount of caffeine generated more deformation of the fiber morphology and non-homogeneity of its diameter. This phenomenon can be attributed to the low solubility of caffeine in Ethanol and DMF, and weak caffeine-copolymer interaction. A similar effect was reported in the research of Sóti et al. using polylactic acid (PLA) fibers (Sóti et al., 2015). In their research, Sóti et al. showed that by increasing the caffeine loading to 50% by weight, the PLA fibers lose there cylindrical shape and surface smoothness, which they attributed to the growth of crystalline regions inside the fibers (Sóti et al., 2015).

Although not shown here, the same phenomenon was also observed with $P_{(80:20)}$ caffeine loading fibers.

5.5.2.2 Fourier transform infrared spectroscopy (FTIR) analyses

Good affinity between a model drug and a polymer is important for the formation of smooth and homogenous fibers, and for a steady drug release. The interactions between the drug model and the polymer can be evaluated using IR spectroscopy.

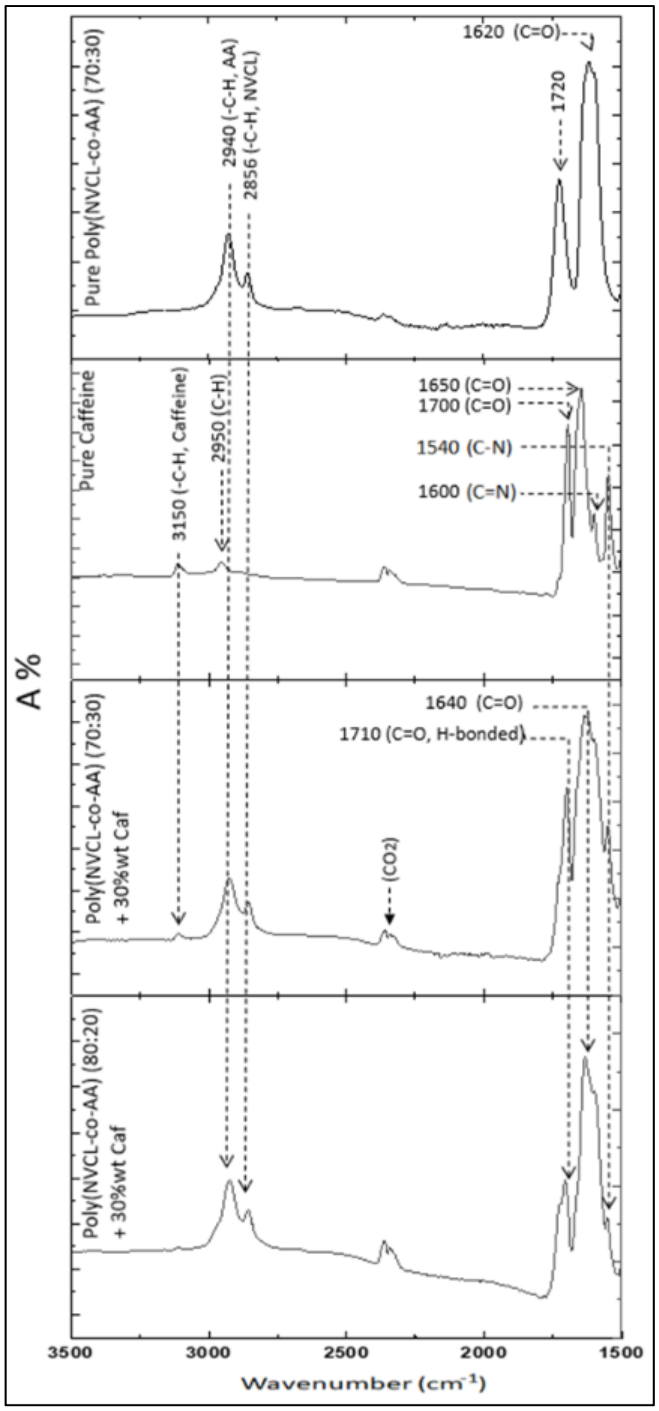

Figure 5.3 FTIR spectra of pure P $_{(70:30)}$, pure caffeine and P $_{(70:30)}$ and P$_{(80:20)}$ with 30 wt% caffeine

Figure 5.3 shows the FTIR spectra of pure $P_{(70:30)}$, pure caffeine and 30 wt% caffeine-loaded $P_{(80:20)}$ and $P_{(70:30)}$ fibers.

Pure $P_{(70:30)}$ infrared spectra present two characteristic bands at 1620 cm^{-1} and 1720 cm^{-1} corresponding to (C=O) stretching vibration, and two other bands at 2856 cm^{-1} and 2940 cm^{-1} corresponding to absorption and related to the aliphatic (–C-H) band of NVCL and AA, respectively.

The caffeine spectra show characteristic absorbance at 1700 cm^{-1} and 1650 cm^{-1} corresponding to (C=O) stretching of the amide group. Other bands were also observed around 1600 cm^{-1} and 1540 cm^{-1} assigned to (C=N) and (C-N) amide stretches (LAKSHMI V., 2011)(Paradkar & Irudayaraj, 2002). The bands at 2950 cm^{-1} and 3150 cm^{-1} may be ascribed to the asymmetric stretching of C-H bonds of methyl ($–CH_3$) groups in the caffeine molecule and the (C-H) stretching vibrations.

The spectra of $P_{(80:20)}$ and $P_{(70:30)}$ fibers to which 30 wt% caffeine was added, show the presence of the (C-N) stretches from caffeine at 1540 cm^{-1} which confirms a homogeneous encapsulation of caffeine into the fibers during electrospinning. The small shifts in band positions from 1720 cm^{-1} for the pure copolymers and 1700 cm^{-1} for the pure caffeine to 1710 cm^{-1} in the caffeine-loaded fibers may indicate the formation of a hydrogen bond between the copolymer and the caffeine molecules. The small shift of carbonyl stretching band of poly(NVCL-*co*-AA) from 1620 cm^{-1} to 1640 cm^{-1} also suggests that there may be a small intermolecular interaction between the caffeine and the copolymers (Sóti et al., 2015)(Illangakoon et al., 2014). A band at 2350 cm^{-1} is attributed to CO_2 molecules in the atmosphere (Park & Lee, 2011). The same results were obtained for the fibers loaded with 10wt% caffeine.

5.5.2.3 Differential scanning calorimeter (DSC) analyses

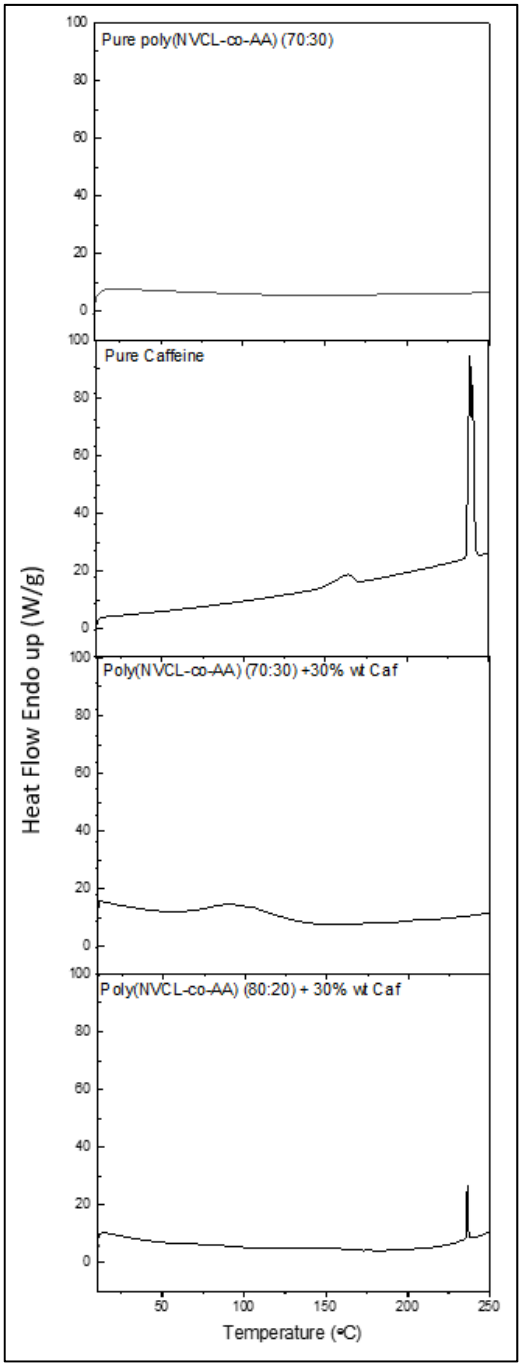

Figure 5.4 DSC curves of pure $P_{(70:30)}$, pure caffeine and $P_{(70:30)}$ and $P_{(80:20)}$ fibers with 30 wt% caffeine

Figure 5.4 shows the DSC thermograms of pure poly(NVCL-*co*-AA) powder, pure caffeine and the fibers of both copolymers loaded with 30wt% caffeine (Caf). The thermogram of the pure copolymer shows a typical amorphous polymer. The thermogram for pure caffeine presented the expected small endothermic peak at around 160ºC (phase transformation from Form II to Form I) and a large one at 238ºC (Hubert et al., 2011). The DSC thermograms of the 30 wt% caffeine-loaded $P_{(70:30)}$ fibers did not show any caffeine fusion peak, suggesting that caffeine was not in crystalline form in the fibers (Illangakoon et al., 2014). Similar curves were also obtained with 10 wt% caffeine-loaded $P_{(70:30)}$ fibers.

Conversely, the DSC thermogram of the 30 wt% caffeine-loaded $P_{(80:20)}$ fibers shows a caffeine melting peak (Form I) at 238ºC, which indicates the presence of caffeine in the crystalline state in the fibers. Similar curves were also obtained with 10 wt% caffeine-loaded $P_{(80:20)}$ fibers. These results may suggest that a better caffeine-copolymer interaction was obtained in the case of $P_{(70:30)}$ most likely due to the higher proportion of AA present in this copolymer compared to $P_{(80:20)}$.

5.5.2.4 X-ray diffraction (XRD) analysis

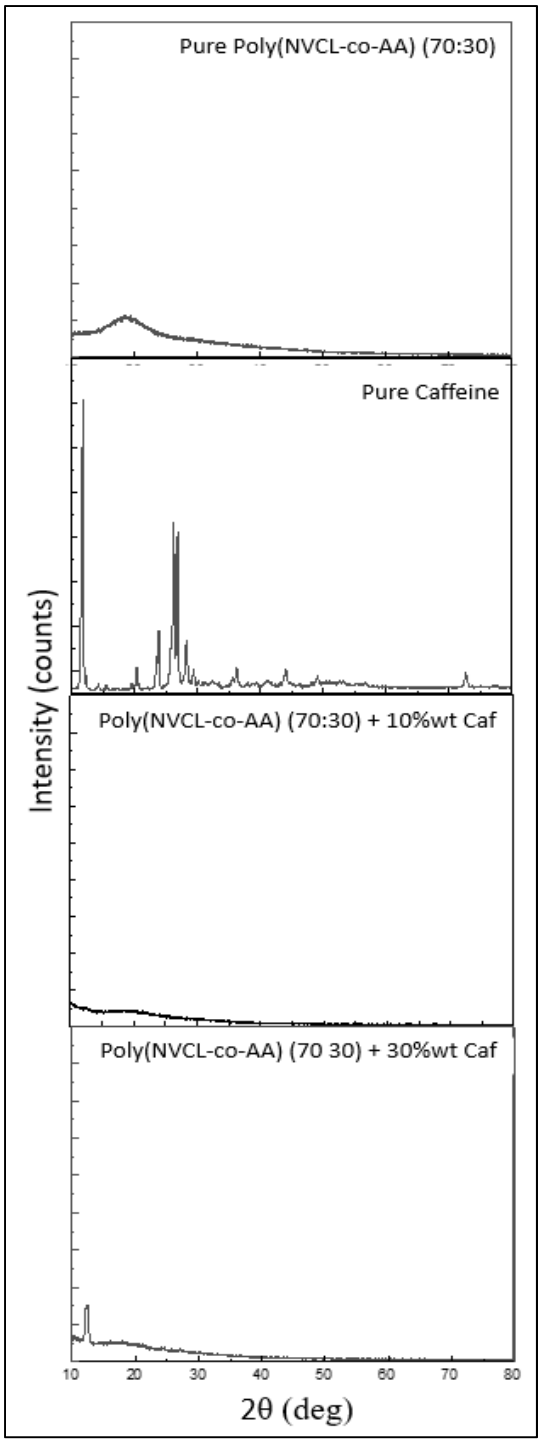

Figure 5.5 XRD patterns of pure $P_{(70:30)}$, pure caffeine and $P_{(70:30)}$ fibers with 10 wt% and 30 wt% caffeine

Figure 5.5 shows the XRD patterns of pure $P_{(70:30)}$ powder, pure caffeine and the caffeine-loaded $P_{(70:30)}$ fibers. The patterns of the caffeine-loaded $P_{(80:20)}$ for both concentrations have not been shown because they confrm the DSC results.

The pattern of fibers containing only pure $P_{(70:30)}$ showed absence of any diffraction peaks, only a broad halo was observed. This confirms that $P_{(70:30)}$ is an amorphous copolymer. The two characteristic diffraction peaks of caffeine appeared at 2θ angles of 11.25°, and 26.25° which confirms the crystallinity of the caffeine. In the pattern of 10 wt% caffeine-loaded fibers, the characteristic diffraction peaks of caffeine could not be observed. A characteristic hump of an amorphous materials was observed. This suggests that caffeine was present in amorphous form inside the fibers confirming the result obtained with the DSC (Illangakoon et al., 2014). However, the 30 wt% caffeine-loaded $P_{(70:30)}$ fibers pattern shows a diffraction peak at a 2θ angle of 11.25°, which indicates that caffeine maintains its crystalinnity during the electrospinning process. These results are different from what was obtained with the DSC, most likely due to the difference of sensitivity of both techniques, and this may be explained by the low dispersion of caffeine in the fibers and the lack of interaction between the copolymer and the caffeine at high concentrations. In a similar fashion Sóti et al. reported the XRD pattern of PLA fibers containing 10 wt% caffeine did not show any crystallinity, unlike the case of PLA containing 50wt% caffeine (Sóti et al., 2015).

5.5.2.5 LCST measurements

Table 5.3 LCST Measurements of $P_{(70:30)}$ and $P_{(80:20)}$ fibers mat with 0, 10 and 30 wt% of caffeine

Copolymer	**Poly(NVCL-*co*-AA) (70:30)**			**Poly(NVCL-*co*-AA) (80:20)**		
Caffeine Concentration (wt %)	0	10	30	0	10	30
LCST (°C)	40	41	41	39	40	40

Table 5.3 presents the LCST of $P_{(70:30)}$ and $P_{(80:20)}$ with 0 wt%, 10 wt% and 30 wt% caffeine concentrations. The increase of the caffeine concentration from 10% to 30%wt did not result

in a noticeable difference in LCST values within the limits of the experimental error, and this may be explained by the low caffeine-copolymer interaction.

5.5.3 Caffeine entrapment

Table 5.4 Caffeine Entrapment into Poly(NVCL-*co*-AA) Electrospun Fiber Mats

Caffeine fibers mat	**EE (%)**	
Poly(NVCL-*co*-AA) (70:30)	10 wt% Caffeine	98.8
	30 wt% Caffeine	100
Poly(NVCL-*co*-AA) (80:20)	10 wt% Caffeine	75
	30 wt% Caffeine	75

Table 5.4 presents the caffeine entrapment into $P_{(70:30)}$ and $P_{(80:20)}$ fiber mats. It can be seen that, the EE values for $P_{(70:30)}$ were above 98% for both 10 wt% and 30 wt% caffeine loading. This confirms the successful encapsulation of the caffeine into the fibers. However, this was not the case for $P_{(80:20)}$, for which only 75% caffeine was encapsulated with 10 wt% and 30 wt%. This may be related to lower of interaction between the copolymer $P_{(80:20)}$ and the caffeine, confirming the results of DSC, XRD and LCST. They, also, support the use of poly(NVCL-*co*-AA) electrospun fibers as a potential hydrophilic model carrier, since the amount of caffeine used during the formulations is almost totally encapsulated in the $P_{(70:30)}$ fibers during electrospinning. This emphasizes the importance of the drug-model affinity to the copolymer in the encapsulation process.

5.5.4 Cell viability and cytotoxicity assays

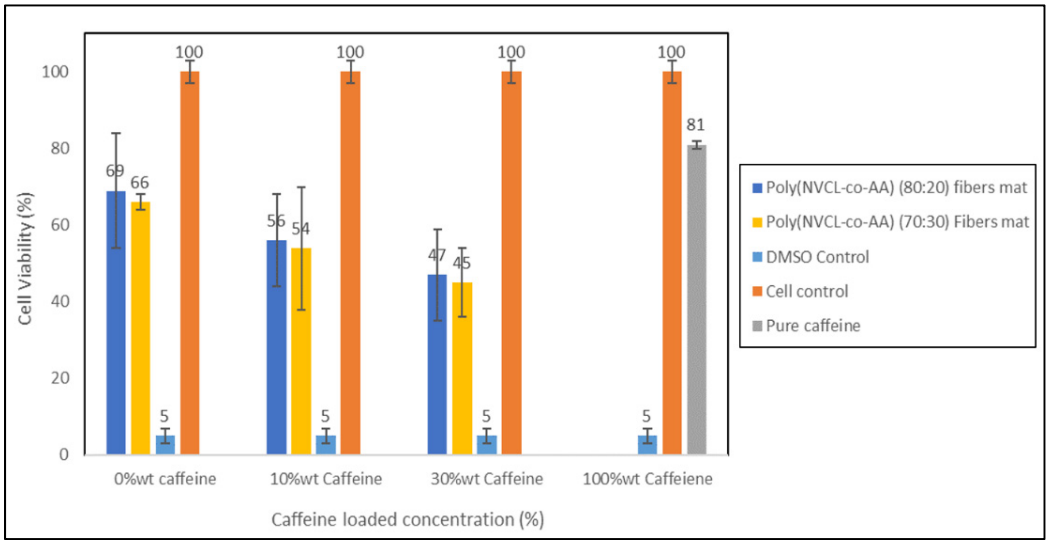

Figure 5.6 Cell viability of MEF cells incubated with $P_{(70:30)}$ and $P_{(80:20)}$ at different caffeine concentrations

Figure 5.6 shows the values of viability of MEF cells incubated in pure caffeine and poly(NVCL-*co*-AA) fiber mats containing 0%, 10%, and 30 wt% caffeine. For all the studied materials, the cell viability values were found to be lower than 70% indicating that the fibers are cytotoxic [ISO:10-953-5]. As expected, the cytotoxicity of $P_{(70:30)}$ and $P_{(80:20)}$ fiber mats without caffeine was quite similar, 69% and 66 %, respectively. Although the average cell viability values found in the cells, incubated with the fiber mats were lower than 70%, the copolymer poly(NVCL-*co*-AA) was reported by several authors to be a non-toxic material (Simone F. Medeiros et al., 2017). In most of these works, cytotoxicity was measured by the indirect method and different types of probes were used to measure cell viability. Herein, the cytotoxicity was assessed by the direct method, where the material was directly in contact with the cells that had grown on the bottom of the well plate. Therefore, it is reasonable to assume that the fiber mats disintegrated under incubation and, most probably, the small fragments had compromised the cell viability. The lowest values of cell viability were

observed in cells incubated with caffeine loaded fiber mats. These findings support our claim that the cytotoxicity observed in this assay was in fact a result of the fiber mats fragmentation. Therefore, considering that *in vivo* tissues would not be as fragile as in vitro cell culture, regarding small fragments of fiber mats, it would be possible to conclude that these results suggest that the $P_{(70:30)}$ and $P_{(80:20)}$ fibers mat loaded with caffeine have considerable potential as a caffeine carrier.

5.5.5 In vitro release study

The fibers prepared introducing 10 wt% caffeine (with respect to the polymer) during electrospinning were used to evaluate the kinetic behavior of the active ingredient.

Figure 5.7 (a,b) shows the caffeine in vitro release profiles as a function of time for the two poly(NVCL-*co*-AA) ratios in fiber mats obtained in acidic medium (pH 1.2) and PBS (pH 7.4). The lines are meant to be just a guide for the eye and not a result of a mathematical function. For each pH, two different temperatures were evaluated, 25ºC (figure 5.7-a) and 42ºC (figure 5.7-b). The choice of temperature and pH for each dissolution test was based on the copolymer LCST, i.e., below and above this parameter. For comparison, dissolution tests were, also, performed for pure caffeine at the same conditions as can be observed in Figure 5.8.
It can be seen from Figure 8 that fast pure caffeine dissolution was observed, over than 65 % within 20 seconds of the test, for all conditions, as a result of the high drug water-solubility. The caffeine dissolution was slightly favored by temperature, as expected.

By comparing Figure 5.7-a and b, the effect of temperature on caffeine release from $P_{(70:30)}$ and $P_{(80:20)}$ copolymers, mainly at pH 7.4, due to the thermo-sensitive behavior of PNVCL segments is clearly demonstrated. At this pH, the effect of PNVCL and PAA are similar, i.e., both segments are in a swollen state. For example, 100 % of caffeine was released from $P_{(70:30)}$ after 120 minutes, while at 42ºC, 72 %. For $P_{(80:20)}$, the release at 25 °C was 70 % and

at 42°C, (39%), which is related to the higher amount of PNVCL. Above the LCST, PNVCL chains tend to collapse into aggregates entrapping the caffeine molecules. In acidic medium (pH 1.2), the same trend was observed for both copolymer ratios, i.e., the caffeine release rate decreased as the temperature of the medium increased from 25 to 42°C. However, the difference in the release rate at the two evaluated temperatures was smaller at pH 7.4, compared with the same temperatures at pH 1.2. At pH 1.2, we have different competitive behaviors governing caffeine release. While the PNVCL segments change from a swollen to a collapsed state with increasing temperature, the PAA segments remain in a collapsed state due to the low pH. This difference in release rate at pH 1.2 at different temperatures is even smaller for the copolymer $P_{(70:30)}$ with higher amount of PAA. The results obtained in the present work are in good agreement with those obtained by Liu et al. (L. Liu et al., 2016), who studied the effect of temperature on captopril (hydrophilic drug) release from poly(NVCL-*co*-MAA) fibers. The authors evaluated the drug release at different temperatures above and below the lower critical solution temperature (LCST), and concluded that the drug release profiles were found to be greatly influenced by temperature.

Regarding the effect of pH on the release rate of caffeine from $P_{(70:30)}$ and $P_{(80:20)}$, the results clearly show that it, also, strongly influences the in vitro release kinetics of the active ingredient. Caffeine itself is a drug that has basic groups in its structure, and therefore, has a *pH*-dependent dissolution behavior, as shown in Figure 8. After 60 seconds of testing, the entire amount of the caffeine was dissolved at pH 1.2, while this percentage decreased to 92 % in pH 7.4. Concerning the caffeine release from $P_{(70:30)}$, at the same temperature (25ºC), it can be observed from Figure 7-a, that the caffeine release decreased from 100 to 46%, after 120 minutes, by changing the pH from 7.4 to 1.2. From $P_{(80:20)}$, the release percentage decreased from 70 to 53 %, by changing the pH from 7.4 to 1.2, at 25 °C and after 120 minutes of testing. These results evidence the effect of PAA segments on drug release. Similar results were reported by Sóti et al. (Sóti et al., 2015), who performed dissolution studies on releasing caffeine from PLA fibers. The results described by Eranka et al.

(Illangakoon et al., 2014) concerning the release of caffeine from polyvinylpyrrolidone (PVP) fibers, also, corroborates our results.

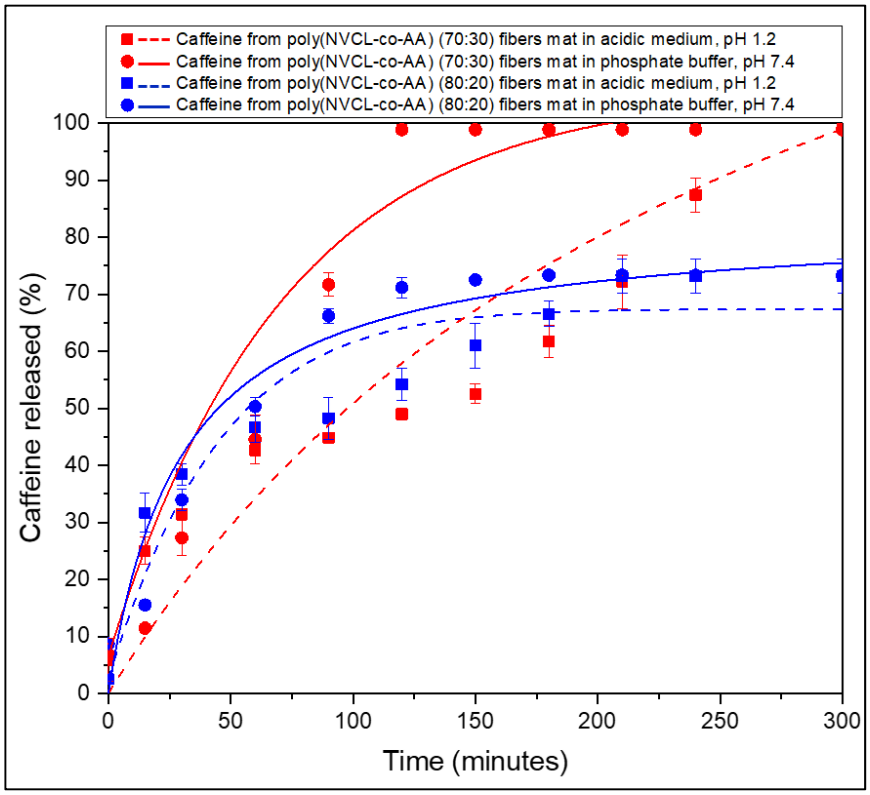

Figure 5.7a In vitro release profile of 10 wt% caffeine from $P_{(70:30)}$ and $P_{(80:20)}$ fiber mats at 25°C in acidic medium, pH 1.2 and in phosphate buffer, pH 7.4

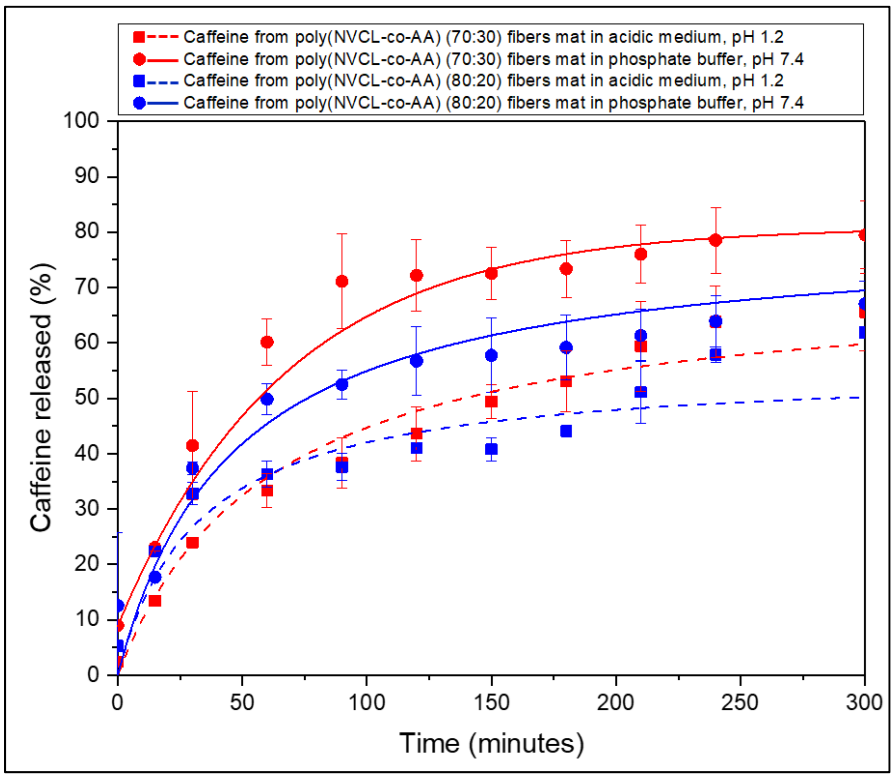

Figure 5.7b In vitro release profile of 10 wt% caffeine from $P_{(70:30)}$ and $P_{(80:20)}$ fiber mats at 42ºC in acidic medium, pH 1.2 and in phosphate buffer, pH 7.4

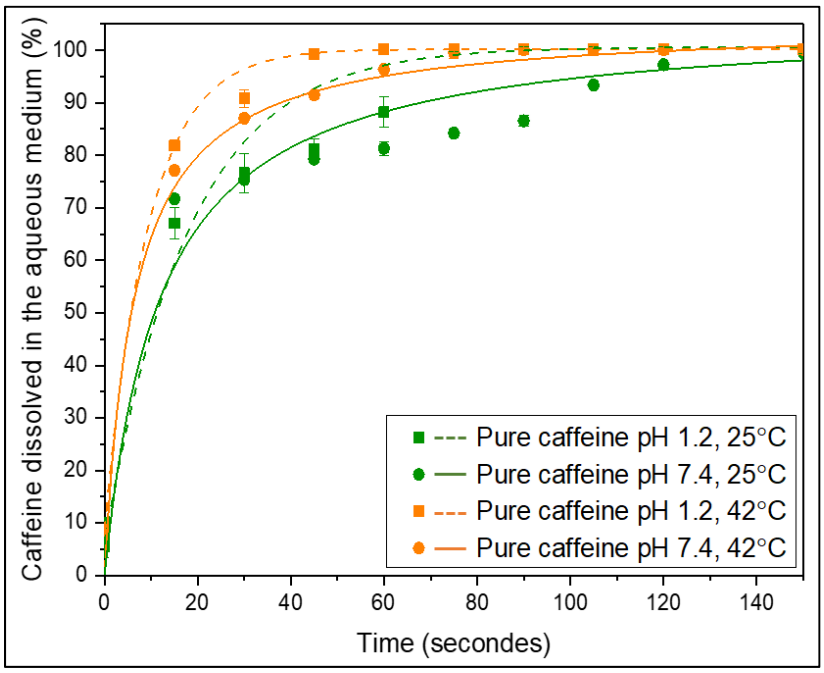

Figure 5.8 Dissolution rate of pure caffeine in acidic medium (pH 1.2) and phosphate buffer (pH 7.4) at 25◦C and 42◦C

5.5.6 Release mechanism

Due to the ability of poly(NVCL-*co*-AA) chains to swell or collapse as a function of temperature and pH variation, it was concluded that diffusion is the main mechanism governing the caffeine release from the fiber mats. To determine the mechanism of drug release, the cumulative drug (until 150 min) release from the poly(NVCL-*co*-AA) fibers was fitted to the Korsmeyer–Peppas model using KinetDS software. Table 5.5 presents the coefficient of determination (R^2), root-mean-square error (RMSE), Akaike's information criterion (AIC), kinetic constant (*k*), and the release exponent (*n*), obtained by a model-dependent method. In this model, the kinetic constant (k) incorporates structural and geometric characteristics of the polymer system, and the release exponent (n) characterizes the mechanism of drug release [eq. (1) and Table 5.2].

The dissolution efficiency (*DE*) values are also presented [eq. (5.2) and Table 5.1]; however, this parameter was calculated by a model-independent method.

From the dissolution experiments, the Korsmeyer–Peppas release model was found to best describe the release behavior of caffeine from poly(NVCL-*co*-AA) fiber mats at different temperature and pH. This is evident from the relatively high correlation values listed in Table 5.5. The kinetic constants (*K*) obtained for all release tests by a model dependent method can, also, be observed individually in Figure 5.9 for caffeine released from poly(NVCL-*co*-AA) fiber mats at 25 and 42 °C.

Table 5.5 Results of Curve Fitting and Kinetic Analysis of 10 wt% caffeine Release Data from $P_{(70:30)}$ and $P_{(80:20)}$ Electrospun Fiber Mats Using the Korsmeyer–Peppas Model and Dissolution Efficiency (DE) Obtained via Independent Model Analysis

Curve fitting parameters	**Poly(NVCL-*co*-AA) (70:30)**				**Poly(NVCL-*co*-AA) (80:20)**			
	25°C		**42°C**		**25°C**		**42°C**	
	pH 1.2	**pH 7.4**	**pH 1.2**	**pH 7.4**	**pH 1.2**	**pH 7.4**	**pH 1.2**	**pH 7.4**
R^2	0.98	0.98	0.97	0.95	0.98	0.94	0.85	0.90
RMSE	1.30	6.60	1.73	5.60	1.61	6.24	2.90	2.32
AIC	17.93	37.41	21.39	35.42	20.52	36.73	27.54	24.86
K (min^{-1})	10.60	0.94	3.45	6.17	15.45	3.02	13.35	24.38
n	0.32	0.95	0.53	0.53	0.26	0.66	0.244	0.18
DE	39.76	58.13	32.93	56.13	44.87	51.42	36.00	50.51

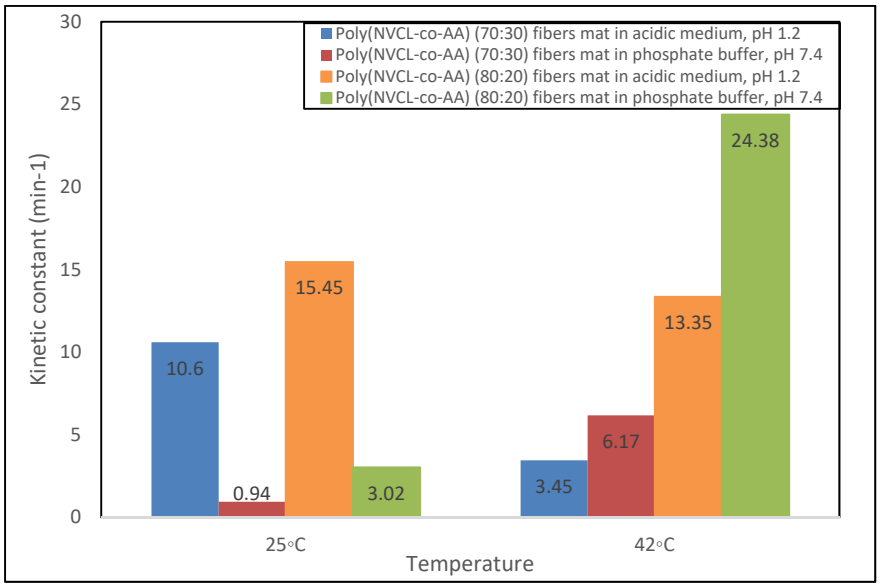

Figure 5.9 Kinetic constant of $P_{(70:30)}$ and $P_{(80:20)}$ Electrospun Fiber Mats at 25 °C and 42ºC in acidic medium, pH 1.2 and in phosphate buffer, pH 7.4

It can be seen from the data presented in Table 5.5 and Figure 5.9 that increasing the temperature from 25ºC (below the LCST) to 42ºC (above the LCST) leads to a decrease of the caffeine release rate (*K*) at pH of 1.2. Below the LCST, a fast release is expected due to the higher hydrophilicity of the poly(NVCL-*co*-AA) fiber mats even in acidic medium. At this temperature hydrogen bonds are formed between lactam seven-membered-ring molecular chains and water molecules, resulting in copolymer chain relaxation and free movement of the caffeine molecules. Above the LCST (42ºC), the copolymer chains collapse due to the polymer-polymer interaction and the loss of the hydrogen bonds caused by the water molecules vibration. This limits the caffeine molecules movement, and as a consequence sustained release rates were obtained. Unlike the acidic medium, the caffeine release rate (*K*) increased when the pH is 7.4, which can be related to the swelling of the PAA chains. Changing the releasing condition from acidic medium to PBS medium (basic), the PAA segments change from an agglomerated state to a swollen state. In PBS (pH 7.4) the

ionization of carboxyl groups from PAA segments causes the dissociation of the polymeric complex, and the fibers swell under the effect of electrostatic repulsion.

The R^2 values higher than 0.9 obtained for both copolymers $P_{(70:30)}$ and $P_{(80:20)}$ release kinetics indicate that the Korsmeyer–Peppas model predicts the data with good accuracy. However, the fact that these values were not in all cases very close to unity also indicates that diffusion is not the only release mechanism governing the kinetics of caffeine release from the fiber mats. Moreover, it is known that release exponent (*n*) values higher than 0.5, mean that the diffusion release mechanism follows a non-Fickian pattern (anomalous diffusion). When *n* is smaller than 0.5 and close to 0 (flat system), this means that the release behavior resembles a Fickian model (Singhvi & Singh, 2011)(Sheng et al., 2006). For all dissolution conditions except 25ºC combined with pH 7.4, the release exponents were equal to or smaller than 0.5, indicating a Fickian diffusion mechanism for all formulations. However, at 25ºC and at a pH of 7.4, release mechanism can be described by a zero order model and this is due to the fast dissolution of caffeine in water, as well as, the strong hydrophilicity of the poly(NVCL-*co*-AA) fiber mats, at this condition. The discussed effect of temperature and pH on caffeine release from fiber mats can be, once more, evidenced by observing *DE* values obtained by a model-independent method. In summary, the increase in temperature results in reduced *DE* for the same pH conditions. On the other hand, the increase in pH for the same temperature results in increased *DE* values (Table 5.5).

Although the Korsmeyer-Peppas model, in general, can be applied to describe the release of caffeine in this study, the calculation of RMSE and AIC parameters indicated that for the tests performed mainly at 25°C and pH 1.2 for $P_{(70:30)}$ fiber mats, as well as, for the tests performed at 25°C and pH 7.4 for $P_{(80:20)}$, the diffusion was not the only mechanism governing the release of caffeine. For the release test made at 25°C and pH 1.2 for $P_{(70:30)}$ fiber mats, this result can be directly associated by the collapsed state of polymer chains in view of the low pH and the higher concentration of *pH*-sensitive PAA in the fibers. RMSE is

a good indicator of the standard deviation and the closer to zero this parameter, the more suitable is the method chosen to evaluate the release mechanism. At 25 °C, when pH increased from 1.2 to 7.4, the high values of RMSE and low value of AIC parameters, indicate a competition between collapsed state of PAA segments and swollen state of PNVCL segments, below the LCST. Although the release mechanism needs to be further elucidated, this study demonstrated that the release of caffeine and probably other hydrophilic similar drugs can be impeded by their entrapment in poly(NVCL-*co*-AA) fiber mats.

5.6 Conclusion

In this study, poly(NVCL-*co*-AA)-based electrospun fiber mats loaded with caffeine have been successfully prepared via electrospinning. Copolymers containing different AA mol% (20 and 30) were evaluated and the caffeine concentration was kept at 10% and 30 wt% (with respect to the copolymer). Scanning electron microscopy showed that the fibers had smooth surfaces and that the average fiber diameter and morphology change as a function of caffeine concentration. IR spectroscopy results demonstrated that there were some intermolecular interactions between caffeine and poly(NVCL-*co*-AA). X-ray diffraction and differential scanning calorimetry studies indicated that highly-loaded caffeine maintains its crystallinity inside the fibers. The caffeine entrapment was dependent on the caffeine – copolymer proportion. $P_{(70:30)}$ membranes showed the highest Encapsulation Efficiency (EE) value (100%). The caffeine kinetics release was studied at two temperatures: below and above the LCST of PNVCL, and at two pH values: acidic medium (pH 1.2) and basic medium (pH 7.4). The release profiles of caffeine from $P_{(70:30)}$ and $P_{(80:20)}$ revealed rapid caffeine release below LCST compared with that above LCST. Above LCST, caffeine release was slower, especially, in acidic medium (pH 1.2). Overall, this study demonstrates that thermo and *pH*-sensitive electrospun fibers may become potential systems for the encapsulation and controlled release of caffeine and similar hydrophilic models.

5.7 Acknowledgments

The authors are grateful to the financial supports from the Natural Sciences and Engineering Research Council of Canada (NSERC), the University Mission of Tunisia in North America (MUTAN) and the Fundação de Amparo à Pesquisa do Estado de São Paulo (FAPESP) of Brazil.

CONCLUSION PERSPECTIVES

The objective of this thesis was to develop a novel electrospun fiber scaffold based on temperature and *pH*-sensitive polymers and copolymers for the control release of different types of drugs as a potential drug delivery system. Achieving this goal was possible in three steps, which answers three specific questions:

How Thermo-sensitive polymers may exhibit better drug release control through electrospun scaffold compared to conventional polymers, which are generally biocompatible and biodegradable?

How the use of both thermo-and *pH*-sensitive polymers can improve the morphology stability of electrospun fibers in contact with water. And how the change in temperature and *pH* as well as the copolymer/drug interaction can influence the release of a hydrophobic drug such as ketoprofen?

How the change in temperature and *pH* as well as the copolymer/drug interaction can influence the releases of hydrophilic drug model such as caffeine from electrospun fibers based on thermo-and *pH*-sensitive copolymers.

First, thermo-sensitive drug delivery systems based on mixtures of PNVCL with PCL, a hydrophobic and biodegradable polymer, were developed using the electrospinning process. The morphology of the electrospun membrane obtained was controlled by the parameters of the process such as the electric field and the flow rate, as well as, by the composition of the electrospun mixtures. The addition of the PCL showed a direct effect on LCST and the hydrophobicity of the membrane. The entrapment of ketoprofen depended on the polymers used in the fiber preparations. The morphology of PCL/PNVCL mixtures has been shown to control drug release. The results reported following the ketoprofen release test provides good evidence that the systems developed allow the adjustment of the drug release kinetics, by varying the type and concentration ratio of the polymers used in the blends and should be tested for other drugs with different affinities with polymers.

The observations of the results of the first article, as well as, the literature review have nevertheless not shown a great improvement in the drug release control of thermosensitive polymers compared to conventional polymers. The causes of these failures relate, on the one hand, to the loss of fibrous morphology in contact with water, and, on the other hand, to the possible lack of interaction between the polymer and the drug. Here where the thermo-and *pH*-sensitive polymers intervene, which showed a better stability of the fibrous morphology in contact with water, on the one hand. On the other hand, these copolymers showed some interaction with the drug which affected the crystallinity and encapsulation efficiency of the drug, and consequently the control of drug release. Not forgetting the great effect of the change in temperature and *pH* of the release medium on the control of drug release of different types of drugs. Four release profiles were obtained by the same membrane encapsulating the drug depending on the combination of the sitting temperature and *pH* of the medium.

Finally, the work carried out during this thesis made it possible to confirm the strong potential of the electrospinning technique and thermo-and *pH*-sensitive polymers in the design of drug delivery systems due to its ability to manufacture flexible fiber scaffold and to control the release of hydrophilic and hydrophobic drug models under the influence of temperature and *pH*. Although aspects remain to be optimized, this project paves the way for the development of a new generation of thermo-and *pH*-sensitive drug delivery systems by electrospinning.

The perspectives resulting from our work are numerous and lies in the continuity of the work carried out in collaboration with the various research teams to extend the applications of the electrospun fiber studied. More precisely the perspectives of this work can be classified according to 3 accesses: the affinity drug / copolymer; the fibers structures; and vivo testing.

Drug/Copolymer affinity: The first step is to test the encapsulation, the drug/copolymer interaction, and the release rate of an hydrophilic drug having better solubility in the solvents

used for the electrospinning of Poly(NVCL-*co*-AA). Second, different hydrophilic and hydrophobic drugs must be tested to confirm the validity of the results obtained with ketoprofen and caffeine.

Fiber structure: The fiber structure plays an important role in the control of the drug release; more specifically the use of coaxial fibers by encapsulating the drug in the fiber core can result in longer and slower drug release. The thermo-and *pH*-sensitive copolymer poly(NVCL-*co*-AA) can be only used in the shell to keep the effect of temperature and pH on drug release.

Vivo testing: In vivo tests are essential to validate the results obtained on a living organism, which takes place in an uncontrolled environment, unlike in vitro testing which takes place in a controlled environment.

ANNEXE I

ENCAPSULATION OF HEPARIN AND DEXAMETHASONE INTO PULLULAN NANOPARTICLE BY ELECTROSPRAY PROSSES

Pullulan (Pull) is a linear polysaccharide produced in large scale from starch, glucose and some agro-industrial (Guerrini et al., 2021). Pull is widely used in biomedical applications such as blood plasma substitutes, oil and oxygen barrier films and carriers and releaser of cytotoxic molecules (D. Kumar et al., 2012)(Pınar et al., 2013). Due to it very interesting properties, such as high solubility in water, oxygen barriers, non-toxicity, non-carcinogenicity, and biodegradability (Pınar et al., 2013)(Guerrini et al., 2021), Pull is an interesting candidate to obtain nanoparticles produced from the electrospray process to be used as drug delivery systems. Figure A I-1 shows the chemical structure of pullulan.

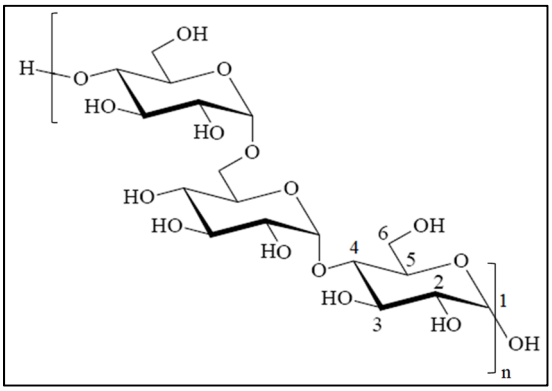

Figure-A I-1 Pullulan chemical structure
Taken from (Guerrini et al., 2021)

The objective of this project is to study the possibility of encapsulating Heparin and Dexamethasone in Pullulan nanoparticles for drug delivery applications. The idea is to produce homogeneous nanoparticles with 300 nm as particle diameter using different molar mass of pullulan. The choice of the diameter was based on the inhalation of the nanoparticle through the respiratory tract(P. Li et al., 2014)(Bazant & Bush, 2021).

The project was carried out in three stages:

- Reduction of pullulan molar mass;
- Optimization of the electrospraying of pullulan particles by controlling the solution and the process parameters;
- Encapsulation of the Heparin and Dexamethasone in Pullulan nanoparticles.

A-1 Reduction of pullulan molar mass

Purified pullulan (Pull, cosmetic grade, Hayashibara Co., Japan) with 91 000g/mol was treated with 0.025M hydrochloric acid solution (HCl) to obtain different molar masses (Guerrini et al., 2021).

In a dry 200 mL three-neck round bottom flask, 4g of purified pullulan was dissolved in HCl solution (80 mL, 0.025 mol/L) using a magnetic stirrer and under a nitrogen atmosphere. The flask was heated at (85±1)ºC for different times depending on the targeted molar mass (from 0 to 2.5h). The reaction was stopped by putting the flask into an ice bath and then the product was obtained by precipitation in ice-cold methanol, washed with cold methanol several times, and dried under vacuum at 30°C for 24 h. The weight-average molar mass ($\overline{M}_w$), number-average molar mass ($\overline{M}_n$) and the dispersity index ($Đ=\overline{M}_w/\overline{M}_n$) are presented in table A I-1 (Guerrini et al., 2021).

Table-A I-1 Molar masses ($\overline{M}_w$ and $\overline{M}_n$) and dispersity (Đ) of Pulluln with different reduction times.

Reduction time (h)	$\overline{M}_w$ (g/mol)	$\overline{M}_n$ (g/mol)	**Đ**
0.0	91,000	42,700	2.13
0.5	60,000	28,800	1.80
1.0	20,000	11,330	1.70
2.0	12,650	7,500	1.70
2.5	10,500	6,560	1.60

A-2 Optimization of the electrospraying of pullulan Particles

Several pullulan aqueous solutions were prepared by varying the solutions concentration for each molar mass to be electrosprayed. In order to understand the parameters controlling the 300 nm particles diameter related to the polymer solutions, the rheological behavior of all pullulan solutions were evaluated using a rotational rheometer (Anton Paar, MCR 302) equipped with cylindrical concentric geometry (CC17). The viscosity was measured for shear rates ranging from 0.01 to 1,000 s-1 at (24 ±1) °C. The results were obtained in duplicate, and the average values are reported in this work. The surface tension of the solutions was measured by a pendant drop apparatus equipped DROPFIT software (UMR 5257).

Once obtained the solutions were electrosprayed in a vertical electrospinning machine (Bionicia FluidNatek L100). The processing parameters used were 100 kV/m electric field, 500µL/h flow rate, 15 cm working distance, 26-gauge needle, 21°C electrospinning temperature and 60% humidity. The electrosprayed nanoparticles were then characterized by scanning electron microscopy. After being coated with gold, the nanoparticles were observed using a SEM (Hitachi S3600N). The diameter of the fibers was evaluated using the Image J software.

Table-A I-2 Properties of pullulan solutions with different concentrations

Pullulan Concentration (%wt)	Solution surface tension (mN/m)	Solution Viscosity (mPa.s)	Particle diameters (nm)
1	72	3.7	194±25
2	67,7	5,3	270±35
5	65,8	21,5	535±30
10	58,7	215	10640±75
15	-	1000	-

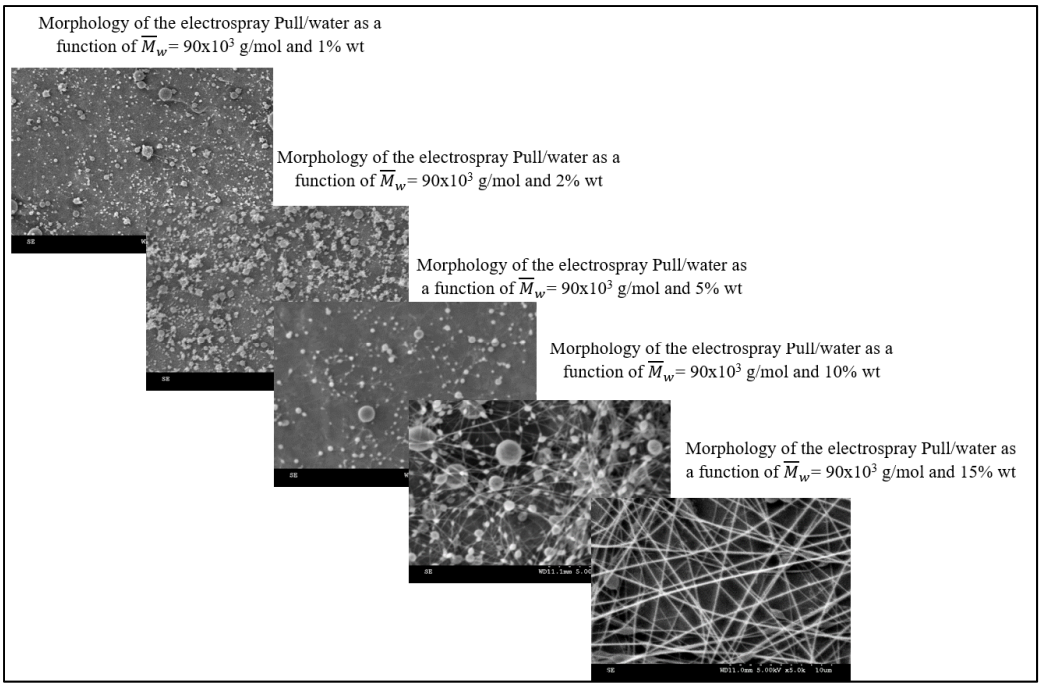

Figure-A I-2 Morphology of the electrospray Pull/water as a function of $\overline{M}_w$ = 91,000 g/mol with different concentrations

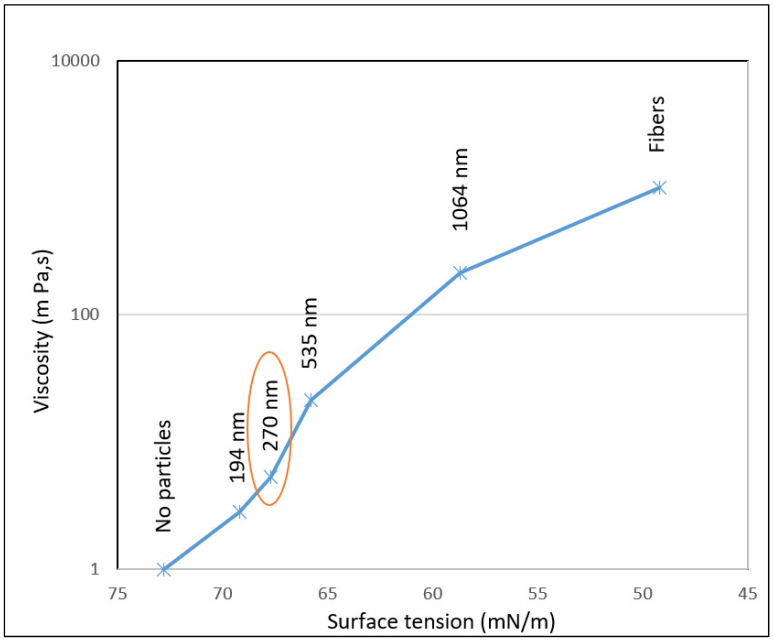

Figure-A I-3 Viscosity versus $\overline{M}_w$ of Pull/water solutions

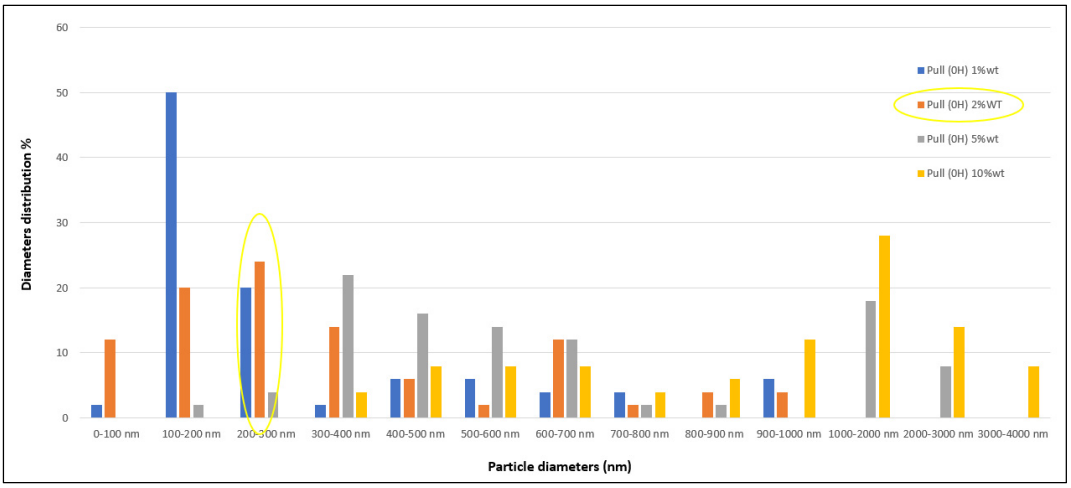

Figure-A I-4 Particle diameters distribution of 1%, 2%, 5% and 10%wt pullulan electrosprayed with water

Preliminary tests have been carried out to optimize the electrospray of pullulan with 91000 g/mol. The electrospray of different concentrations of pullulan shows that it was possible to produce pullulan nanoparticles having around 300 nm particle diameter with 2%wt as concentration, corresponding to 5.3 mPa.s as solutions viscosity and 67.7 mN/m as surface tension. Increasing the viscosity to 1000 mPa.s results to the production of fibers (figure A I-2).

The same thing was also done with 20 000, 60 000 and 12 650 g/mol pullulan molar mass to identify the viscosity and the surface tension able to produce nanoparticles of around 300 nm (figure A I-5).

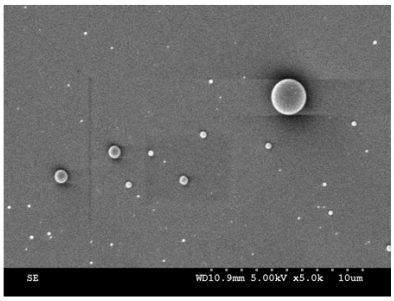

Morphology of the electrospray Pull/water as a function of $\overline{M}_w$= 60,000 g/mol and 2% wt

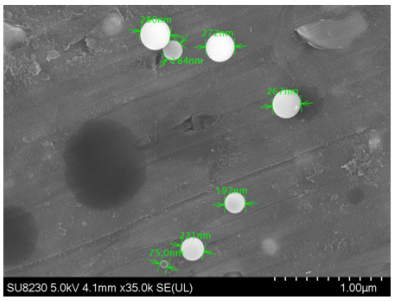

Morphology of the electrospray Pull/water as a function of $\overline{M}_w$= 20,000 g/mol and 15% wt

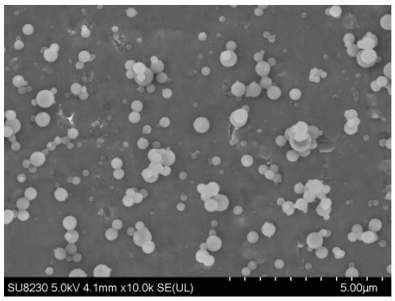

Morphology of the electrospray Pull/water as a function of $\overline{M}_w$= 12,650 g/mol and 30% wt

Figure-A I-5 Morphology of the electrospray Pull/water with different molar mass and concentrations

A-3 Encapsulation of the Heparin and Dexamethasone in Pullulan nanoparticles

Heparin and Dexamethasone was supplied by Sigma-Aldrich and was used without further purification. The last step of this project is to encapsulate the heparin and the dexamethasone in the nanoparticles of pullulan. The concentration of the two drugs was set to be 5%wt (Figure A I-6).

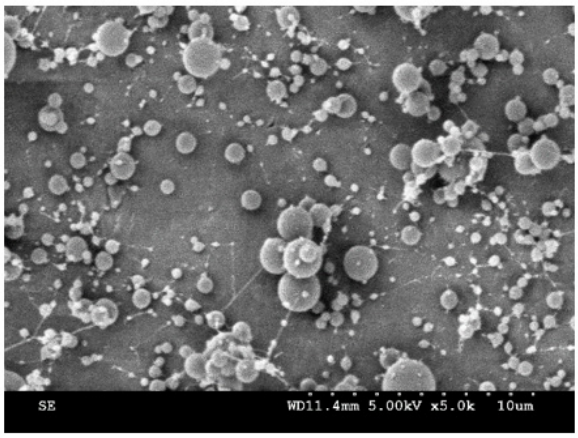

Morphology of the electrospray Pull/water as a function of $\overline{M}_w$= 90,000 g/mol and 2% wt + 5%wt Heparin

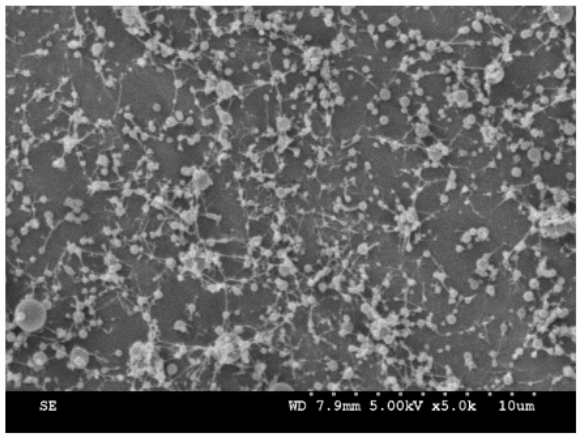

Morphology of the electrospray Pull/water as a function of $\overline{M}_w$= 90,000 g/mol and 2% wt + 5%wt Dexamethasone

Figure-A I-6 Morphology of the electrospray Pull/water as a function of $\overline{M}_w$ = 91,000 g/mol with 5%wt Heparin and Dexamethasone

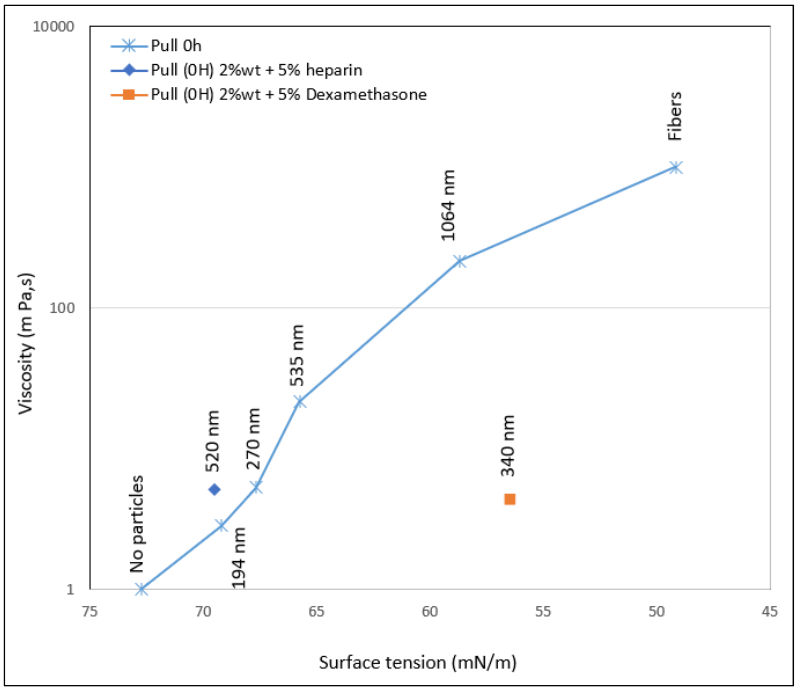

Figure-A I-7 Viscosity versus surface tension (ɣ)
of Pull/water solutions

By adding 5%wt (pullulan) of heparin and dexamethasone in the pullulan solution, the viscosity decreased from 21.5 to 20.5 mPa.s which is within experimental error. Despite the decrease of the viscosity, fine-discounted fibers were obtained in the case of dexamethasone. This can be explained by the decreases of the surface tension from 67.7 to 56.5 mN/m. At the same time, the average particle diameter slightly increased from 270 nm to 340 nm.

LIST OF BIBLIOGRAPHICAL REFERENCES

Aguilar, M. R., Elvira, C., Gallardo, A., Vázquez, B., & Román, J. . (2007). Smart Polymers and Their Applications as Biomaterials. *Topics in Tissue Engineering*, *3*, Chapitre 6.

Ardila Nelson; Arkoun ,Mounia; Heuzey,Marie-Claude; Ajji,Abdellah; Panchal,Chandra J., N. M. (2016). Chitosan–bacterial nanocellulose nanofibrous structures for potential wound dressing applications. *Cellulose*, *23*, 3089–3104.

Arshad, I., Ali, S., Amin, U., Shabbir, M., Raza, M., Sharif, A., & Akhtar, M. F. (2018). Effect of hydrophilic and hydrophobic polymer on the release of ketoprofen and allopurinol from bilayer matrix transdermal patch. *Advances in Polymer Technology*, *37*(8), 3076–3083. https://doi.org/10.1002/adv.22078

Basar, A. O., Castro, S., Torres-Giner, S., Lagaron, J. M., & Turkoglu Sasmazel, H. (2017). Novel poly(ε-caprolactone)/gelatin wound dressings prepared by emulsion electrospinning with controlled release capacity of Ketoprofen anti-inflammatory drug. *Materials Science and Engineering C*, *81*(July), 459–468. https://doi.org/10.1016/j.msec.2017.08.025

Bazant, M. Z., & Bush, J. W. M. (2021). A guideline to limit indoor airborne transmission of COVID-19. *Proceedings of the National Academy of Sciences of the United States of America*, *118*(17), 1–12. https://doi.org/10.1073/pnas.2018995118

Beachley, V., & Wen, X. (2010). Polymer nanofibrous structures: Fabrication, biofunctionalization, and cell interactions. *Progress in Polymer Science*, *35*, 868–892.

Bhagwat, R. R., & Vaidhya, I. S. (2013). Novel Drug Delivery Systems: An Overview. *International Journal Of Pharmaceutical Sciences and Research*, *4*(3), 970–982.

Bhardwaj, N., & Kundu, S. C. (2010). Electrospinning: A fascinating fiber fabrication technique. *Biotechnology Advances*, *28*, 325–347.

Calderón, M. Á. R., & Zhao, W. (2014). Applications of polymer nanofibers in bio-materials, biotechnology and biomedicine: A review. *TMS Annual Meeting*, *125*, 401–414. https://doi.org/10.1002/9781118889879.ch50

Chakraborty, D. D., Nath, L. K., & Chakraborty, P. (2018). Recent Progress in Smart Polymers : Behavior , Mechanistic Understanding and Application. *Polymer-Plastics Technology and Engineering*, *57*(10), 945–957. https://doi.org/10.1080/03602559.2017.1364383

Cheng, J., Jun, Y., Qin, J., & Lee, S.-H. (2017). Electrospinning versus microfluidic spinning of functional fibers for biomedical applications. *Biomaterials*, *114*, 121–143.

Cohen, A. A. (2008). Kant's biological conception of history. *Journal of the Philosophy of History*, *2*(1), 1–28. https://doi.org/10.1163/187226308X268845

Cortez-Lemus, N. A., & Licea-Claverie, A. (2016). Poly(N-vinylcaprolactam), a comprehensive review on athermoresponsive polymer becoming popular. *Progress in Polymer Science*, *53*, 1–51.

Dai, S., Ravi, P., & Tam, K. C. (2008). pH-Responsive polymers: synthesis, properties and applications. *Soft Matter*, *4*, 435–449.

Dash, S., Murthy, P. N., Nath, L., & Chowdhury, P. (2010). Kinetic modeling on drug release from controlled drug delivery systems. *Acta Poloniae Pharmaceutica - Drug Research*, *67*(3), 217–223.

Deepak, A., Goyal, A. K., & Rath, G. (2018). Nanofiber in transmucosal drug delivery. *Journal of Drug Delivery Science and Technology*, *43*(September 2017), 379–387. https://doi.org/10.1016/j.jddst.2017.11.008

Dimitrov, I., Trzebicka, B., Müller, A. H. ., Dworak, A., & Tsvetanov, C. B. (2007). Thermosensitive water-soluble copolymers with doubly responsive reversibly interacting entities. *Progress in Polymer Science*, *32*(11), 1275–1343.

Galaev, I., & Mattiasson, B. (2008). *Smart Polymers:Applications in Biotechnology and Biomedicine.* (second Edition (ed.)). Taylor & Francis Group.

Gao, Yanshan, Teoh, T. W., Wang, Q., & Williams, G. R. (2017). Electrospun organic-inorganic nanohybrids as sustained release drug delivery systems. *Journal of Materials Chemistry B*, *5*(46), 9165–9174. https://doi.org/10.1039/c7tb01825h

Gao, Yuan, Truong, Y. B., Zhu, Y., & Kyratzis, I. L. (2014). Electrospun Antibacterial Nanofibers : Production , Activity , and In Vivo Applications. *Journal of Applied Pharmaceutical Science*, *40797*, 1–13. https://doi.org/10.1002/app.40797

Gaspar, S., & Ramos, F. (2016). Caffeine: Consumption and Health Effects. *Encyclopedia of Food and Health*, 573–578.

Ghafoor, B., Aleem, A., Najabat Ali, M., & Mir, M. (2018). Review of the fabrication techniques and applications of polymeric electrospun nanofibers for drug delivery systems. *Journal of Drug Delivery Science and Technology*, *48*(August), 82–87. https://doi.org/10.1016/j.jddst.2018.09.005

Goh, Y.-F., Shakir, I., & Hussain, R. (2013). Electrospun fibers for tissue engineering , drug delivery , and wound dressing. *J Mater Sci*, 3027–3054. https://doi.org/10.1007/s10853-013-7145-8

Guerrini, L. M., Oliveira, M. P., Stapait, C. C., Maric, M., Santos, A. M., & Demarquette, N. R. (2021). Evaluation of different solvents and solubility parameters on the morphology and diameter of electrospun pullulan nanofibers for curcumin entrapment. *Carbohydrate Polymers*, *251*(September 2020), 117127. https://doi.org/10.1016/j.carbpol.2020.117127

Gupta, P., Elkins, C., Long, T. E., & Wilkes, G. L. (2005). Electrospinning of linear homopolymers of poly(methyl methacrylate): exploring relationships between fiber formation, viscosity, molecular weight and concentration in a good solvent. *Polymer*, *46*, 4799–4810.

Haider, A., Haider, S., & Kang, I.-K. (2015). A comprehensive review summarizing the effect of electrospinning parameters and potential applications of anofibers in biomedical and biotechnology. *Arabian Journal of Chemistry*, 1–23.

Hu, S. H., Liu, T. Y., Liu, D. M., & Chen, S. Y. (2007). Nano-ferrosponges for controlled drug release. *Journal of Controlled Release*, *121*(3), 181–189. https://doi.org/10.1016/j.jconrel.2007.06.002

Huang, C. H., Kuo, T. Y., Lee, C. F., Chu, C. H., Hsieh, H. J., & Chiu, W. Y. (2014). Preparation of a thermo- and pH-sensitive nanofibrous scaffold with embedded chitosan-based nanoparticles and its evaluation as a drug carrier. *Cellulose*, *21*(4), 2497–2509. https://doi.org/10.1007/s10570-014-0290-7

Huang, Z.-M., Zhang, Y. .-Z., Kotaki, M., & Ramakrishna, S. (2003). A review on polymer nanofibers by electrospinning and their applications in nanocomposites. *Composites Science and Technology*, *63*, 2223–2253.

Hubert, S., Briancon, S., Hedoux, A., Guinet, Y., Paccou, L., Fessi, H., & Puel, F. (2011). Process induced transformations during tablet manufacturing: Phase transition analysis of caffeine using DSC and low frequency micro-Raman spectroscopy. *International Journal of Pharmaceutics*, *420*(1), 76–83. https://doi.org/10.1016/j.ijpharm.2011.08.028

Illangakoon, U. E., Gill, H., Shearman, G. C., Parhizkar, M., Mahalingam, S., Chatterton, N. P., & Williams, G. R. (2014). Fast dissolving paracetamol/caffeine nanofibers prepared by electrospinning. *International Journal of Pharmaceutics*, *477*(1–2), 369–379. https://doi.org/10.1016/j.ijpharm.2014.10.036

Immich, A. P. S., Tornero, J. A., Casas, F. C., & Arias, M. J. L. (2017). Electrospun PLLA Membranes for Caffeine Delivery: Diffusional Approach. *Journal of Biomedical Science and Engineering*, *10*(12), 563–574. https://doi.org/10.4236/jbise.2017.1012042

Islam, S., Chin, B., Andri, A., Amalina, A., & Afifi, M. (2019). A review on fabrication of nanofibers via electrospinning and their applications. *SN Applied Sciences*, *1*(10), 1–16. https://doi.org/10.1007/s42452-019-1288-4

James, H. P., John, R., Alex, A., & K.R, A. (2014). Smart polymers for the controlled delivery ofdrugs–a concise overview. *Acta Pharmaceutica Sinica B*, *4*, 120–127.

Jiang, H., Hu, Y., Li, Y., Zhao, P., Zhu, K., & Chen, W. (2005). A facile technique to prepare biodegradable coaxial electrospun nanofibers for controlled release of bioactive agents. *Journal of Controlled Release*, *108*, 237–243.

Jiang, J., Xie, J., Ma, B., Bartlett, D. E., Xu, A., & Wang, C. H. (2014). Mussel-inspired protein-mediated surface functionalization of electrospun nanofibers for pH-responsive drug delivery. *Acta Biomaterialia*, *10*(3), 1324–1332. https://doi.org/10.1016/j.actbio.2013.11.012

Kanani S. Hajir, A. G. B. (2011). Effect of Changing Solvents on Poly(ε-Caprolactone) NanofibrousWebs Morphology. *Journal of Nanomaterials*, *2010*, 724153–724163.

Kenawy, E.-R., Abdel-Hay, F. I., El-Newehy, M. H., & Wnek, G. E. (2009). Processing of polymer nanofibers through electrospinning as drug delivery systems. *Materials Chemistry and Physics*, *113*, 296–302.

Kenawy, E. R., Abdel-Hay, F. I., El-Newehy, M. H., & Wnek, G. E. (2007). Controlled release of ketoprofen from electrospun poly(vinyl alcohol) nanofibers. *Materials Science and Engineering A*, *459*(1–2), 390–396. https://doi.org/10.1016/j.msea.2007.01.039

Khoo, W., & Koh, C. T. (2016). A review of electrospinning process and microstructure morphology control. *ARPN Journal of Engineering and Applied Sciences*, *11*(12), 7774–7781.

Kim, H. S., & Yoo, H. S. (2010). MMPs-responsive release of DNA from electrospun nanofibrous matrix for local gene therapy: In vitro and in vivo evaluation. *Journal of Controlled Release*, *145*(3), 264–271. https://doi.org/10.1016/j.jconrel.2010.03.006

Kim Jeong-Hyun; Lee, Mi Hee; Kwon,Byeong Ju; Park, Jong-Chul, H.-L. ; L. (2012). Evaluation of Electrospun (1,3)-(1,6)-b-D-Glucans/ Biodegradable Polymer as Artificial Skin for Full-Thickness Wound Healing. *TISSUE ENGINEERING A*, *18*, 2315–2322.

Kitsara, M., Agbulut, O., Kontziampasis, D., Chen, Y., & Menasché, P. (2017). Fibers for hearts: A critical review on electrospinning for cardiac tissue engineering. *Acta Biomaterialia*, *48*, 20–40.

Kocak, C., Tuncer, C., & Bütün, V. (2017). pH-Responsive polymers. *The Royal Society of Chemistry*, *8*, 144–176.

Kozanoğlu, S., Özdemir, T., & Usanmaz, A. (2011). Polymerization of N-Vinylcaprolactam and Characterization of Poly(N-Vinylcaprolactam). *Journal of Macromolecular Science, Part A*, *48*, 467–477.

Kumar, A., Srivastava, A., Galaev, I. Y., & Mattiasson, B. (2007). Smart polymers: Physical forms and bioengineering applications. *Progress in Polymer Science*, *32*, 1205–1237.

Kumar, D., Saini, N., Pandit, V., & Ali, S. (2012). An Insight To Pullulan: A Biopolymer in Pharmaceutical Approaches. *International Journal of Basic and Applied Sciences*, *1*(3). https://doi.org/10.14419/ijbas.v1i3.101

Kumar Thakur, V., & Kumar Thakur, M. (2015). Handbook of Polymers for Pharmaceutical Technologies, Biodegradable Polymers. In *Biodegradable Polymers* (Vol. 3).

LAKSHMI V., N. DAS. (2011). Biodegradation of Caffeine by Trichosporon asahii Isolated from Caffeine Contaminated Soil. *International Journal of Engineering Science and Technology*, *3*(11), 7988–7997.

Lansdowne, L. E. (2020). *Drug Delivery*. Technology Networks.

Laukkanen, A., Valtola, L., Winnik, F. M., & Tenhu, H. (2004). Formation of Colloidally Stable Phase Separated Poly(N-vinylcaprolactam) in Water: A Study by Dynamic Light Scattering, Microcalorimetry, and Pressure Perturbation Calorimetry. *Macromolecules*, *37*, 2268–2274.

Lee, B.-S., Jeon, S.-Y., Park, H., Lee, G., & Yang, H.-S. (2014). New Electrospinning Nozzle to Reduce Jet Instability and Its Application to Manufacture of Multi-layered anofibers. *SCIENTIFIC REPORTS*, *4*, *6758;*, 1–9.

Lee, J. H., & Yeo, Y. (2015). Controlled drug release from pharmaceutical nanocarriers. *Chemical Engineering Science*, *125*, 75–84. https://doi.org/10.1016/j.ces.2014.08.046

Leung, M. F., Zhu, J., Harris, F. W., & Li, P. (2005). Novel synthesis and properties of smart core-shell microgels. *Macromolecular Symposia*, *226*, 177–186. https://doi.org/10.1002/masy.200550817

Li, D., & Xia, Y. (2004). Direct Fabrication of Composite and Ceramic Hollow Nanofibers by Electrospinning. *NANO Letters*, *4*, 933–938.

Li, H., Liu, K., Williams, G. R., Wu, J., Wu, J., & Wang, H. (2018). Dual temperature and pH responsive nano fi ber formulations prepared by electrospinning. *Colloids and Surfaces B: Biointerfaces*, *171*(July), 142–149. doi.org/10.1016/j.colsurfb.2018.07.020

Li, H., Liu, K., Williams, G. R., Wu, J., Wu, J., Wang, H., Niu, S., & Zhu, L.-M. (2018). Dual temperature and pH responsive nanofiber formulations prepared by electrospinning. *Colloids and Surfaces B: Biointerfaces*, *171*, 142–149.

Li, H., Sang, Q., Wu, J., Williams, G. R., Wang, H., & Niu, S. (2018). Dual-responsive drug delivery systems prepared by blend electrospinning. *International Journal of Pharmaceutics*, *543*(1–2), 1–7. https://doi.org/10.1016/j.ijpharm.2018.03.009

Li, P., Wang, C., Zhang, Y., & Wei, F. (2014). Air filtration in the free molecular flow regime: A review of high-efficiency particulate air filters based on Carbon Nanotubes. *Small*, *10*(22), 4543–4561. https://doi.org/10.1002/smll.201401553

Li, W.-J., Shanti, R. M., & Tuan, R. S. (2007). Electrospinning Technology for Nanofibrous Scaffolds in Tissue Engineering. In *Nanotechnologies for the Life Sciences* (Vol. 9). https://doi.org/10.1002/9783527610419.ntls0097

Li, Xiaohu, Yang, W., Li, H., Wang, Y., Bubakir, M. M., Ding, Y., & Zhang, Y. (2015). Water Filtration Properties of Novel Composite Membranes CombiningSolution Electrospinning and Needleless Melt Electrospinning Methods. *Journal of Applied Polymer Science*, 41601–41609.

Li, Xiaoqiang, Kanjwal, M. A., Lin, L., & Chronakis, I. S. (2013). Electrospun polyvinyl-alcohol nanofibers as oral fast-dissolving delivery system of caffeine and riboflavin. *Colloids and Surfaces B: Biointerfaces*, *103*, 182–188. https://doi.org/10.1016/j.colsurfb.2012.10.016

Lin, X., Tang, D., Lyu, H., & Zhang, Q. (2016). Poly(N-isopropylacrylamide)/polyurethane core–sheath nanofibres by coaxial electrospinning for drug controlled release. *Micro & Nano Letters*, *11*(5), 260–263.

Liu, H., Yang, Q., Zhang, L., Zhuo, R., & Jiang, X. (2016). Synthesis of carboxymethyl chitin in aqueous solution and its thermo- and pH-sensitive behaviors. *Carbohydrate Polymers*, *137*, 600–607. https://doi.org/10.1016/j.carbpol.2015.11.025

Liu, J., Debuigne, A., Detrembleur, C., & Jérome, C. (2014). Poly(N -vinylcaprolactam): A Thermoresponsive Macromolecule with Promising Future in Biomedical Field. *Advanced Healthcare Materials*, *3*, 1941–1968.

Liu, L., Bai, S., Yang, H., Li, S., Quan, J., Zhu, L., & Nie, H. (2016). Controlled release from thermo-sensitive PNVCL-co-MAA electrospun nanofibers: The effects of hydrophilicity/hydrophobicity of a drug. *Materials Science and Engineering C*, *67*, 581–589.

Liu, Y., Meng, L., Lu, X., Zhang, L., & He, Y. (2008). Thermo and pH sensitive fluorescent polymer sensor formetal cations in aqueous solution. *Polymers for Advanced Technologies*, *November 2007*, 229–236. https://doi.org/10.1002/pat

Lu, J., Zhu, W., Dai, L., Si, C., & Ni, Y. (2019). Fabrication of thermo- and pH-sensitive cellulose nanofibrils-reinforced hydrogel with biomass nanoparticles. *Carbohydrate Polymers*, *215*(29), 289–295. https://doi.org/10.1016/j.carbpol.2019.03.100

Luo, C. J., Stride, E., & Edirisinghe, M. (2012). Mapping the Influence of Solubility and Dielectric Constant on Electrospinning Polycaprolactone Solutions. *Macromolecules*, *45*, 4669–4680.

Medeiros, S., Filizzola, J. O. ., Oliveira, P. F. ., Silva, T. M., Lara, B. R., Lopes, M. V, Rossi-Bergmann, B., Elaissari, A., & Santos, A. M. (2016). Fabrication of biocompatible and stimuli-responsive hybrid microgels with magnetic properties via aqueous precipitation polymerization. *Materials Letters*, *175*, 296–299. https://doi.org/10.1016/j.matlet.2016.04.004

Medeiros, S.F., Santos, A. ., Fessi, H., & Elaissari, A. (2011). Stimuli-responsive magnetic particles for biomedical applications. *International Journal of Pharmaceutics*, *403*, 139–161.

Medeiros, Simone F., Barboza, J. C. S., Ré, M. I., Giudici, R., & Santos, A. M. (2010). Solution Polymerization of N-vinylcaprolactam in1,4-dioxane. Kinetic Dependence on Temperature,Monomer, and Initiator Concentrations. *Journal of Applied Polymer Science*, *118*, 229–240.

Medeiros, Simone F., Lopes, M. V., Rossi-Bergmann, B., Ré, M. I., & Santos, A. M. (2017). Synthesis and characterization of poly(N-vinylcaprolactam)-based spray-dried microparticles exhibiting temperature and pH-sensitive properties for controlled release of ketoprofen. *Drug Development and Industrial Pharmacy*, *43*(9), 1519–1529. https://doi.org/10.1080/03639045.2017.1321660

Mendyk, A., Jachowicz, R., Fijorek, K., Dorożyński, P., Kulinowski, P., & Polak, S. (2012). KinetDS : An Open Source Software for Dissolution Test Data Analysis. *Dissolution Technologies*, *778051*, 5–11. https://doi.org/10.14227/DT190112P6

Milla, A. L. G., Meireles, A. B., & Corre, D. K. (2018). Mini Review Trends in polymeric electrospun fibers and their use as oral biomaterials. *Experimental Biology and Medicine*, 665–676. https://doi.org/10.1177/1535370218770404

Mutlu, G., Calamak, S., Ulubayram, K., & Guven, E. (2018). Curcumin-loaded electrospun PHBV nanofibers as potential wound-dressing material. *Journal of Drug Delivery Science and Technology*, *43*, 185–193. https://doi.org/10.1016/j.jddst.2017.09.017

Natu, M. V., de Sousa, H. C., & Gil, M. H. (2010). Effects of drug solubility, state and loading on controlled release in bicomponent electrospun fibers. *International Journal of Pharmaceutics*, *397*(1–2), 50–58. https://doi.org/10.1016/j.ijpharm.2010.06.045

Paradkar, M. M., & Irudayaraj, J. (2002). A rapid FTIR spectroscopic method for estimation of caffeine in soft drinks and total methylxanthines in tea and coffee. *Journal of Food Science*, *67*(7), 2507–2511. https://doi.org/10.1111/j.1365-2621.2002.tb08767.x

Park, J., & Lee, I. (2011). Controlled release of ketoprofen from electrospun porous polylactic acid (PLA) nanofibers. *J Polym Res*, 1287–1291. https://doi.org/10.1007/s10965-010-9531-0

Pasparakis, G., & Tsitsilianis, C. (2020). LCST polymers: Thermoresponsive nanostructured assemblies towards bioapplications. *Polymer*, *211*(October), 123146. https://doi.org/10.1016/j.polymer.2020.123146

Pawar, M. D., Rathna, G. V. N., Agrawal, S., & Kuchekar, B. S. (2015). Bioactive thermoresponsive polyblend nanofiber formulations for wound healing. *Materials Science and Engineering C*, *48*, 126–137.

Perez, R., & Kim, H.-W. (2015). Core–shell designed scaffolds for drug delivery and tissue engineering. *Acta Biomaterialia*, *21*, 2–19.

Persano, L., Camposeo, A., Tekmen, C., & Pisignano, D. (2013). Industrial Upscaling of Electrospinning andApplications of Polymer Nanofibers: A Review. *Macromolecular Journals*, *298*, 504–520.

Pınar, O., Yangılar, F., Oğuzhan, P., & Yangılar, F. (2013). Pullulan : Production and usage in food ındustry. *African Journal of Food Science and Technology*, *4*(3), 57–63.

Poornima, B., & Korrapati, P. S. (2017). Fabrication of chitosan-polycaprolactone composite nanofibrousscaffold for simultaneous delivery of ferulic acid and resveratrol. *Carbohydrate Polymers*, *157*, 1741–1749.

Qin, X., & Wu, D. (2012). Effect of different solvents on poly(caprolactone) (PCL) electrospun nonwoven membranes. *Journal of Thermal Analysis and Calorimetry*, *107*, 1007–1013.

Qu, H., Wei, S., & Guo, Z. (2013). Coaxial electrospun nanostructures and their applications. *Journal of Materials Chemistry A*, *1*(38), 11513–11528. https://doi.org/10.1039/c3ta12390a

Reda, R. I., Wen, M. M., & El-kamel, A. H. (2017). Ketoprofen-loaded Eudragit electrospun nanofibers for the treatment of oral mucositis. *International Journal of Nanomedicine*, 2335–2351.

Rezabeigi, E., & Demarquette, N. R. (2019). Ultraporous Membranes Electrospun from Nonsolvent-Induced Phase-Separated Ternary Systems. *Macromolecular Rapid Communications*, *40*(9), 1–11. https://doi.org/10.1002/marc.201800880

Rezabeigi, E., Sta, M., Swain, M., McDonald, J., Demarquette, N. R., Drew, R. A. L., & Wood-Adams, P. M. (2017). Electrospinning of porous polylactic acid fibers during nonsolvent induced phase separation. *Journal of Applied Polymer Science*, *134*(20). https://doi.org/10.1002/app.44862

Rezabeigi, E., Wood-Adams, P. M., & Demarquette, N. R. (2018). Complex Morphology Formation in Electrospinning of Binary and Ternary Poly(lactic acid) Solutions. *Macromolecules*, *51*(11), 4094–4107. https://doi.org/10.1021/acs.macromol.8b00083

Riccitiello, F., Luise, A. De, Aniello, S. D., Vittoria, V., Di, A., Calarco, A., & Peluso, G. (2018). Effect of resveratrol release kinetic from electrospun nano fi bers on osteoblast and osteoclast differentiation. *European Polymer Journal*, *99*(October 2017), 289–297. https://doi.org/10.1016/j.eurpolymj.2017.12.035

Romeo, V., Gorrasi, G., & Vittoria, V. (2007). Encapsulation and Exfoliation of Inorganic Lamellar Fillers into Polycaprolactone by Electrospinning. *Biomacromolecules*, *8*, 3147–3152.

Salome A, C., Godswill C, O., & Ikechukwu I, O. (2013). Kinetics and Mechanisms of Drug Release from Swellable and Non Swellable Matrices: A Review. *Research Journal of Pharmaceutical, Biological and Chemical Sciences*, *4*, 97–103.

Santana-melo, G. F., Rodrigues, B. V. M., Ricci, R., Marciano, F. R., Webster, T. J., Vasconcellos, L. M. R., & Lobo, A. O. (2017). Electrospun ultrathin PBAT / nHAp fibers influenced the in vitro and in vivo osteogenesis and improved the mechanical properties of neoformed bone. *Colloids and Surfaces B: Biointerfaces*, *155*, 544–552. https://doi.org/10.1016/j.colsurfb.2017.04.053

Sarabi-Mianeji, S., Scott, J., & Pagé, D. J. Y. S. (2015). Impact of Electrospinning Process Parameters on the Measured Current and Fiber Diameter. *Polymer Engineering & Science*, *55*(11), 2576–2582.

Schmaljohann, D. (2006). Thermo- and pH-responsive polymers in drug delivery. *Advanced Drug Delivery Reviews*, *58*.

Seif, S., Franzen, L., & Windbergs, M. (2015). Overcoming drug crystallization in electrospun fibers - Elucidating key parameters and developing strategies for drug delivery. *International Journal of Pharmaceutics*, *478*(1), 390–397. https://doi.org/10.1016/j.ijpharm.2014.11.045

Sell, S. A., McClure, M. J., Garg, K., Wolfe, P. S., & Bowlin, G. L. (2009). Electrospinning of collagen/biopolymers for regenerative medicine and cardiovascular tissue engineering. *Advanced Drug Delivery Reviews*, *61*, 1007–1019.

Shaikh, R. P., Pillay, V., Choonara, Y. E., Du Toit, L. C., Ndesendo, V. M. K., Bawa, P., & Cooppan, S. (2010). A review of multi-responsive membranous systems for rate-modulated drug delivery. *AAPS PharmSciTech*, *11*(1), 441–459. https://doi.org/10.1208/s12249-010-9403-2

Sheng, J. J., Kasim, N. A., Chandrasekharan, R., & Amidon, G. L. (2006). Solubilization and dissolution of insoluble weak acid , ketoprofen : Effects of pH combined with surfactant. *European Journal of Pharmaceutical Sciences*, *29*, 306–314. https://doi.org/10.1016/j.ejps.2006.06.006

Shengtong, S., & Peiyi, W. (2011). Infrared Spectroscopic Insight into Hydration Behavior of Poly(N-vinylcaprolactam) in Water. *The Journal of Physical Chemistry B*, *8*, 11609–11618.

Sill, T. J., & Recum, H. A. Von. (2008). Electrospinning : Applications in drug delivery and tissue engineering. *Biomaterials*, *29*, 1989–2006. https://doi.org/10.1016/j.biomaterials.2008.01.011

Simko Jirí ; Lukás, David, M. E. (2014). A mathematical model of external electrostatic field of a special collector for electrospinning of nanofibers. *Journal of Electrostatics*, *72*, 161–165.

Singhvi, G., & Mahaveer, S. (2011). REVIEW: IN-VITRO DRUG RELEASE CHARACTERIZATION MODELS. *International Journal of Pharmaceutical Studies and Research*, *II*(2229–4619), 77–84.

Singhvi, G., & Singh, M. (2011). REVIEW: IN-VITRO DRUG RELEASE CHARACTERIZATION MODELS. *International Journal of Pharmaceutical Studies and Research*, *II*(I), 77–84.

Song, Q., Chen, H., Zhou, S., Zhao, K., Wang, B., & Hu, P. (2016). Thermo- and pH-sensitive shape memory polyurethane containing carboxyl groups. *Polymer Chemistry*, *7*(9), 1739–1746. https://doi.org/10.1039/c5py02010g

Sóti, P. L., Nagy, Z. K., Serneels, G., Vajna, B., Farkas, A., Van Der Gucht, F., Fekete, P., Vigh, T., Wagner, I., Balogh, A., Pataki, H., Mezo, G., & Marosi, G. (2015). Preparation and comparison of spray dried and electrospun bioresorbable drug delivery systems. *European Polymer Journal*, *68*, 671–679. doi.org/10.1016/j.eurpolymj.2015.03.035

Srivastava, A., Yadav, T., Sharma, S., Nayak, A., & Kumari, A. (2016). *Polymers in Drug Delivery*. *January*, 69–84.

Sta, M., Aguiar, G., Forni, A. A. J., Medeiros, S. F., Santos, A. M., & Demarquette, N. R. (2020). Design and characterization of PNVCL-based nanofibers and evaluation of their potential applications as scaffolds for surface drug delivery of hydrophobic drugs. *Journal of Applied Polymer Science*, *137*(11). https://doi.org/10.1002/app.48472

Sta, Marwa, Aguiar, G., Forni, A. A. J. A. A. J. J., Medeiros, S. F. S. F., Santos, A. M. A. M., & Demarquette, N. R. N. R. (2020). Design and characterization of PNVCL-based nanofibers and evaluation of their potential applications as scaffolds for surface drug delivery of hydrophobic drugs. *Journal of Applied Polymer Science*, *137*(11), 48472–48786. https://doi.org/10.1002/app.48472

Sun, K., Ge, Y., Li, Z., & Zhang, X. (2013). Post-processing of Chitosan Based Nanofibers Prepared by Electrospinning. *Advanced Materials Research*, *873*(1662–8985), 652–662.

Teo, W. E. (2012). *Electrospinning Parameters: Voltage.* http://electrospintech.com/voltage.html

Tipduangta, P., Belton, P., Fábián, L., Wang, L. Y., Tang, H., Eddleston, M., & Qi, S. (2016). Electrospun Polymer Blend Nanofibers for Tunable Drug Delivery: The Role of Transformative Phase Separation on Controlling the Release Rate. *Molecular Pharmaceutics*, *13*(1), 25–39. https://doi.org/10.1021/acs.molpharmaceut.5b00359

Ullrich, S., de Vries, Y. C., Kühn, S., Repantis, D., Dresler, M., & Ohla, K. (2015a). Feeling smart: Effects of caffeine and glucose on cognition, mood and self-judgment. *Physiology and Behavior*, *151*, 629–637. https://doi.org/10.1016/j.physbeh.2015.08.028

Ullrich, S., de Vries, Y. C., Kühn, S., Repantis, D., Dresler, M., & Ohla, K. (2015b). Feeling smart: Effects of caffeine and glucose on cognition, mood and self-judgment. *Physiology and Behavior*, *151*, 629–637. https://doi.org/10.1016/j.physbeh.2015.08.028

Vihola A; Valtola, L; Tenhu, H; Hirvonen, J., H. L. (2005). Cytotoxicity of thermosensitive polymers poly(N-isopropylacrylamide), poly(N-vinylcaprolactam) and amphiphilically modified poly(N-vinylcaprolactam). *Biomaterials*, 3055–3065.

Vihola, H., Laukkanen, A., Valtola, L., Tenhu, H., & Hirvonen, J. (2005). Cytotoxicity of thermosensitive polymers poly(N-isopropylacrylamide), poly(N-vinylcaprolactam) and amphiphilically modified poly(N-vinylcaprolactam). *Biomaterials*, *26*(16), 3055–3064. https://doi.org/10.1016/j.biomaterials.2004.09.008

Wang, Bin, Liu, H. J., Jiang, T. T., Li, Q. H., & Chen, Y. (2014). Thermo-, and pH dual-responsive poly(N-vinylimidazole): Preparation, characterization and its switchable catalytic activity. *Polymer*, *55*(23), 6036–6043. https://doi.org/10.1016/j.polymer.2014.09.051

Wang, Bochu, Wang, Y., Yin, T., & Yu, Q. (2010). *APPLICATIONS OF ELECTROSPINNING TECHNIQUE IN DRUG DELIVERY Applications of Electrospinning Technique in Drug Delivery*. *6445*. https://doi.org/10.1080/00986441003625997

Wang, W., Lu, K. J., Yu, C. H., Huang, Q. L., & Du, Y. Z. (2019). Nano-drug delivery systems in wound treatment and skin regeneration. *Journal of Nanobiotechnology*, *17*(1), 1–15. https://doi.org/10.1186/s12951-019-0514-y

Wang, X., Yu, D., Li, X., Bligh, S. W. A., & Williams, G. R. (2015). Electrospun medicated shellac nano fi bers for colon-targeted drug delivery. *International Journal of Pharmaceutics*, *490*(1–2), 384–390. https://doi.org/10.1016/j.ijpharm.2015.05.077

Ward, M. A., & Georgiou, T. K. (2011). Thermoresponsive Polymers for Biomedical Applications. *Polymers*, *3*, 1215–1242.

Webster, M., Miao, J., Lynch, B., Green, D., Jones-Sawyer, R., Linhardt, R. J., & Mendenhall, J. (2013). Tunable Thermo-Responsive Poly(Nvinylcaprolactam) Cellulose Nanofibers: Synthesis, Characterization, and Fabrication. *Macromol. Mater. Eng.*, *298*, 447–453.

Wei, L., Cai, C., Lin, J., & Chen, T. (2009). Dual-drug delivery system based on hydrogel/micelle composites. *Biomaterials*, *30*(13), 2606–2613. https://doi.org/10.1016/j.biomaterials.2009.01.006

Wu, Q., Wang, L., Fu, X., Song, X., Yang, Q., & Zhang, G. (2014). Synthesis and self-assembly of a new amphiphilic thermosensitive poly(N-vinylcaprolactam)/ poly(e-caprolactone) block copolymer. *Polym. Bull*, *71*, 1–18.

Yang, X., Li, W., Sun, Z., Yang, C., & Tang, D. (2020). Electrospun P(NVCL-co-MAA) nanofibers and their pH/temperature dual-response drug release profiles. *Colloid and Polymer Science*, *298*(6), 629–636. https://doi.org/10.1007/s00396-020-04647-y

Yu, Z., Gu, H., Tang, D., Lv, H., Rend, Y., & Gu, S. (2015). Fabrication of PVCL-co-PMMA nanofibers with tunable volume phase transition temperatures and maintainable shape for anti-cancer drug release. *The Royal Society of Chemistry*, *5*, 64944–64950.

Zamani, M., Prabhakaran, M. P., & Ramakrishna, S. (2013). Advances in drug delivery via electrospun and electrosprayed nanomaterials. *International Journal of Nanomedicine*, *8*, 2997–3017. https://doi.org/10.2147/IJN.S43575

Zavgorodnya, O., Carmona-Moran, C. A., Kozlovskaya, V., Liu, F., Wick, T. M., & Kharlampieva, E. (2017). Temperature-responsive nanogel multilayers of poly(N-vinylcaprolactam) for topical drug delivery. *Journal of Colloid and Interface Science*, *506*, 589–602.

Zhang, C., Yuan, X., Wu, L., Han, Y., & Sheng, J. (2005). Study on morphology of electrospun poly(vinyl alcohol) mats. *European Polymer Journal*, *41*, 423–432.

Zhang, H., Niu, Q., Wang, N., Nie, J., & Ma, G. (2015). Thermo-sensitive drug controlled release PLA core/PNIPAM shell fibers fabricated using a combination of electrospinning and UV photo-polymerization. *European Polymer Journal*, *71*, 440–450.

Zhang, Q., Weber, C., Schubert, U. S., & Hoogenboom, R. (2017). Thermoresponsive polymers with lower critical solution temperature: From fundamental aspects and measuring techniques to recommended turbidimetry conditions. *Materials Horizons*, *4*(2), 109–116. https://doi.org/10.1039/c7mh00016b

Zomer Volpato, F., Almodóvar, J., Erickson, K., Popat, K. C., Migliaresi, C., & Kipper, M. J. (2012). Preservation of FGF-2 bioactivity using heparin-based nanoparticles, and their delivery from electrospun chitosan fibers. *Acta Biomaterialia*, *8*(4), 1551–1559. https://doi.org/10.1016/j.actbio.2011.12.023